学位論文

Neuroendocrinological studies on the central regulatory mechanisms of teleost reproduction with special reference to hypothalamic GnRH neurons

(視床下部GnRH ニューロンを中心とした 真骨魚類生殖中枢制御機構に関する神経内分泌学的研究)

平成 25 年 12 月博士（理学）申請

東京大学大学院理学系研究科

生物科学専攻

苅郷 友美

学位論文

Neuroendocrinological studies on the central regulatory mechanisms of teleost reproduction with special reference to hypothalamic GnRH neurons

視床下部 GnRH ニューロンを中心とした真骨魚類生殖中枢制御機構に関する神経内分泌学的研究

平成 25 年 12 月博士（理学）申請

東京大学大学院理学系研究科

生物科学専攻

苅郷 友美

Abstract

Animals receive various information from their environment and adapt to it by changing their internal homeostatic regulations. Among them, adaptive regulation of breeding conditions depending on both internal and external environments such as seasonality and nutrition, is one of the most important examples of such adaptations. The hypothalamic-pituitary-gonadal (HPG) axis is the central regulator of reproduction in almost all vertebrates, and GnRH1 neurons in the hypothalamus have been suggested to play a central role in the HPG axis regulation. In order to understand the central regulatory mechanisms of reproduction, the basic properties of GnRH1 neurons themselves have been studied mainly in rodents. However, the analysis of the neural circuitry for the HPG axis regulation appears to be incomplete mainly because of the technical limitation in mammalian studies. In the present thesis, to overcome such problems in the previous studies and to reveal the general principles underlying the HPG axis regulation mechanisms of vertebrates in common, I analyzed the HPG axis regulation mechanisms focusing on the hypophysiotropic GnRH1 neurons and pituitary gonadotropes by taking advantage of teleosts for the neuroendocrinological studies.

In Chapter 1, I analyzed the general properties of GnRH1 neurons and gonadotropin secretion during the ovulatory cycle using medaka as a model. First I recorded the electrical activities of GnRH1 neurons in the ventral preoptic area (vPOA), which directly project to the pituitary, and found that the spontaneous firing activities of vPOA GnRH1 neurons showed time-of-day-dependent changes; the firing rate in the afternoon was higher than that in the morning. Also, I examined the daily changes in the pituitary gonadotropin transcription level and

found that the expression levels of *lhb* and *fshb* mRNA varied according to the time of day, peaking during night. I also demonstrated that GnRH increases *lhb* mRNA transcription several hours after GnRH stimulation in an isolated whole pituitary culture, which explains the time gap between the peaks of GnRH1 release and *lhb* mRNA transcription. From these results, I proposed a working hypothesis concerning the temporal regulation of the ovulatory cycle in the brain and pituitary of female medaka.

After analyzing the basic properties of GnRH1 neurons and gonadotropin gene transcription during the ovulatory cycle in medaka, I analyzed the effects of GnRH in the pituitary concerning hormone secretion in Chapter 2. In order to analyze the effect of GnRH on LH and FSH cells separately, I first generated transgenic medaka lines that express a fluorescent Ca^{2+} indicator protein, inverse-pericam, specifically in the LH cells or FSH cells. By using these transgenic lines, I performed cell-type specific Ca^{2+} imaging and demonstrated that LH and FSH cells show different Ca^{2+} dynamics in response to GnRH. The results suggested that LH and FSH release are regulated by GnRH in different manners.

Finally, in Chapter 3, I searched for the regulator of GnRH1 neurons. As the candidate transmitters conveying neuronal inputs to the GnRH1 neurons, I focused on a neuropeptide kisspeptin and a monoaminergic neurotransmitter dopamine. Kisspeptin is known as one of the most potent activators of HPG axis in mammals, but it was shown that, in neither medaka nor goldfish, the kisspeptin administration *in vivo* induced an increase in the plasma LH concentration nor ovulation, and the kisspeptin administration *in vitro* did not change the GnRH1 neuronal activities at all. These results suggest that kisspeptin is dispensable for stimulation of the teleost GnRH1 neurons, at least in the same manner as in

mammals. On the other hand, I demonstrated that dopamine administration significantly inhibits the activities of GnRH1 neurons. The dopaminergic fibers projected to the cell bodies of the vPOA GnRH1 neurons and to the pituitary by intertwining with the GnRH1 fibers in the pituitary. Taken together, dopamine neurons possibly inhibit the GnRH1 neurons as well as the gonadotropes, suggesting that the dopaminergic inhibition of gonadotropin secretion is conserved among mammalian and teleost species.

In my thesis, I revealed several novel aspects of the HPG axis regulation mechanisms with special focus on the hypophysiotropic GnRH1 neurons and the pituitary, by taking advantage of medaka as a model system for the study of such mechanisms in vertebrates.

TABLE OF CONTENTS

Abbreviations 1

General Introduction 3

Chapter 1. 11

Time-of-Day-Dependent Changes in GnRH1 Neuronal Activities and Gonadotropin mRNA Expression in Medaka: Estrous Cyclicity

Chapter 2. 43

Physiological Study of GnRH-Induced Differential Regulations of Gonadotropins, LH and FSH:
Analysis of Ca^{2+} Dynamics in Transgenic Medaka

Chapter 3. 77

Identification of the Regulator of GnRH1 Neurons in Some Teleosts

General Discussion 111

Acknowledgements 121

References 122

Abbreviations

2APB	2-aminoethoxydiphenyl borate
ACSF	artificial cerebrospinal fluid
BAC	bacterial artificial chromosome
BCIP	5-bromo-4-chloro-3-indoyl-phosphate
DIG	digoxigenin
Dl	area dorsalis telencephali pars lateralis
Dm	area dorsalis telencephali pars medialis
Dp	area dorsalis telencephali pars posterior
E2	17β-estradiol
EGFP	enhanced green fluorescent protein
FSH	follicle stimulating hormone
GFP	green fluorescent protein
GnRH	gonadotropin-releasing hormone
gpa	glycoprotein α
GSI	gonadosomatic index
GTH	gonadotropin
HPG axis	hypothalamic-pituitary-gonadal axis
hrGFP	humanized renilla green fluorescent protein
i.c.v.	intracerebroventricular administration
i.p.	intraperitoneal administration
IHC	immunohistochemistry
IP	inverse-pericam
IP_3	inositol 1,4,5-trisphosphate
ir	immunoreactive
ISH	*in situ* hybridization
LH	luteinizing hormone
mdGnRH	medaka GnRH
NBT	4-nitroblue tetrazolium chloride
OT	tectum opticum
OVX	ovariectomy

PBST	phosphate buffered saline with tween 20
PKA	protein kinase A
PKC	protein kinase C
POA	preoptic area
POm	nucleus preopticus pars magnocellularis
POp	nucleus preopticus pars parvocellularis
PPD	proximal pars distalis
RGS	regulators of G protein signaling
TH	tyrosine hydroxylase
Vp	area ventralis telencephali pars posterior
vPOA	ventrolateral POA

General Introduction

Animals receive diverse information from the external environments and change their internal conditions for the adaptation to the environments, which enable them to respond appropriately to the external cues. Among such regulations, the control of reproduction is one of the most important regulations for the animals. Especially, the seasonally breeding animals show dynamic changes in the serum hormone concentrations and the gonadal size according to the seasonal cues such as day length, temperature, and nutrition.

The neuroendocrine control mechanisms of reproduction have been addressed intensely for a long time, and the hypothalamic-pituitary-gonadal axis (HPG axis) is believed as the "central dogma" in the central regulation of reproduction in almost all vertebrate species. Since the identification of gonadotropin releasing hormone (GnRH) by Schally and Guillemin in the 1970's (1-3), GnRH neurons have been considered as the final common pathway in hypothalamus for the control of reproduction. The function of hypophysiotropic GnRH neurons (called as GnRH1 neurons in most animals) is well-conserved among vertebrates. GnRH is a neuropeptide produced by GnRH1 neurons, which are located in the basal hypothalamic and/or preoptic area (POA) (4). The GnRH1 neurons stimulate gonadotropin secretion from the pituitary. In mammals, the GnRH1 neurons are located in the hypothalamic region and project their axons to the median eminence, and GnRH1 peptide is conveyed to the pituitary via the portal vessel (4). In teleost fish, the hypothalamic GnRH1 neurons directly innervate the pituitary (5-7) and stimulate the gonadotropin secretion from the gonadotropes. Two types of gonadotropins, luteinizing hormones (LH) and follicle stimulating hormone (FSH) are released from the pituitary and stimulate ovulation or follicle maturation respectively in females (illustrated in Fig. 0).

The earlier studies on the GnRH1 system were the histological analysis and the measurement of the amount of released hormones in the serum, gonadotropins, and GnRH, after intracerebroventricular applications or treatment of the hypothalamic explants or cultures with candidate regulatory factors of the HPG axis. Because of the technical limitations in those days, further analysis on the intrinsic electrical properties of the GnRH1 neurons and their neural networks has not been studied at the cellular level. However, physiological studies of GnRH1 neurons were greatly facilitated after the generation of transgenic mice and rats expressing green fluorescent protein (GFP) in GnRH1 neurons around the beginning of the 21st century (8-11). After the generation of transgenic animals, considerable numbers of electrophysiological analyses of GnRH1 neurons have been performed especially in mice and rats. The GFP transgenic labeling technique of GnRH1 neurons brought about a breakthrough in the cellular analysis of the features of GnRH1 neurons themselves under specific physiological conditions. However, the elucidation of the neural circuit for the HPG axis regulation is still difficult. This is partly because the brains of rodents are too large to perform experiments while keeping the neural circuitries intact, which, therefore, necessitates preparation of brain slices; the neural circuits are inevitably disrupted during the preparation of thin brain slices. Recently, it has been gradually clarified that a knowledge obtained in rodents is not necessarily consistent with those in other species, and there are some species variations in the HPG axis regulatory mechanism even in mammals. This is exactly the reason we should examine and compare results from various species, instead of using just a few specific animals such as rodents. Unfortunately, the cellular level studies on the HPG axis regulation in the non-mammalian vertebrates has lagged behind those in the mammalian species because of the lack of appropriate model

animal species, and only one report has been published concerning the non-mammalian GnRH1 neuronal activities in a cichlid fish (12) before I started the present work.

To overcome these previously described problems and to study the general principles underlying the HPG axis regulation mechanisms of vertebrates in general, I started to study the regulation mechanisms of gonadotropes by the GnRH1 neurons, by making the most of the following advantages of teleosts for the study of reproductive endocrinology. First, the gonadotropins, LH and FSH, are secreted from distinct populations of gonadotropes, LH and FSH cells, that express those hormones separately (13), whereas LH and FSH are secreted from a single type of pituitary gonadotropes in mammals, which makes the study of control mechanisms of different gonadotropins difficult. Second, the adenohypophysis is directly innervated by the neurosecretory fibers in teleosts, and is not intercalated by portal vessels as in mammals (14). These features are helpful for the analysis of hypophysiotropic neural control of gonadotrophins at the single cell level. Among the teleost species, medaka has the following advantages for neuroendocrinological analyses of reproduction. First, various molecular genetic tools such as transgenic technologies are available. Second, their small and transparent brains enable us to use a whole-brain in vitro preparation, in which intact neural circuits are maintained. Third, their 1-day ovulatory cycle facilitates the analysis of the regulatory mechanisms of GnRH1 neurons and gonadotropins in rather natural and physiological conditions throughout the ovulatory cycle. Therefore, I started the present thesis work by using medaka as a teleost model.

To begin with, I started my study by examining the characteristics of GnRH1 neurons and gonadotropin secretion during the ovulatory cycle of medaka, because

there had been no report on the neural activity of GnRH1 neurons and gonadotropin secretion during natural ovulatory cycles in any vertebrate species. By retrograde labeling of the neurons projecting to the pituitary, I found that GnRH1 neurons in the ventral preoptic area (vPOA) directly project to the pituitary. I therefore recorded the neural activities from these GnRH1 neurons using transgenic medaka, in which GnRH1 neurons are labeled by GFP. Taking advantage of 1-day ovulatory cycle of medaka, I recorded neural activities of GnRH1 neurons during ovulatory cycle and found that the spontaneous firing activity of GnRH1 neurons showed time-of-day-dependent changes: the firing activity in the afternoon was higher than in the morning. Also, I examined the daily changes in the pituitary gonadotropin transcription level. The expression levels of *lhb* and *fshb* mRNA also showed changes related to the time of day, peaking during the lights-off period. Next, I analyzed effects of GnRH on the pituitary gonadotropes. I demonstrated that GnRH increases *lhb* mRNA transcription several hours after the stimulation in isolated pituitary preparations, which was very slow compared to the well-known immediate LH releasing effect of GnRH. From these results, I proposed a working hypothesis concerning the temporal regulation of the ovulatory cycle in the brain and pituitary of female medaka (Chapter 1).

In Chapter 2, I analyzed the control mechanisms of GnRH on the release of LH and FSH, respectively. Two types of gonadotropins, LH and FSH are important pituitary hormones for sexual maturation and reproduction, and both of them are known to be centrally regulated by GnRH. However, the mechanisms of differential regulation by GnRH of the release of two types of gonadotropins with different secretory profiles are still unknown. Taking advantages of teleost pituitary, where LH and FSH are secreted from separate cellular populations unlike in mammals, I

generated transgenic medaka lines that express Ca^{2+} indicator proteins, inverse-pericam, specifically in the LH or FSH cells. I performed cell-type specific Ca^{2+} imaging of LH and FSH cells, respectively. Using the whole brain-pituitary preparations of these transgenic fish in which all neural circuits and GnRH neuronal projection to the pituitary are kept intact, I found that LH and FSH cells showed different Ca^{2+} responses to GnRH. I also succeeded in detecting the effect of endogenous GnRH peptide on LH cells, which was released by electrical stimulation of the axons of GnRH1 neurons. The results suggest the differential regulatory mechanisms for LH and FSH release by GnRH and that neural control of LH release by GnRH1 neurons are functionally important *in vivo* in animals (Chapter 2).

GnRH neurons may alter their firing activity according to the environmental cues or the animals' conditions to alter their reproductive states. However, only a few neuronal inputs have been identified as regulators of GnRH1 neurons. To understand how animals change their reproductive state via GnRH1 neurons, I searched for the candidate neural inputs to the GnRH1 neurons. First, I focused on the neuropeptide kisspeptin, which is recently known as a potent activator of GnRH1 neuronal activity in mammals. However, *in vivo* intraperitoneal or intracerebroventricular administration of kisspeptin failed to induce plasma LH elevation or ovulation in sexually mature female goldfish. Moreover, electrophysiological experiments showed that Kiss1 did not change the firing frequency of GnRH1 neurons in medaka. Thus, it was strongly suggested that in some teleosts kisspeptins are dispensable for LH release at least in the same manner as reported in mammals. Next, I focused on a monoamine neurotransmitter dopamine, which had been suggested to have inhibitory effects on the HPG axis of

some vertebrates. I found close appositions between the dopaminergic fibers and the GnRH1 cell bodies in vPOA as well as the characteristic association of projecting dopaminergic and GnRH fibers in the pituitary. I also demonstrated electrophysiologically that dopamine inhibits the vPOA GnRH neuronal activity. In addition, LH and FSH cells in the pituitary received dopaminergic projections (Chapter 3). These results suggest that dopamine neurons possibly inhibit the HPG axis at two levels: at the level of GnRH1 neuron cell bodies in the POA, and at the level of the gonadotropes in the pituitary.

Figure 0

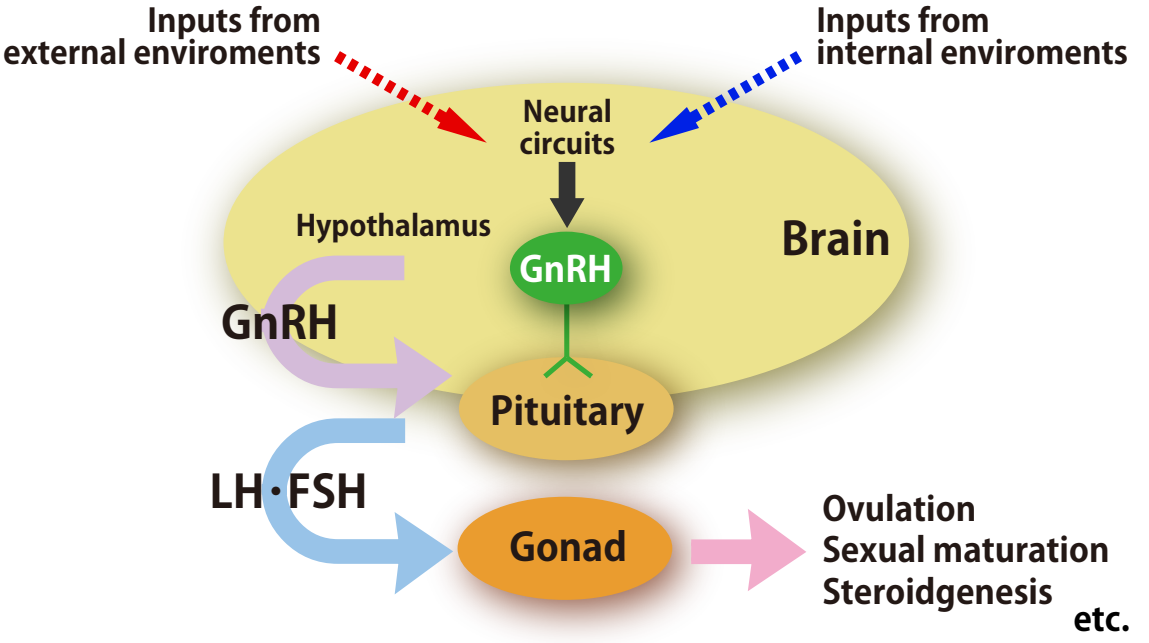
Inputs from
external enviroments
Inputs from
internal enviroments
Neural
circuits
Hypothalamus
GnRH
Brain
GnRH
Pituitary
LH·FSH
Gonad
Ovulation
Sexual maturation
Steroidgenesis
etc.

Chapter 1

Time-of-Day-Dependent Changes in GnRH1 Neuronal Activities and Gonadotropin mRNA Expression in Medaka: Estrous Cyclicity

Abstract

Gonadotropin-releasing hormone (GnRH) neurons in the preoptic area and hypothalamus control the secretion of GnRH and form the final common pathway for hypothalamic–pituitary–gonadal (HPG) axis regulation in vertebrates. Temporal regulation of reproduction by coordinating endogenous physiological conditions and behaviors is important for successful reproduction. Here, I examined the temporal regulation of reproduction by measuring time-of-day dependent changes in the electrical activity of GnRH1 neurons and in the levels of expression of pituitary gonadotropin mRNA using a daily spawning teleost, medaka (*Oryzias latipes*). First, I performed on-cell patch clamp recordings from GnRH1 neurons that directly project to the pituitary, using *gnrh1*-GFP transgenic medaka. The spontaneous firing activity of GnRH1 neurons showed time-of-day dependent changes: overall, the firing activity in the afternoon was higher than in the morning. Next, I examined the daily changes in the pituitary gonadotropin transcription level. The expression levels of *lhb* and *fshb* mRNA also showed changes related to time of day, peaking during the lights-off period. Finally, I analyzed effects of GnRH on the pituitary. I demonstrated that incubation of isolated pituitary with GnRH increases *lhb* mRNA transcription several hours after GnRH stimulation, unlike the well-known immediate LH releasing effect of GnRH. From these results, I propose a working hypothesis concerning the temporal regulation of the ovulatory cycle in the brain and pituitary of female medaka.

Introduction

Gonadotropin-releasing hormone (GnRH) neurons of the preoptic area and hypothalamus are responsible for the secretion of GnRH and form the final common pathway in the central regulation of reproductive functions. A rapid and large increase in GnRH levels, the GnRH surge, is a trigger for a surge in pituitary luteinizing hormone (LH) and a prerequisite for ovulation. This preovulatory LH surge has been demonstrated in many vertebrate species (15-21).

Temporal regulation is important for successful reproduction, and numerous physiological and behavioral processes that depend on neuronal and hormonal activities must be coordinated to achieve that goal. For example, ovulation, sexual behavior, fertilization, and maintenance of pregnancy require specific temporal patterns of hormone secretion in spontaneous ovulators such as rats, hamsters, and mice (22-24). A good example of temporal regulation of reproduction is the regulation of the daily LH surge, which has been observed in many vertebrates. The LH surge in most women begins early in the morning (25). Similarly, in nocturnal rodents, the LH surge begins immediately preceding their active period, around the time of lights off (26). Comparable phenomena are known to occur in non-mammals; for example, goldfish show an LH surge at dawn on the day of spawning (21). The mechanisms that control the occurrence of an LH surge at particular time of day are thus suggested to be conserved throughout the evolutionary lineage of vertebrates, but are not well understood.

In the present study, I examined the temporal regulation of reproduction by measuring time-of-day dependent changes in the electrical activity of GnRH1 neurons and in the levels of expression of pituitary gonadotropin mRNA using a

daily spawning teleost, medaka. Medaka is a diurnal teleost that spawns every morning under breeding condition and presents several advantages for the study of temporal regulation mechanisms of reproduction. First, their one-day ovulatory cycle facilitates the analysis of the regulatory mechanisms of GnRH1 neurons and gonadotropins in rather natural and physiological conditions throughout the ovulatory cycle. In addition, their small and transparent brains enable us to use a whole-brain *in vitro* preparation, in which intact neural circuits are maintained for electrical recording and imaging.

I found time-of-day dependent changes in the firing activities of GnRH1 neurons and transcription of pituitary gonadotropin mRNA. The increased activity of GnRH1 neurons in the afternoon is suggested to rapidly induce the LH surge in the same day and also to induce transcription of *lhb* mRNA after a delay to promote synthesis of LH that becomes the source for the LH surge in the next ovulatory cycle. This is the first report to strongly suggest a relationship between GnRH1 neuronal activity and LH secretion by examining their time-of-day dependent changes throughout the ovulatory cycle.

Materials and Methods

Animals

Male and female wild-type d-rR medaka (*Oryzias latipes*), *gnrh1:hrGFP* transgenic medaka (27), and *gnrh1*:EGFP transgenic medaka were maintained in pairs under a 14-h light and 10-h dark photoperiod (light on at 8:00 and light off at 22:00) with a water temperature of 27 °C. Female subjects were sexually mature (body weight: 0.22 ~ 0.26 g) and spawned for at least three consecutive days [gonadosomatic index

(GSI): 8.0 ~ 14.0]. Fish were fed two to three times daily with live brine shrimp and flake food. All animals were maintained and used in accordance with guidelines established by the University of Tokyo for the use and care of experimental animals.

Histology

To identify GnRH1 neurons in the POA, I performed *in situ* hybridization using a DIG labeled RNA probe that specifically labels medaka *gnrh1* mRNA following a standard protocol (28) with some minor modifications. After DIG-3 treatment, I added an alkaline phosphatase substrate, NBT/BCIP (337 mg/ml NBT and 175 mg/ml BCIP) in DIG-3. I then took photographs at 10 min, 30 min and 240 min after application of NBT/BCIP, while the reaction continued. Innervation of the pituitary by GnRH1 neurons was examined using a dual fluorescence method by retrograde labeling of biocytin and GnRH immunohistochemistry (or *in situ* hybridization) as described previously (29). Briefly, I anesthetized fish and dissected out the whole brain and pituitary of male and female d-rR medaka and then inserted a small crystal of biocytin (Sigma, St. Louis, MO) into the pituitary. After incubation of the brain in fish artificial cerebrospinal fluid (ACSF) containing (in mM): NaCl 134, KCl 2.9, $CaCl_2$ 2.1, $MgCl_2$ 1.2, HEPES 10, and glucose 15 (adjusted to pH 7.4 with NaOH) for 30 - 60 min, brains were fixed with 4 % paraformaldehyde in PBS. The fixed brain was sectioned frontally at 30 μm using a cryostat (CM 3050S, Leica microsystems, Wetzlar, Germany) and mounted onto MAS-GP typeA coated glass slides (Matsunami, Osaka, Japan). Then, the retrogradely labeled biocytin signals were visualized with AlexaFluor 488 conjugated streptavidin (1:500; Invitrogen, Carlsbad, CA) by reaction with ABC *Elite* kit (Vector, Burlingame, CA). GnRH immunoreactivity was visualized by anti-medaka (md)GnRH antiserum (1:10,000)

and AlexaFluor555 conjugated anti-rabbit IgG (1:800; Invitrogen). The fluorescent signals were observed using a LSM-710 confocal laser-scanning microscope (Carl Zeiss, Oberkochen, Germany). Anti-mdGnRH (GnRH1) antiserum was produced as follows; mdGnRH peptide (pE-H-W-S-F-G-L-S-P-G-NH_2) was synthesized chemically by Sawady Technology (Tokyo, Japan). An antiserum against mdGnRH (lot no. 2) was raised against the full-length mdGnRH decapeptide by immunization of a rabbit (Gift from Dr. Kataaki Okubo, The University of Tokyo, (7)). The specificity of the antiserum was assessed by a dot blot analysis. Briefly, synthetic mdGnRH (GnRH1), chicken-type GnRH (GnRH2), and salmon-type GnRH (GnRH3) peptides were serially diluted 1:5 from a starting concentration of 500 ng/μl down to a concentration of 160 pg/μl, and 1 ml of these peptide solutions were spotted on nylon membranes (Hybond-N^+; Amersham Pharmacia Biotech, Amersham, UK). The subsequent immunoreaction with the antiserum against mdGnRH was performed in the same manner as for the tissue samples, as described below. This dot blot test demonstrated that the mdGnRH antiserum cross-reacted with chicken-type GnRH and salmon-type GnRH by less than 0.8% (data not shown). I also used fluorescent *in situ* hybridization with an HNPP (2-hydroxy-3-naphthoic acid-2′- phenylanilide phosphate) fluorescence detection kit (Roche) to label GnRH1 neurons. The results of *in situ* hybridization were consistent with that of immunohistochemistry. I used wild type d-rR medaka for all histological experiments.

Electrophysiology

For the electrophysiological analysis, I used both a *gnrh1*:hrGFP transgenic line (27) and a *gnrh1*:EGFP transgenic line. Because the two transgenic lines showed

similar results, I combined all data from the two lines. Fish were anesthetized by immersion in tricaine methanesulfonate (MS-222; dissolved 0.02% in tap water) and then decapitated. *In vitro* whole brain preparation for the patch-clamp recordings from genetically GFP-labeled GnRH1 neurons was carried out as follows. First, the brain and attached pituitary were dissected out and placed in a hand-made chamber filled with ACSF. Then, the optic nerve was removed from the brain to make it easier for the patch pipettes to access the brain, and the ependymal layer of preoptic area was carefully peeled off with fine forceps. Under an upright fluorescent microscope with infrared differential interference contrast optics (Eclipse E600FN, Nikon, Tokyo, Japan), the exposed GnRH1-GFP neurons were easily identified visually from the ventral side of the brain. The patch pipette was carefully directed toward the GnRH1-GFP neurons with the aid of an MP-225 micromanipulator (Sutter Instruments, Novato, CA) by comparing the images on the infrared differential interference contrast monitor and the GFP fluorescence through the ocular lens. Patch pipettes of borosilicate glass capillaries with 1.5-mm outer diameter (GD-1.5; Narishige, Tokyo, Japan) were pulled using a Flaming-Brown micropipette puller (P-97; Sutter Instruments, Novato, CA). The tip resistance of patch pipettes in ACSF was about 8~15 MΩ, and seal resistances for on-cell recordings were about 15 to 60 MΩ. ACSF was also used as the pipette solution for loose-patch recordings. Targeted single-unit extracellular loose-patch recordings were performed with patch-clamp amplifiers (CEZ-2400; Nihon Koden, Tokyo, Japan and and BVC-700A; Dagan, Minneapolis, MN) and I analyzed spontaneous firing activity of single GnRH1-GFP neurons extracellularly by continuously recording changes in currents that are associated with action potential generation (action currents). The action currents were filtered at 1 kHz with a

low-pass four-pole Bessel filter and digitized at 10kHz using a Digidata 1320A interface and pClamp8 software (Molecular Devices, Sunnyvale, CA). All recordings were initiated within two hours after dissecting out the whole brain with pituitary. Electrical recordings were performed every four hours (n=10~13 for each time point).

Quantification of time-of-day dependent changes in pituitary gonadotropin mRNA

Female medaka were sacrificed under MS-222 anesthesia, and the pituitaries were collected for real-time PCR analysis. Pituitaries were collected six times a day, every four hours (1:00, 5:00, 9:00, 13:00, 17:00, and 21:00), from 14 or 16 fish per each sampling. Total RNA was extracted from the pituitaries using the FastPure RNA kit (Takara, Shiga, Japan) according to the manufacture's protocol. Two pituitaries were homogenized in a tube by vortexing with the FastPure kit lysis buffer for more than one minute (n=7 or 8 for each time point). Genomic DNA was removed by DNaseI (Ambion, Applied Biosystems, Foster City, CA) treatment on a column membrane. Total RNA was reverse-transcribed with a High Capacity RNA-to-cDNA kit (Applied Biosystems, Foster City, CA) according to the manufacturer's instructions. Real-time PCR was performed as previously described (30). The PCR product was verified by the melting curve analysis. The data were normalized to a housekeeping gene, *b-actin*, and average expression levels were calculated. Primer pairs used for real-time PCR are listed in Table 1-1 and were designed as follows: (i) one side of the primer pairs was designed in the exon-exon boundary, and the other one was designed inside of the exon to detect mature mRNA and (ii) the both primer pairs were designed in the same intron to detect the mRNA precursor.

GnRH effects on lhb mRNA and lhb primary transcript transcription in the isolated pituitary

I collected the pituitaries at around 10:00 and immediately began pre-incubation in normal medium (NM; Leibovitz's L-15 medium (pH 7.4; cat. no. L5520; Sigma) supplemented with L-glutamine (2 mM), D-glucose (10 mM), penicillin-streptomycin (100 U of penicillin and 0.1 mg streptomycin/ml; Life Technologies), and 5% fetal bovine serum (FBS; JRH Biosciences, Lenexa, KS) at 25 °C for two hours. 10 nM 17β-estradiol (E2) was added for control group (C group), and 10 nM E2 and 100 nM mdGnRH for GnRH administration group (G group; n=5~8, two pituitaries for each sample). Given the data available for goldfish (21), I expect that 10 nM E2 would be a reasonable physiological level for a female teleost. I determined the concentration of synthetic mdGnRH peptide by reference to (31): application of 100 nM GnRH induces rapid intracellular calcium rise in dissociated goldfish gonadotropes. After two-hour preincubation with or without mdGnRH, each sample was washed with NM and then incubated in NM for 0, 4, 8, 12, or 16 hours. The experimental scheme is shown in Fig. 1-4A. After incubation, the pituitaries were homogenized, and *lhb* mRNA was quantified in the same manner as were time-of-day dependent changes in pituitary gonadotropin mRNA. Because *lhb* mRNA level was greatly increased by co-treatment of GnRH with estrogen (32-35), I added estrogen to NM when isolated pituitaries were pretreated with GnRH. I also performed preliminary tests to show that estrogen treatment alone did not change *lhb* mRNA expressions (data not shown).

Data analysis

All values are shown as mean ± SEM. For electrophysiological experiments, the action currents were recorded between 5 and 10 or 15 min after the start of

recordings and were counted using Clampfit10.2 (Molecular Devices). The mean firing rate (spikes/seconds) was determined by dividing the total number of action currents detected during the 5 or 10 min recording period by the total recording time (seconds) (Fig. 1-2E). Instantaneous frequency (the interval between events, converted to frequency in Hz) was also calculated from the data for the 5 or 10 min recording period (Fig. 1-2F). Quiescence was defined as a 1-min bin containing one event or less. The percentage of bins that were quiescent (Fig. 1-2G), and the maximum duration of quiescence (number of consecutive quiescent bins) during the recording period (5 min or 10 min) (Fig. 1-2H) were determined for each recording. When quiescence continued for the whole duration of recording (5 min), the maximum duration of quiescence was defined as 5 min or 10 min. Because female medaka have a one-day ovulatory cycle, I arbitrarily categorized the recorded data into six groups, each with four-hour period (Fig. 1-2: group a, 23:30~3:30; b, 3:30~7:30; c, 7:30~11:30; d, 11:30~15:30; e, 15:30~19:30; and f, 19:30~23:30; n=10, 10, 12, 11, 12, and 13, respectively). The mean value for each group was calculated and multiple comparison tests were performed using the Tukey-Kramer test (significance levels < 0.05). For the analysis of the time-of-day dependent changes in the pituitary mRNA levels, the expression level for each time period was normalized by the average mRNA expression level at 5:00. Outliers for each time point and gene were excluded using the Smirnov-Grubbs test (significance levels < 0.05). Outliers represented less than one data point in each sample group. Tukey-Kramer multiple comparison tests were performed for each time period and gene (significance levels < 0.05). For the GnRH-induced increase of *lhb* mRNA levels in pituitary primary culture, each data point was normalized by the averaged expression level measured just after the pre-incubation without mdGnRH and outliers were excluded using the

Smirnov-Grubbs test (significance levels < 0.05). Outliers represented less than one data point in each sample group. Expression levels were analyzed using a two-way factorial ANOVA and Dunnet's post hoc test (significance levels < 0.05).

Results

Ventral population of GnRH1 neurons project to the pituitary

The axons of GnRH1 neurons project directly to the pituitary in teleosts; this is quite different from mammalian GnRH1 neurons, the axons of which project to the median eminence and stimulate gonadotrophs indirectly via hypophyseal portal vessels (29). Two major populations of GnRH1 neurons are present in the telencephalon of medaka: one in the region spanning area ventralis pars dorsalis, supracommissuralis, and posterior (Vd/Vs/Vp) of telencephalon (referred to as the dorsal POA in (27)) (Fig. 1-1A), and the other in the region ranging from the lateral part of area ventralis pars ventralis of telencephalon (Vv) to the ventrolateral POA (ventral POA in (27)) (Fig. 1-1B). In the present paper, I refer to these populations as the dorsal and the ventral populations of GnRH1 neurons, respectively. A schematic illustration of these two populations is shown in Fig. 1-1C.

I examined the localization of the hypophysiotropic GnRH1 neurons using double fluorescence analysis, with retrograde labeling of neurons after biocytin injections to the pituitary and either GnRH immunohistochemistry or *in situ* hybridization for GnRH mRNA. I embedded the crystal of biocytin into various areas of the pituitary and labeled the pituitary-projecting neurons. The results clearly demonstrate colocalization of GnRH immunoreactivity and retrograde labeling in a part of the ventral population of GnRH1 neurons (Fig. 1-1B). On the other hand, I did not find

any colocalization with retrograde labeling in the dorsal population (Fig. 1-1A). This result in adult medaka was consistent with a previous report that GFP-positive axons from the POA project to the pituitary in GnRH1-GFP medaka embryos (27). Because of inevitable technical limitations of the retrograde tracing method, I cannot completely discount the possibility of a pituitary projection from the dorsal GnRH1 neurons; however, at most it would be a minor projection compared with the strong projection from the ventral population of GnRH1 neurons.

I also conducted a semi-quantitative comparison of levels of expression of GnRH mRNA in the dorsal and ventral populations of GnRH1 neurons by comparing the time to visualize digoxigenin precipitates during *in situ* hybridization in identical sections (see (36) for this method). I obtained similar results after repeating the same experiments several times, and a representative image is shown in Fig. 1-1D. Because the ventral GnRH1 neurons were visualized in less than 10 min, while it took more than 30 min to visualize the dorsal GnRH1 neurons (Fig. 1-1D), I suggest that the ventral GnRH1 neurons express much higher level of GnRH1 mRNA than the dorsal GnRH1 neurons.

GnRH1 neurons show time-of-day dependent changes in electrical activities

Because the hypophysiotropic GnRH1 neurons project to the pituitary and release GnRH to stimulate LH release from pituitary gonadotropes, changes in GnRH neuronal activities are considered to be the immediate indications of GnRH and LH release. I focused my electrical recordings on the vPOA GnRH1 neurons, and will simply refer to these cells as “GnRH1 neurons” in this thesis. Using a targeted loose-patch single-unit recording technique, I analyzed spontaneous firing activity of single GnRH1-GFP neurons extracellularly by continuously recording

action currents for up to 120 min. Virtually all the recorded GnRH1-GFP neurons (Fig. 1-2A) showed irregular spontaneous activities (n = 66 neurons from 41 fish; Fig.1-2B). Two GnRH1 neurons were quiescent during the recording period.

Electrical recordings were performed every four hours, and I found that spontaneous activity changes with time of day. The LH surge in female medaka has been roughly estimated to start from eight to nine hours after the time of light-on (37), which corresponds to 16:00 to 17:00 in our lighting schedule. I divided a day into six four-hour periods and categorized the data recorded during each period. Fig.1-2C and D show representative traces of spontaneous firing activity of GnRH1-GFP neurons at the time preceding the putative LH surge (at 13:00, group d) and at the time just before the putative LH surge (at 16:00, group e), respectively. GnRH1 neuronal activity is clearly low at 13:00 and high at 16:00. The data for every four-hour period, showing the mean firing rate, median instantaneous frequency, and percentage and maximum duration of time in quiescence, are shown in Fig. 1-2E–H. The mean firing rate of GnRH1 neurons was highest at the time just before and during the putative LH surge (group e: 1.42±0.82 spikes/second, n = 12) and the lowest at the time immediately preceding it (group d: 0.24±0.08 spikes/second, n = 11; Fig. 1-2E). The median instantaneous frequency was also highest at the time just before and during the putative LH surge (group e: 1.39±0.51 spikes/second, n = 12) and the lowest at the time preceding it (group d: 0.41±0.14 spikes/second, n = 11; Fig. 1-2F). GnRH1 neurons recorded during 11:30~15:30 showed the highest percentage of quiescence, compared with other times of day (statistically significant differences were found between groups a and d, and groups b and d, *: $p<0.05$; Fig. 1-2G). In addition, the maximum duration of quiescence in the recording period during 11:30~15:30 was the longest, compared with those of

other time periods (statistically significant differences were found between groups a and d, groups b and d, groups c and d, and groups e and d, *: $p<0.05$; Fig. 1-2H). Two neurons were quiescent for the entire recording period: one out of twelve GnRH1 neurons recorded in group c, and one out of thirteen GnRH1 neurons recorded in group f. Taking all these results into consideration (Fig. 1-2E~H), electrical activity obviously changes with time of day, with a significant increase in GnRH neuronal activity in the afternoon which may produce an associated increase in release of GnRH to the pituitary (see Discussion).

Time-of-day dependent changes in gonadotropin mRNA/primary transcript expression levels in the pituitary

Time-of-day dependent changes in levels of expression of *lhb* and *fshb* mRNAs and their primary transcripts in the breeding female pituitaries were analyzed. *Lhb* and *fshb* mRNAs and primary transcripts in pituitaries were measured six times a day at 4-h intervals (1:00, 5:00, 9:00, 13:00, 17:00, and 21:00; n=8, 7, 8, 7, 7 and 8, respectively). For quantification of gene expression at better time resolution, I designed the PCR primer pairs in the introns so that I could selectively quantify the amount of mRNA precursor before splicing, referred to as the primary transcript (38).

Both *lhb* mRNA and the primary transcript showed clear time-of-day dependent changes (Fig. 1-3A). In *lhb* mRNA, expression level was highest at 5:00 and showed significantly lower levels from 17:00 to 1:00. The change in *lhb* primary transcript was time-shifted forward, and the transcription level peaked from 1:00 to 5:00 and showed significantly lower levels from 13:00 to 21:00. *Fshb* mRNA is supposed to peak at 5:00, similar to *lhb* mRNA, although I did not find statistical significance. The *Fshb* primary transcript also showed time-of-day dependent changes, with

transcription level highest at 5:00 and significantly lower from 17:00 to 1:00 (Fig. 1-3B).

These results suggest that 1) transcriptional levels of *lhb* and *fshb* change with time of day, 2) because of their shorter half-life period *lhb* and *fshb* primary transcript levels show more significant time-of-day dependent changes than those of *lhb* and *fshb* mature mRNA, and 3) the peak time is similar for *lhb* and *fshb* transcription, highest during the light-off period and lowest during the latter half of light-on period, with slightly different dynamics in which the *lhb* primary transcript started to increase earlier than *fshb* primary transcript and was kept longer at higher transcription level. Thus, the *lhb* and *fshb* expression levels may be differentially regulated.

GnRH upregulates the expression of lhb mRNA on a slow time scale

In many vertebrates, GnRH is known to trigger release of LH from the pituitary via activation of GnRH receptors in the LH producing cells. In medaka, I have reported that the mdGnRH peptide triggers an intracellular calcium ($[Ca^{2+}]_i$) rise in LH producing cells in the pituitary within several seconds after mdGnRH application, which should reflect the fast release of LH from the pituitary (39). A rapid $[Ca^{2+}]_i$ rise after GnRH application has also been reported in dissociated goldfish gonadotrope cells (31). Therefore, I examined the effects of mdGnRH peptide on the transcription of *lhb* mRNA in isolated pituitary preparations. The expression levels of *lhb* mRNA started to increase twelve hours after 2-hour pre-incubation with 100 nM GnRH and was significantly different 16 hours after preincubation ($p<0.001$), whereas they did not show any changes after preincubation without GnRH (Fig. 1-4B). The amount of *lhb* primary transcript

started to increase eight hours after the end of preincubation with GnRH and became significantly different at 16 hours ($p<0.01$; Fig. 1-4B). This result indicates that the facilitatory effect of mdGnRH peptide on *lhb* transcription in the pituitary proceeds on a slower time scale than the rapid LH release after GnRH application, which takes nearly ten hours or more.

Discussion

In the present study, I examined the mechanisms of temporal regulation of reproduction by analyzing time-of-day dependent changes in the electrical activity of GnRH1 neurons and transcription of *lhb/fshb* mRNA, as well as GnRH-induced changes in *lhb* transcription, using the teleost medaka, which spawn on a daily basis.

vPOA GnRH1 neurons directly regulate the pituitary in medaka

By retrograde labeling of neurons after biocytin injection to the pituitary, I demonstrated that vPOA GnRH1 neurons directly project to the pituitary in medaka. This is consistent with the fact that *gnrh1* in teleosts is homologous to *GnRH1* in mammals, which plays a role in hypophysiotropic regulation (40). In addition, I have shown that ventral GnRH1 neurons have higher levels of expression of *gnrh1* mRNA than do those of the dorsal population. These data led us to conclude that the ventral population of GnRH1 neurons in the POA (vPOA GnRH1 neurons) play a major role in hypophysiotropic functions and mainly contribute to the stimulation of gonadotropin release, and I therefore recorded their electrical activities.

Firing activity of medaka GnRH1 neurons shows time-of-day dependent changes

Using a model teleost, medaka, I recorded the activities of GnRH1 neurons at various time of the day and found changes in their activity levels corresponding to the reproductive cycle. Medaka is the only vertebrate species in which all three subtypes of GnRH neurons have been genetically labeled by GFP. In medaka, non-hypophysiotropic GnRH neurons, GnRH2 and GnRH3 neurons, show regular firing activities (41, 42), as has been reported for the dwarf gourami (43); (see also review by (44)). On the other hand, I report here that the GnRH1 neurons show irregular and episodic spontaneous firing activities, which is distinct from that of the extrahypothalamic GnRH2 and GnRH3 neurons in medaka (Fig. 1-2B). Similar irregular and episodic firing activities have been reported in the GnRH1 neurons of other vertebrates such as mice, rats, monkeys and cichlid fish (9, 11, 12, 45, 46).

The spontaneous firing activity of medaka GnRH1 neurons clearly showed time-of-day dependent changes in frequency; the overall tendency was low in the morning and high in the afternoon. Similar to the strong correlation between the multiple unit activities (MUA) and the pulsatile release of LH (47), the electrical activity of a single GnRH1 neuron is also expected to be correlated with GnRH release from the GnRH1 neuron. Concerning the dynamic changes in the spontaneous activity of GnRH1 neurons, there are some reports on the occurrence of time-of-day dependent changes in GnRH1 neuronal activity using the daily surge mice model (48). A series of electrophysiological studies by Christian and Moenter (49) demonstrated that spontaneous firing in GnRH1 neurons was low in the morning (AM) and high in the afternoon (PM) in ovariectomized and estrogen treated (OVX+E) mice, and that no such difference is apparent in OVX mice.

Although the intact female mice show an LH surge every four to five days, the OVX+E mice show LH surge every PM. The time-of-day dependent changes in the firing activity in mice were thought to reflect an increase in GnRH release, which in turn triggers an LH surge. Their studies suggest that some kind of circadian neural mechanisms may be important for the regulation of GnRH neuronal activities (50). I surmise that there are two possible factors concerning time-of-day dependent changes in GnRH1 neuronal activities in general: changes in synaptic inputs to the GnRH1 neurons and the changes in the intrinsic excitability of the GnRH1 neurons themselves. In mice, the existence of both mechanisms has been suggested, which may exert synergistic effects on the neuronal activities of GnRH1 neurons (49, 51). The frequency of excitatory fast synaptic transmission to the GnRH1 neurons, especially excitatory GABAergic transmission, was found to be high in the PM (at the start of lights-off period) and low in the AM (during lights-on period) in OVX + E mice (50). Also, high voltage activated Ca^{2+} currents in the GnRH1 neurons varied with the time of day: currents in GnRH1 neurons recorded from OVX + E mice were lower than those from OVX mice in the AM but were higher in the PM (52). These results were consistent with an increase of GnRH neuronal activity preceding LH surge.

There are reports also in rodents suggesting that signals arising from the suprachiasmatic nucleus (SCN), which is considered to be the master circadian clock, affect the hypothalamic neuronal functions such as the regulation of timing of LH surge (reviewed in (53)). In addition, direct neural connections between SCN neurons and GnRH neurons in the hypothalamus have been demonstrated anatomically (54, 55). Finally, the GnRH1 neurons themselves have been reported to express endogenous clock genes (56), which may modify their sensitivity to

various signals by changing the expression levels of certain receptors.

Although previous studies of the diurnal regulatory mechanisms of GnRH1 neurons have been performed using OVX+E mice, I here succeeded in recording, for the first time in vertebrate brains, time-of-day dependent changes in the electrical activity of GnRH1 neurons in the intact brain of daily ovulating medaka without manipulations of the sex steroid milieu. This approach will enable us to use medaka to examine the temporal relationships between the natural ovulatory cycles and GnRH neuronal activity under physiological conditions. Analyzing the contribution of estrous and circadian cyclicity on time-of-day dependent changes in the GnRH neuron activities will be an interesting topic for future research.

Pituitary expression of lhb and fshb mRNA also shows time-of-day dependent changes

I demonstrated that *lhb* and *fshb* mRNA expression in medaka pituitaries showed time-of-day dependent changes, particularly in the primary transcript. Both mRNA and primary transcript for these two genes showed similar time-of-day dependent changes, although *lhb* primary transcript started to change earlier than *lhb* mRNA. Because primary transcripts were measured before splicing, I should in principle be able to use this approach to detect changes in the expression of genes of interest more sensitively than with mRNA. Interestingly, I found a time lag between the peak of *lhb* and *fshb* transcription and the peak of GnRH neuronal activity. This time lag may be due to the effect of GnRH on *lhb* transcription, which took ten hours or more (Fig. 1-4).

In the experiment using isolated pituitaries incubated with GnRH, *lhb* transcription started to increase eight hours after the completion of GnRH peptide treatment and was maintained at increased levels for several hours.

Non-mammalian GnRH receptors, which possess a C-terminal tail that contributes to agonist-dependent receptor desensitization and internalization, show robust agonist-dependent internalization (57). Three subtypes of GnRH receptors are expressed in medaka, and all of them possess a cytoplasmic C-terminal tail (58, 59). Therefore, medaka GnRH receptors are expected to show robust agonist-dependent internalization when they are treated with GnRH. Nonetheless, the increased *lhb* transcription level was maintained for more than 12 hours in my experiments. This prolonged response may be because of *in vitro* incubation of pituitary isolated from the brain; in contrast, *in vivo* the transcription of *lhb* mRNA may be inhibited by other factors such as dopamine, which inhibits LH release in teleosts (60, 61). These results, taken together with my results, suggest that once the LH synthetic pathway has been switched on GnRH receptor internalization itself may not inhibit *lhb* mRNA transcription, and that the effect of agonists may last for ten hours or more.

Conclusions

I propose a working hypothesis concerning temporal regulation of the ovulatory cycle in the brain and pituitary of female medaka (see Fig. 1-5). Activity of GnRH1 neurons increases towards the evening of Day 1 (Fig. 1-2), leading to increased release of GnRH. The released GnRH peptide regulates LH on two different time scales. First, it stimulates the pituitary gonadotropes to release LH on a short time scale (i.e., in several seconds; (39)) thereby causing the LH surge, which then triggers ovulation during the time period before lights-on. At the same time, GnRH facilitates transcription of *lhb* on a slower time scale, ten hours or more (Fig. 1-4); the resulting protein product, LH, will be the source for the next LH surge, on Day2.

Thus, medaka represents an excellent model system for studying the neural mechanisms of control of vertebrate reproduction under the natural conditions, and is expected to provide us with important insights in future work.

Figure legends

Figure 1-1

GnRH1 neurons in the ventral POA project directly to the pituitary and express higher level of *gnrh1* mRNA than do dorsal POA GnRH1 neurons. (A, B) Double fluorescence analysis with retrograde labeling of neurons after biocytin injection to the pituitary (green) and GnRH immunohistochemistry (magenta) demonstrates that the GnRH1 neurons of the vPOA project directly to the pituitary (B). White arrowheads in the merged picture indicate neurons that show colocalization of retrograde tracer and mdGnRH peptide. I did not find any colocalization of retrograde labeling (green) and *gnrh1* mRNA (magenta) in the population of dorsal GnRH1 neurons (A). Taken together, I conclude that the ventral population of GnRH1 neurons in POA (vPOA GnRH1 neurons) play a major role in hypophysiotropic function and mainly contribute to the stimulation of gonadotropin release. V, ventricle; IHC, immunohistochemistry. Scale bars, 20 μm. (C) Illustrations of a frontal section and a lateral view (left = rostral) of the medaka brain, showing the plane of section corresponding to panels A, B, and D; note that midline is located in the center of the picture in A. Blue squares indicate the dorsal (D) and ventral (V) populations of GnRH1 neurons shown in A, B, and D. Dm, area dorsalis telencephali pars medialis; Dl, area dorsalis telencephali pars lateralis; Dp, area dorsalis telencephali pars posterior; POm, nucleus preopticus pars magnocellularis; POp, nucleus preopticus pars parvocellularis; OT, tectum opticum; Vp, area ventralis telencephali pars posterior. (D) Representative time-lapse photographs of digoxigenin precipitates visualized for *gnrh1* mRNA detection by *in situ* hybridization in the identical section. Photographs were taken at 10 min, 30

min and 240 min after the application of an alkaline phosphatase substrate, NBT/BCIP. *In situ* hybridization shows two separate populations of *gnrh1* mRNA positive neurons in the area ranging from the telencephalon to the POA. The ventral population of GnRH1 neurons was visualized much earlier during the precipitation, strongly suggesting that the expression of *gnrh1* mRNA is higher in the ventral than the dorsal population. Scale bar, 25 μm.

Figure 1-2

Electrical activity of the vPOA GnRH1-GFP neurons in sexually mature female medaka. (A) Enlarged view of the cell bodies of vPOA GnRH1-GFP neurons imaged by conventional fluorescence microscopy. Scale bar, 10 μm. (B) Targeted on-cell patch clamp recording from a vPOA GnRH1-GFP neuron (for 15 seconds). (C, D) Spontaneous firing activities of GnRH1-GFP neurons for one minute in the time period preceding the putative LH surge (at 13:00; C) and just before and during the putative LH surge (at 16:00, D). Bars above the traces indicate the lighting conditions of the aquarium room; light on from 8:00 ~ 22:00 (white boxes) and light off from 22:00 ~ 8:00 (gray boxes). The striped boxes indicate the recording time windows, and the scale bars indicate the action current amplitude and time scale. The table at the bottom of D indicates the recording time groups. (E, F) Comparisons of the mean firing rate (spikes/second; E) and the median instantaneous frequency (Hz; F) indicate that vPOA GnRH1-GFP neurons show higher firing rates and higher median instantaneous frequencies in group e (15:30~19:30, n = 12), compared with group d (11:30 ~ 15:30, n = 11). (G, H) Comparisons of the percentage and the maximum duration of quiescence demonstrate that vPOA GnRH1-GFP neurons show a significantly higher

percentage of quiescent time and a longer duration of quiescence in group d (15:30 ~ 19:30, n = 11), compared with other groups. *, $p < 0.05$ (Tukey-Kramer test) compared to group d.

Figure 1-3

Time-of-day dependent changes in the expression of gonadotropin mRNA/primary transcript in the pituitary of sexually mature female medaka. (A) Both *lhb* mRNA and primary transcript show clear time-of-day dependent changes. In *lhb* mRNA, the expression level is highest at 5:00 and remains at relatively low levels between 17:00 and 1:00. This pattern is time-shifted forward for *lhb* primary transcript such that the expression level is highest at 1:00 and 5:00 and remains low between 13:00 and 21:00. (B) Time-of-day dependent changes in levels of *fshb* mRNA are not clear, but levels peak at 5:00 as do those of *lhb* mRNA. *Fshb* primary transcript shows time-of-day dependent changes, and the expression level is highest at 5:00 and remains low between 17:00 and 1:00. The vertical axes of the graphs represent relative expression levels that were normalized relative to the average expression level at 5:00. Tukey-Kramer tests indicate the following levels are statistically significant: a ($p < 0.001$), b ($p<0.01$), and c ($p < 0.05$) are lower compared to 5:00, and d ($p<0.001$), e ($p<0.01$) are lower compared to 1:00.

Figure 1-4

GnRH upregulates expression of *lhb* mRNA on a slow time scale in isolated pituitaries *in vitro*. (A) Experimental scheme. Pituitaries were surgically isolated and treated with normal medium (NM) and 10 nM E2 and NM ("without mdGnRH" group), or with 10 nM E2 and 100 nM mdGnRH ("with mdGnRH" group). Two hours

after treatment, pituitaries were washed with NM and incubated in NM for several hours. Pituitaries were collected 0, 4, 8, 12, and 16 hours after the completion of the GnRH or control treatment, and expression of *lhb* mRNA/primary transcript was measured. (B) Relative expression of *lhb* mRNA/primary transcript in the pituitaries was measured using real-time PCR. The level of expression of *lhb* mRNA starts to increase twelve hours after the completion of GnRH treatment, and shows no change in pituitaries not treated with GnRH. Relative expression of *lhb* primary transcript starts to increase more than eight hours after the completion of GnRH treatment. The vertical axes of the graphs represent relative expression levels, normalized by the average expression level measured just after the 2-hour incubation without mdGnRH. Statistically significant differences were obtained using a two-way factorial ANOVA to compare the "with" and "without GnRH" groups (*lhb* mRNA, $p<0.01$; *lhb* primary transcript, NS ($p=0.053$)), to compare each sampling time (*lhb* mRNA, $p<0.01$; *lhb* primary transcript, $p<0.01$), and to examine the interaction effect (*lhb* mRNA, $p<0.01$; *lhb* primary transcript, $p<0.05$). Dunnet's post hoc test, *** $p < 0.001$ and ** $p<0.01$ compared to the level of expression in the "without GnRH" group at time 0 (without GnRH time 0, 4, 8, 12, 16, n= 7, 7, 7, 7, and 5; with GnRH time 0, 4, 8, 12, 16, n=8, 8, 8, 8, and 6, respectively).

Figure 1-5

Working hypothesis for the temporal regulation of the ovulatory cycle in the female medaka. Towards the evening of Day1, GnRH1 neuronal activity increases, leading to increased GnRH release. The GnRH peptide stimulates pituitary gonadotropes to release LH within several seconds and causes the LH surge, which triggers ovulation during the night. The GnRH peptide simultaneously acts on the pituitary

gonadotropes to increase the transcription of *lhb* mRNA over the course of several hours, and the synthesized LH will be the source for LH surge on Day2. See text for detail.

Figure 1-1

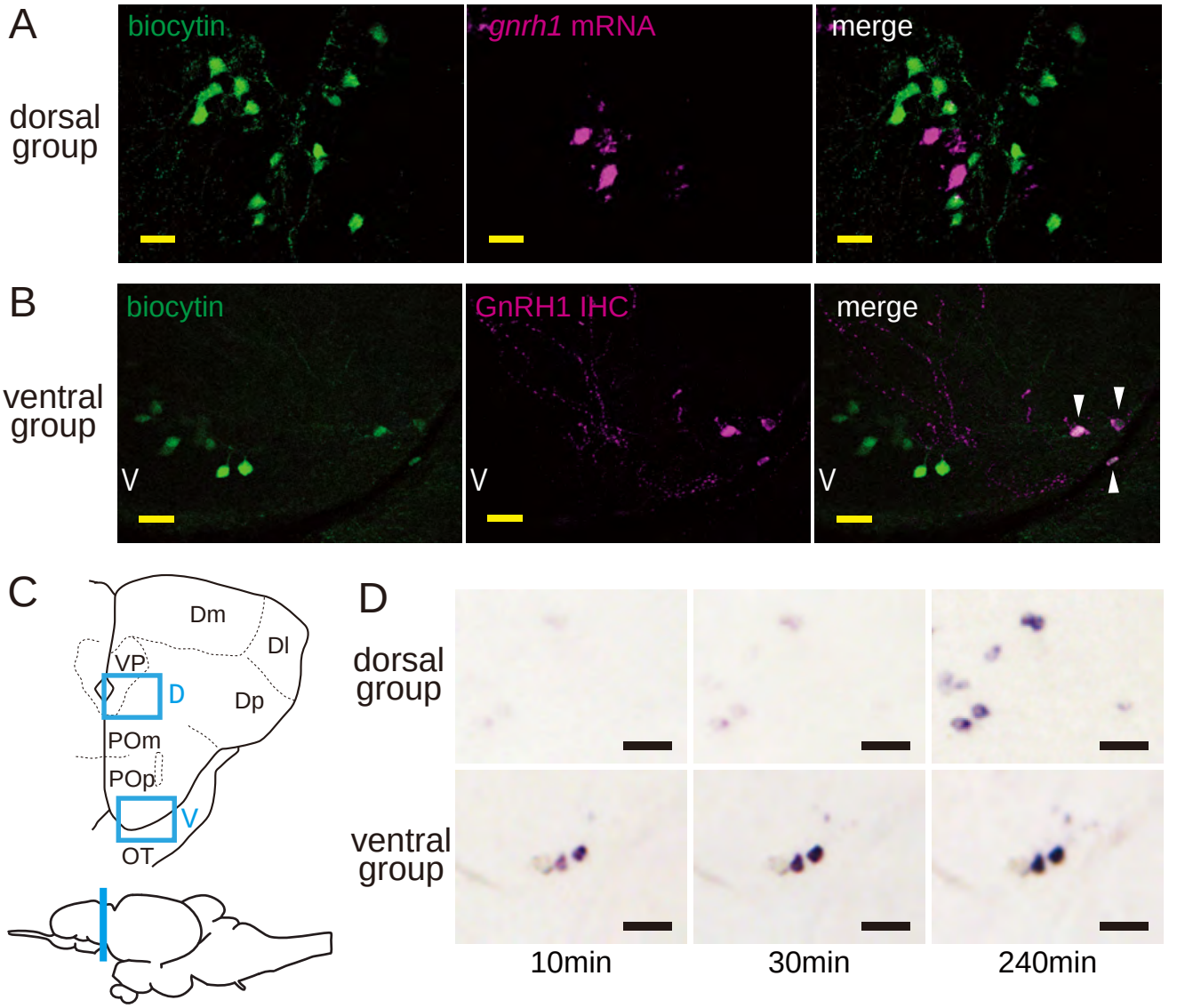
A
dorsal group
biocytin
gnrh1 mRNA
merge
B
ventral group
biocytin
GnRH1 IHC
merge
V
V
V
C
Dm
Dl
VP
D
Dp
POm
POp
V
OT
D
dorsal group
ventral group
10min
30min
240min

Figure 1-2

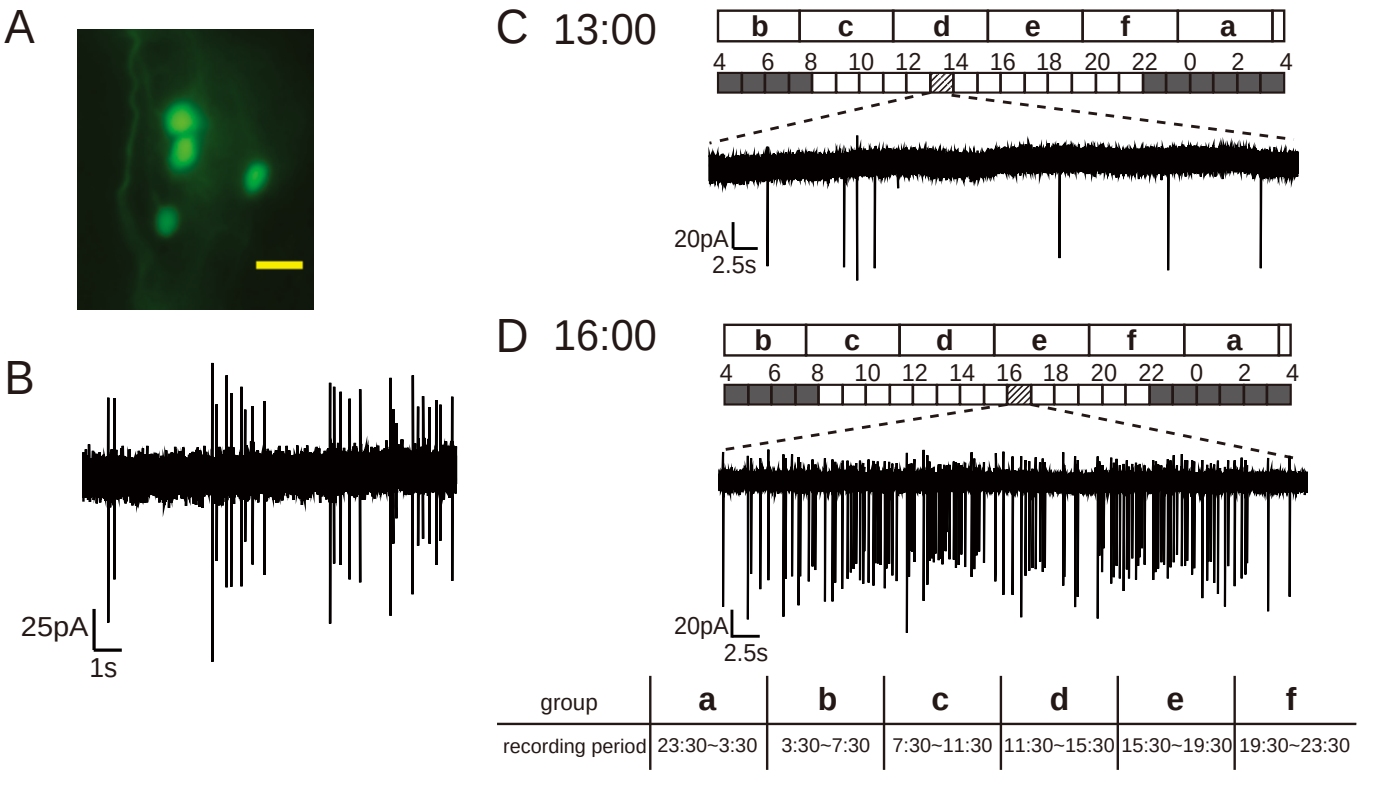
A
B
25pA
1s
C 13:00
b c d e f a
4 6 8 10 12 14 16 18 20 22 0 2 4
20pA
2.5s
D 16:00
b c d e f a
4 6 8 10 12 14 16 18 20 22 0 2 4
20pA
2.5s
group a b c d e f
recording period 23:30~3:30 3:30~7:30 7:30~11:30 11:30~15:30 15:30~19:30 19:30~23:30

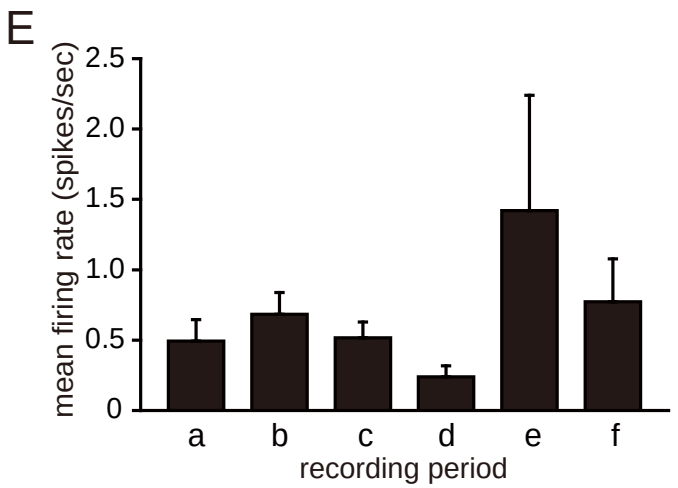
E
mean firing rate (spikes/sec)
0 0.5 1.0 1.5 2.0 2.5
a b c d e f
recording period

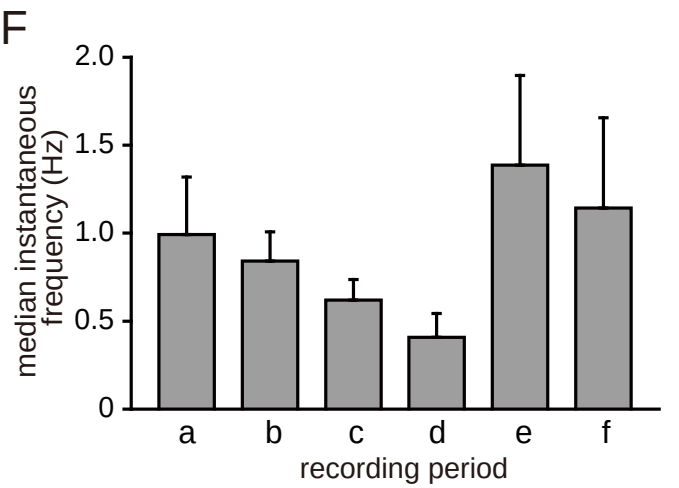
F
median instantaneous frequency (Hz)
0 0.5 1.0 1.5 2.0
a b c d e f
recording period

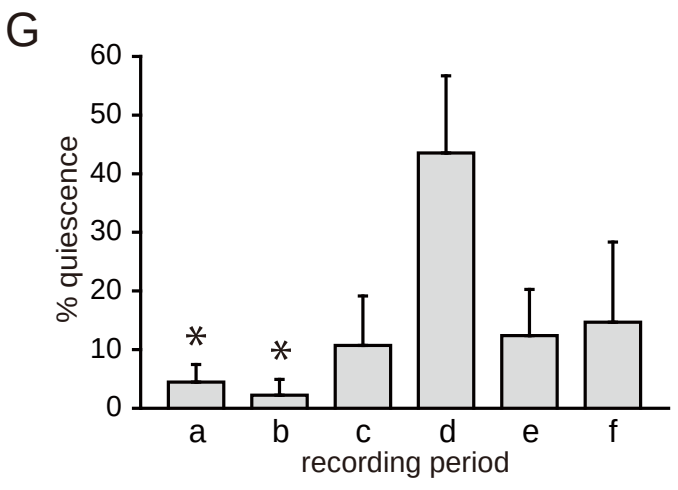
G
% quiescence
0 10 20 30 40 50 60
a b c d e f
recording period

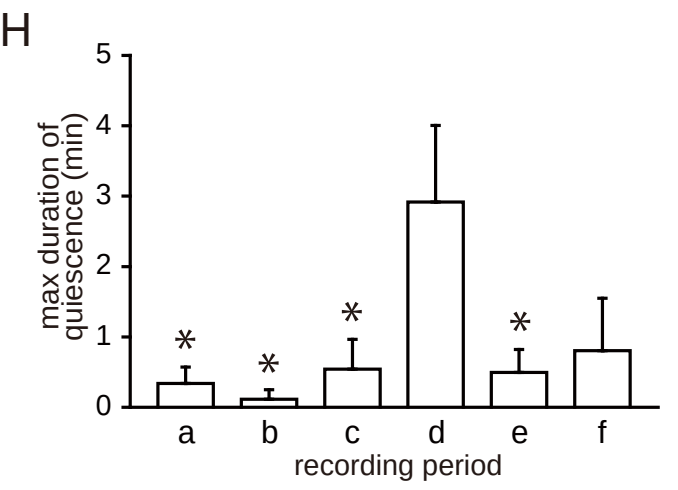
H
max duration of quiescence (min)
0 1 2 3 4 5
a b c d e f
recording period

Figure 1-3

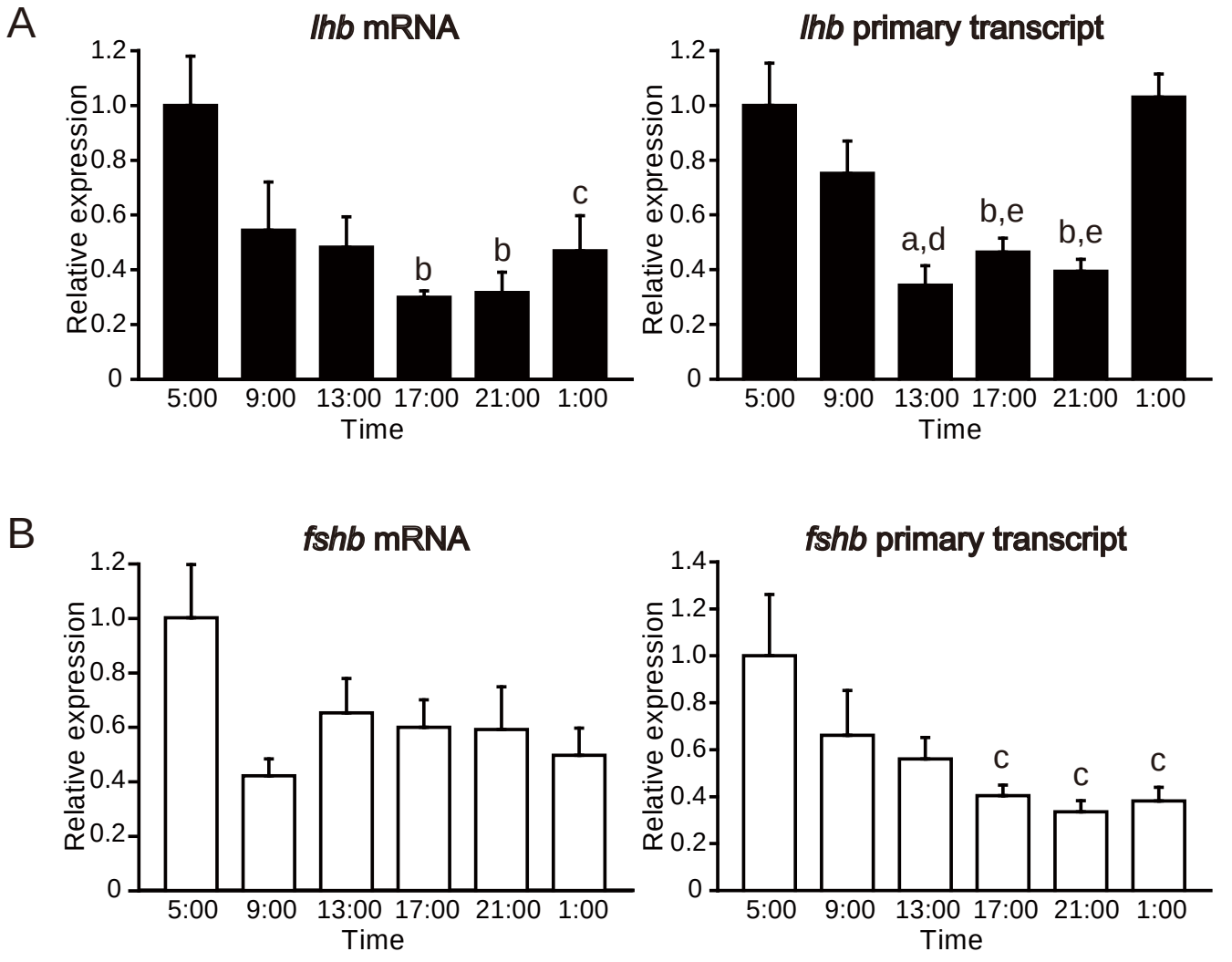
A
lhb mRNA
Relative expression
1.2
1.0
0.8
0.6
0.4
0.2
0
b
b
c
5:00
9:00
13:00
17:00
21:00
1:00
Time
lhb primary transcript
Relative expression
a,d
b,e
b,e
Time
B
fshb mRNA
Relative expression
Time
fshb primary transcript
Relative expression
1.4
c
c
c
Time

Figure 1-4

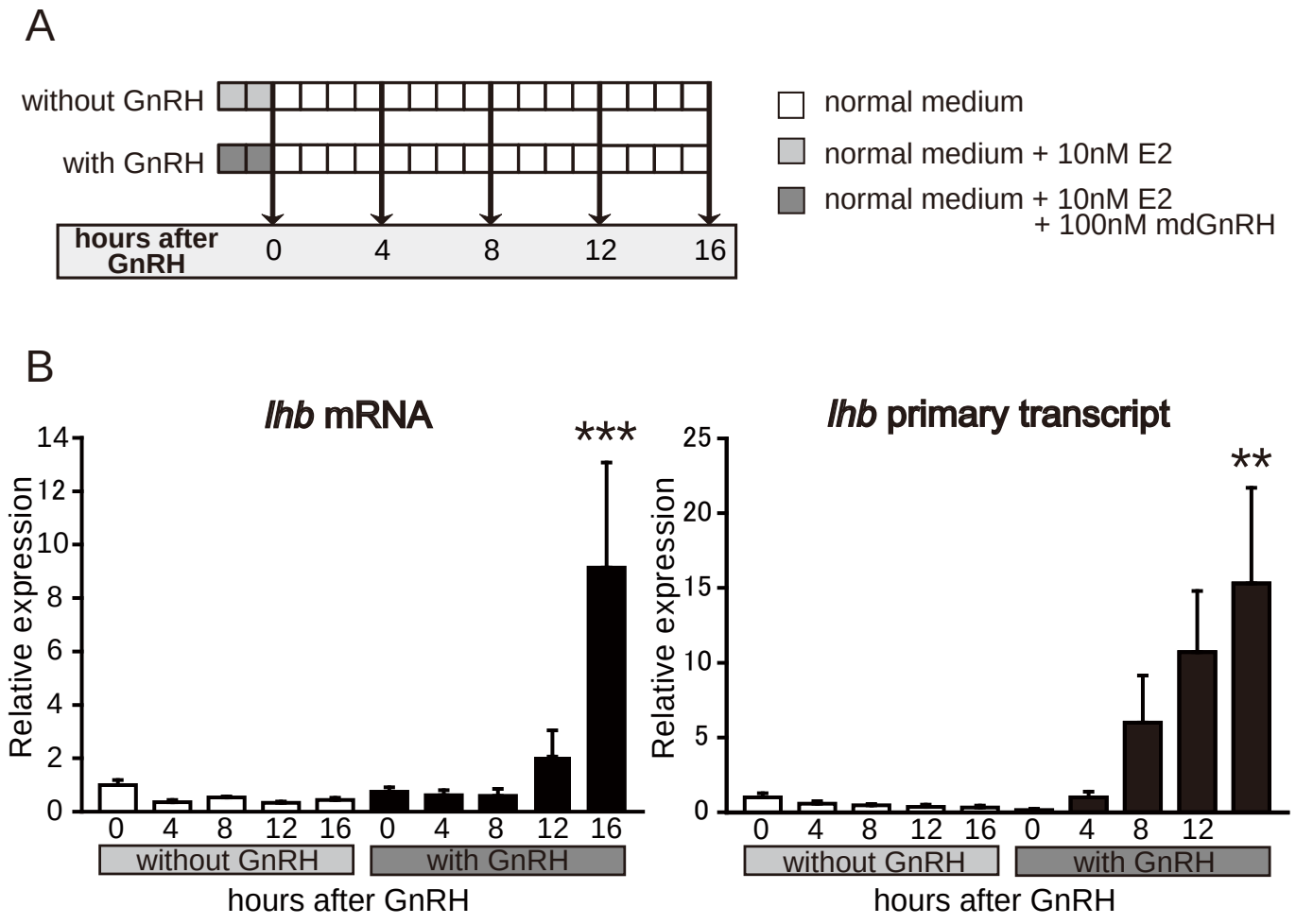
A
without GnRH
with GnRH
hours after GnRH
0
4
8
12
16
normal medium
normal medium + 10nM E2
normal medium + 10nM E2
+ 100nM mdGnRH
B
lhb mRNA
***
Relative expression
14
12
10
8
6
4
2
0
0 4 8 12 16 0 4 8 12 16
without GnRH
with GnRH
hours after GnRH
lhb primary transcript
**
Relative expression
25
20
15
10
5
0
0 4 8 12 16 0 4 8 12
without GnRH
with GnRH
hours after GnRH

Figure 1-5

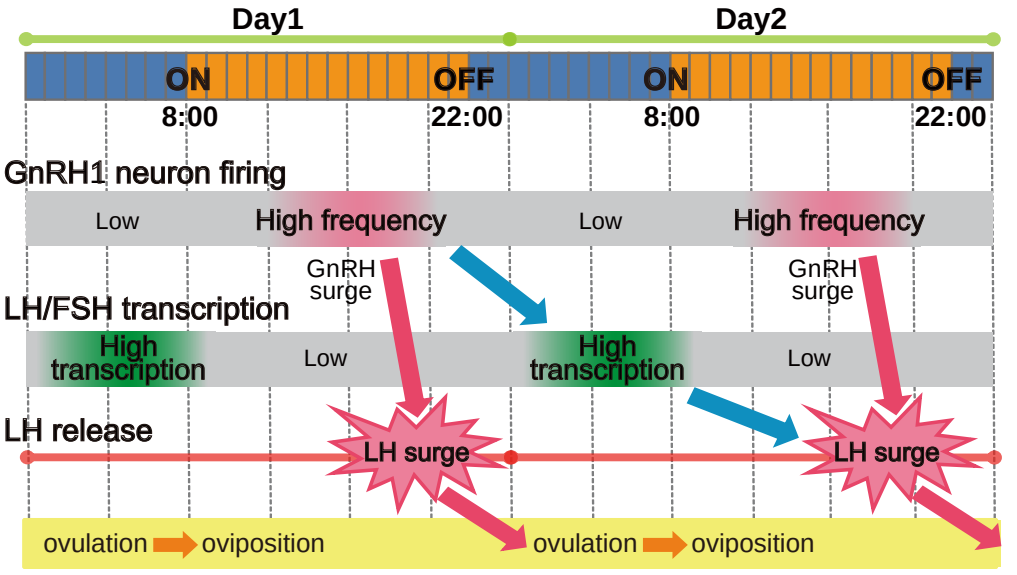
Day1
Day2
ON
OFF
ON
OFF
8:00
22:00
8:00
22:00
GnRH1 neuron firing
Low
High frequency
Low
High frequency
GnRH surge
GnRH surge
LH/FSH transcription
High transcription
Low
High transcription
Low
LH release
LH surge
LH surge
ovulation
oviposition
ovulation
oviposition

Table 1-1

Primer pairs used for real-time PCR

F: forward, R: reverse

Usage for	F/R	Nucleotide sequence
lhb mRNA	F	5'-TGCCTTACCAAGGACCCCTTGATG-3'
	R	5'-AGCTCTCCACAGGGATGCTG-3'
lhb primary transcript	F	5'-TAAAGGCTTCAAAGTGGTGCAGTC-3'
	R	5'-TGGAGTGCATGTAAGGGAAGAAC-3'
fshb mRNA	F	5'-TGGAGATCTACAGGCGTCGGTAC-3'
	R	5'-AGGGTATGTGACTGACGGATCCAC-3'
fshb primary transcript	F	5'-TTTGGAATATTATCCCCCAACCGC-3'
	R	5'-ATGTGGTGAACCCAAAAACTCTGC-3'
actb mRNA	F	5'-CCCCACCCAAAGTTTAG-3'
	R	5'-CAACGATGGAGGGAAAGACA-3'

Chapter 2

Physiological Study of GnRH-Induced Differential Regulations of Gonadotropins, LH and FSH: Analysis of Ca^{2+} Dynamics in Transgenic Medaka

Abstract

Two types of gonadotropins, luteinizing hormone (LH) and follicle stimulating hormone (FSH) are important pituitary hormones for sexual maturation and reproduction, and both of them are centrally regulated by gonadotropin-releasing hormone (GnRH) from the hypothalamus. In mammals, these two gonadotropins are secreted from a single type of gonadotropes. The mechanisms of differential regulation by GnRH of the release of two types of gonadotropins with different secretory profiles are still unknown. In teleosts, however, LH and FSH are secreted from separate cellular populations unlike in mammals. This feature makes them useful for studying the regulatory mechanisms of LH and FSH secretions independently. Here, I generated transgenic medaka lines that express Ca^{2+} indicator proteins, inverse-pericam, specifically in the LH or FSH cells. I performed cell-type specific Ca^{2+} imaging of LH and FSH cells, respectively, using the whole brain-pituitary preparations of these transgenic fish in which all neural circuits and GnRH neuronal projection to the pituitary are kept intact. LH and FSH cells showed different Ca^{2+} responses to GnRH. The results suggest differential regulation mechanisms for LH and FSH release by GnRH. Moreover, I also succeeded in detecting the effect on LH cells of endogenous GnRH peptide, which was released by electrical stimulation of the axons of GnRH1 neurons. Thus, my newly-developed experimental model system using the whole brain-pituitary *in vitro* preparation of the transgenic medaka is a powerful tool for analyzing the differential regulatory mechanisms of the release of LH and FSH by multi-synaptic neural inputs to the pituitary.

Introduction

Pituitary gonadotropins, LH and FSH, are the most important regulators of vertebrate reproduction. In mammals, FSH stimulates the maturation of ovarian follicles, whereas LH induces the follicular rupture, ovulation in female. The synthesis and release of LH and FSH are regulated by GnRH, which is synthesized by neurons in the hypothalamus, GnRH neurons (62). In addition to the gonadotropins, GnRH is suggested to be functionally conserved throughout vertebrates (40). On the basis of accumulating physiological and molecular phylogenic homology data, it is now generally accepted that the two subtypes of teleost gonadotropins, GTH-I and GTH-II, correspond to the tetrapod FSH and LH, respectively (13). Thus, it is suggested that the functions of LH and FSH may have differentiated early in the vertebrate lineage, and the functional and secretory properties of LH and FSH have much in common for each throughout vertebrate species.

The great majority of physiological studies concerning the regulation of gonadotropin release have been performed using mammalian primary cell cultures, particularly from rats (63-66). However, there are some inevitable difficulties in studying the differential regulation mechanisms of gonadotropin release in mammals because of the fact that each mammalian gonadotrope produces both LH and FSH. By contrast, teleost is a good model to overcome some difficulties of mammalian preparations and to study the neural control of the adenohypophysis because of their unique characteristics. First, LH and FSH are secreted from distinct populations of LH and FSH cells that express those hormones separately (reviewed in (13) and as for medaka in (30)). Second, the adenohypophysis is

directly innervated by neurosecretory fibers, and is not intercalated by portal vessels (14). Third, the teleost pituitary is highly compartmentalized, and the same types of cells are clustered (13). Also, especially in medaka, their pituitary is small and transparent enough to keep them healthy and to observe their fluorescence of Ca^{2+} indicators or fluorescent proteins from outside of the whole brain-pituitary preparations without dispersing or slicing.

To take advantage of such features, I here generated a transgenic medaka that expresses a genetically encoded calcium indicator, inverse-pericam (IP) (67), in LH and FSH cells for the first time in vertebrates to study differential release mechanisms of those hormones at the cellular level. IP is a genetically encoded calcium indicator that shows stronger fluorescence at lower Ca^{2+} concentrations and weaker fluorescence at higher Ca^{2+} concentrations, which is the inverse of the general Ca^{2+} indicators. I chose IP to make it easier to identify the labeled cells at the resting low Ca^{2+} concentrations, which helped the screening process. As the GnRH-induced Ca^{2+} rise in gonadotropes has been reported to be accompanied by an increase in the membrane capacitance (surface membrane area) of gonadotropes (65, 66), Ca^{2+} rise could be considered as the indicator of the exocytotic release of hormones from the gonadotropes.

By using these transgenic medaka lines, I succeeded, for the first time, in analyzing the stimulatory effects of GnRH separately on the LH and FSH cells at the cellular level. Furthermore, in the present study, I used whole brain-pituitary *in vitro* preparations to keep the neural circuit to the pituitary and the networks inside the pituitary intact by taking advantage of the small and transparent brain and pituitary of a small teleost fish, medaka. I succeeded in analyzing GnRH-induced Ca^{2+} changes differentially in the individual LH and FSH cell by

using the whole brain-pituitary preparations. Moreover, I also succeeded in detecting the effect of endogenous GnRH peptide on LH cells, which was released by electrical stimulation of the axons of GnRH1 neurons. These results suggest that my newly developed experimental model system using the transgenic medaka lines is a powerful tool for analyzing the differential regulatory mechanisms of the release of LH and FSH by neural inputs to the pituitary.

Materials and Methods

Animals

Male and female wild type drR medaka and all transgenic medaka (*lhb:IP*, *fshb:IP*, *gnrh1:EGFP* (39), and *gnrh1:EGFP* x *lhb:IP*) were maintained in pairs under a 14-h light and 10-h dark photoperiod (light on at 8:00 and light off at 22:00) at water temperature of 27 °C. I used sexually matured female and male medaka (body weight: female 261±14 mg, male 240±18 mg; gonadosomatic index (GSI): 7.27±0.35 % in female) that spawned for at least three consecutive days. I did not find any significant sexual differences in results, and I therefore combined the data from both sexes. The fish were fed two to three times a day with live brine shrimp and flake food. All animals were maintained and used in accordance with the guidelines of the University of Tokyo for the use and care of experimental animals.

Generation of constructs for transgenic medaka

The medaka *lhb* and *fshb* loci were isolated by screening a bacterial artificial chromosome (BAC) library (*lhb*: ola1-108H20, *fshb*: ola1-110G16). The primer pairs used for promoter PCR amplification were as follows; for LHβ promoter, Forward:

5'- AAAAATCAGCGAGAGTCGCTGGTT -3', and Reverse: 5'-TGTGAAAAATAAAATTGACTC -3', for FSHβ promoter, Forward: 5'-ACATCCATTGGCCTCTGTAAATGA -3', and Reverse: 5'-CCTCTGCCTGGTGCAGTACC -3'. The fragment containing the 5'-flanking region (about 2.5 kb) along with exon 1 of *lhb* or *fshb* was PCR amplified from the screened BAC clone. In each gene, exon 1 coded a 5'-untranslated region, and the initiation methionine codon was present at the 5' end of exon 2. Each fragment was fused with the inverse-pericam-coding sequence (67) followed by the polyadenylation signal of the bovine growth hormone (BGH) gene and subcloned into the cloning vector pGEM-T (Promega, Madison, WI) (Fig. 2-2 A). These constructs were purified and dissolved in 10 mM Tris-HCl (pH 8.0) containing 0.1 mM EDTA.

Generation of transgenic medaka lines

DNA constructs were diluted into 10~50ng/μL with PBS and 0.02% phenol red and injected into the cytoplasm of one- or two-cell-stage embryos (F0). The injected embryos were intercrossed to identify the germ line founders. Individual adults from positive pairs were then outcrossed to identify the individual founder fish. Heterozygous transgene carriers in the F1 generation were identified by their presence of fluorescence in the embryos. To obtain homozygous transgenic offsprings, the carriers were crossed with each other. In the present study, I used homozygous progeny.

Histology

The pituitary was fixed by 4% paraformaldehyde in PBS. The fixed pituitary was frontally cryo-sectioned at 30 μm using a cryostat (CM 3050S, Leica microsystems,

Wetzlar, Germany) and mounted onto MAS-GP typeA coated glass slides (Matsunami, Osaka, Japan) as described before (30). For double labeling immunohistochemistry (IHC) for LH or FSH cells and GnRH fibers in the pituitary, I used *gnrh1:EGFP* transgenic medaka line that was generated by Ms. Akiko Takahashi (The University of Tokyo). The GnRH fibers were visualized by anti-EGFP antiserum (68) (diluted 1:1000 with PBST) and AlexaFluor488 conjugated anti-rabbit IgG (diluted 1:800 with PBST; Invitrogen, Carlsbad, CA). LH and FSH cells were visualized by anti-medaka LHβ antiserum or anti-medaka FSHβ antiserum (diluted 1:10000 with PBST) (69) and AlexaFluor555 conjugated anti-mouse IgG (diluted 1:800 with PBST; Invitrogen). For double labeling of *lhb* or *fshb* mRNA and IHC for inverse-pericam, I used *lhb:IP* or *fshb:IP* transgenic medaka. *Lhb* or *fshb* mRNA were visualized with a standard protocol described in (30) using DIG-labeled *lhb* or *fshb* probe. After ISH probe hybridization, the sections were incubated with anti-EGFP antiserum (diluted 1:1000 with DIG-1 buffer), rinsed twice with DIG-1 buffer, and incubated with TSA (tyramide signal amplification)-plus biotin reagent (PerkinElmer) for 30 min, rinsed with DIG-1 buffer twice, and incubated with ABC reagents (1% A solution and 1% B solution in DIG-1 buffer, Vector, Burlingame, CA) for 1 h. The sections were rinsed twice with DIG-1 buffer, incubated with Alexa Fluor 488-conjugated streptavidin (diluted 1:500 with DIG-1 buffer, Invitrogen) and alkaline phosphatase-conjugated anti-DIG antibody (diluted 1:1000 with DIG-1 buffer, Roche) for 2 h. Then, the sections were rinsed twice with DIG-1 buffer. After the EGFP signals were detected, the alkaline phosphatase activity, which was used to label *lhb* or *fshb* mRNA, was detected using Fast-Red substrate kit (abcam, Cambridge, UK) according to the manufacturer's instructions. The incubation for this substrate was carried out until

visible signals were detected and was stopped by washing in PBS containing 0.5 mM EDTA. Then, the sections were coverslipped with CC/Mount (Diagnostic BioSystems, Pleasanton, CA). The fluorescence was observed under confocal laser-scanning microscope LSM-710 (Carl Zeiss, Oberkochen, Germany) at 1-μm optical section. I also observed the whole brain-pituitary preparations using MVX10 stereoscopic microscope (Olympus, Tokyo, Japan).

Ca^{2+} imaging

Preparation and intracellular Ca^{2+} imaging with Fura-2

The fish were anesthetized by immersion in tricaine methanesulfonate (MS-222; dissolved 0.02% in tap water) and then decapitated. The brain was dissected out with intact pituitary and kept in fish artificial cerebrospinal fluid (ACSF) containing (in mM): NaCl 134, KCl 2.9, $CaCl_2$ 2.1, $MgCl_2$ 1.2, HEPES 10, and glucose 15 (adjusted to pH 7.4 with NaOH). I prepared Fura-2 solution (ACSF with 10 μM Fura2-AM (DOJINDO, Kumamoto, Japan) and 0.02% CremophorEL (Fluka, St. Louis, MO), vortexed it for 10 seconds and sonicated it for 4 seconds on ice using a sonicator (MS-50, HEAT SYSTEMS-ULTRASONICS, INC., Farmingdale, NY). After spinning down, the whole brain-pituitary preparation was incubated in Fura-2-AM solution for 30~60 min at room temperature to load Fura-2 in the cytoplasm of pituitary cells. After the incubation, the preparation was washed with ACSF and placed in a hand-made chamber filled with ACSF in the ventral side-up direction (Fig. 2-1B). The preparation was perfused with ACSF at a continuous flow rate (2mL/min). Fura-2 fluorescence were detected by the Chroma 74000 filter set (D340×, D380× exciter; 505DCLP dichroic mirror; HQ535/50m emitter) housed in the Lambda DG-4 Xenon light source, excitation filter exchanger (Sutter

Instruments, Novato, CA), and the BX-51WI upright epifluorescence microscope (Olympus, Tokyo, Japan). The fluorescence was recorded (exposure: 100 ms; interval: 5 sec) using QuantEM 512SC EMCCD camera (Photometrics, Tucson, AZ) and the Metafluor imaging software (Molecular Devices Corp., Downingtown, PA). For Fura-2, the intensity ratio of emission (at 510 nm) from the alternating 340 and 380 nm excitation was monitored.

Preparation and Ca^{2+} imaging with inverse-pericam

The whole brain-pituitary preparation from *lhb:IP* or *fshb:IP* transgenic medaka was prepared as described above. For the detection of IP fluorescence, I replaced the excitation filter in the Lambda DG-4 Xenon light source and excitation filter exchanger for FF01-474/23-25 (Semrock, Rochester, NY). Positions of the LH and FSH cells were visually identified under epifluorescence illumination, and fluorescence images of IP were recorded (exposure: 50 ms; interval: 5 sec). In all experiments using repetitive mdGnRH applications (Fig. 2-5), the interval (washout time) between the 1st and the 2nd trial was 10 minutes, and that between the 2nd and the 3rd one was 20~30 minutes. The mdGnRH applications under various antagonists in Fig. 2-5 were performed 10 minutes after pretreatment with antagonists.

GnRH response of LH cells evoked by electrical axonal stimulation of GnRH neurons

For this category of experiments, I used double-transgenic medaka (*gnrh1:EGFP* crossed with *lhb:IP*) to label both GnRH1 fibers and LH cells. I crossed homozygous transgenic offsprings of *gnrh1:EGFP* and *lhb:IP* and obtained double heterozygous *gnrh1:EGFP* x *lhb:IP* transgenic medaka. I prepared the whole brain-pituitary

preparation as described above. I used the same filter set as that for IP imaging. First, I set the focus on the bundle of GnRH1 fibers that run rostrocaudally in the hypothalamus and project to the pituitary (Fig. 2-6A, B). For the stimulation electrode, I used a mono-polar electrode (an electrolytically polished stainless steel insect pin, 1 μm in tip diameter, which was lacquer-coated, leaving a 50-100μm uncoated bared tip). I attached the mono-polar hand-made stimulation electrode to the EGFP-labeled GnRH1 fiber bundle unilaterally under the fluorescent microscope. After attaching the stimulation electrode, I performed Ca^{2+} imaging of the LH cell layer, while stimulating the GnRH1 fiber bundle (500-μs pulses at +250 μA every 20 ms for 20 trains) via an electronic stimulator equipped with an isolator (SEN-3301 and SS-302J, NIHON KOHDEN, Tokyo, Japan).

Drugs

The medaka GnRH (mdGnRH) peptide (pE-H-W-S-F-G-L-S-P-G-NH_2) was synthesized chemically by Sigma-Aldrich Japan (Tokyo, Japan). I used 100 nM mdGnRH for the co-application with $CdCl_2$ or 2APB (Fig. 2-5C,D,G,H) and 50 nM GnRH for other experiments with *lhb:IP* and *fshb:IP*. Analog M ($_D$-pE-$_D$-F-$_D$-W-S-Y-$_D$-W-L-R-P-G-NH_2), a competitive GnRH receptor antagonist (70), was purchased from Sigma-Aldrich (L6524, St. Louis, MO) or synthesized by GL Biochem (Shanghai, China). Both mdGnRH and analog M were dissolved in 100 μM pure water and diluted by ACSF to an optimal concentration. 2-Aminoethoxydiphenyl borate (2APB), an IP_3 receptor antagonist, was dissolved by dimethyl sulfoxide (DMSO) in 100 mM and diluted by ACSF.

Data analysis

All values are shown as mean ± SEM. In all imaging experiments, the time when drug reached the experimental chamber was defined as Frame 0. F_0 was calculated as an average of five frames, Frame -8 to -4. The fluorescence intensity change ($\Delta F/F_0$) was calculated as $(F_0-F)/F_0$, and the peak $\Delta F/F_0$ was picked up from 25 frames, Frame -3 to 21 in *lhb:IP*, and from 50 frames, Frame -3 to 46 for *fshb:IP*. All Fura2 experiments were analyzed in the same paradigm for *lhb:IP*, using the ratio of emission intensity (340 nm/380 nm; R) instead of the IP fluorescence intensity, and the ΔR values were calculated as $R-R_0$, where R_0 is the averaged ratio of the Frame -8 to -4. In the rise time analysis (Fig. 2-3E), I calculated $(F_0-F)/F_0$ for each cell (LH; 27~36 cells and FSH; 22~32 cells from one experiment), drew averaged trace for each experiment, and compared the half rise time from the onset to the peak of GnRH responses among the averaged traces (n=7). The Ca^{2+} fluctuation events were identified with the event detection algorithm in TaroTools (Igor macro set written by Dr. Taro Ishikawa, Jikei University School of Medicine) (Fig. 2-4). The peak detection procedure for this algorism is as follows. First, the raw data was linearly approximated for defining the baseline level. Next, the time points when the difference between the baseline and the raw trace is larger than the threshold value were picked up chronologically. Then, the maximum value of the raw trace that is found just before the first point when the polarity of the backward derivative of the 3-point moving averaged trace changed from positive to negative, were defined as a peak. For the Ca^{2+} peak detection, I used 0.001 as the threshold value. For the detection of simultaneous Ca^{2+} peaks, I selected all fluorescent pituitary cells found from one focus plane and detected Ca^{2+} peaks from each cell and plotted the Ca^{2+} peak events as a raster plot (Fig. 2-4B, E). I calculated and plotted percentage of cells that showed Ca^{2+} peaks at each time point (gray line in Fig. 2-4C,

F). I detected peaks from 3-point moving averaged trace (black line in Fig. 2-4C, F) with the same algorithms used for the Ca^{2+} peak detection using 3% as the threshold value (Fig. 2-4C, F).

Mann-Whitney *U* tests were performed for the comparison between the peak $\Delta F/F_0$ of vehicle and GnRH application, and that between 50% rise time of LH and FSH cells. Steel's multiple comparison tests were performed for repetitive GnRH application experiments, compared to the 1st GnRH application. These statistical analyses were performed using Kyplot5 (Kyence, Tokyo, Japan). Significance levels were set as $P < 0.05$. All the imaging data were analyzed using ImageJ (Wayne Rasband, National Institutes of Health, Bethesda, MD) with MBF ImageJ plug-ins (Tony Collins, McMaster University, Ontario, Canada) and Igor Pro 6.22A (WaveMetrics Inc., Lake Oswego, OR) with TaroTools.

Results

GnRH-induced Ca^{2+} rise in pituitary cells

To test the usefulness of the whole brain-pituitary preparations for Ca^{2+} imaging, I first examined Ca^{2+} response induced by GnRH application in unidentified pituitary cells. I loaded Fura2-AM to the entire pituitary and recorded Ca^{2+} response induced by GnRH. Generally, the pituitary of teleosts consists of various cell types arranged in characteristic clusters, and the LH and FSH cells are separated in different clusters in the pituitary (13, 30). FSH cells were localized in the dorsal proximal pars distalis (PPD), and LH cells in the ventral PPD (shown in Fig. 2-1A as a schematic illustration, see (30, 71) for detailed distribution). I set the focus at the surface of PPD, the presumptive LH cell area (white dotted square in

Fig. 2-1A). I used a synthetic medaka GnRH (mdGnRH) peptide, which is suggested to be the intrinsic GnRH peptide secreted by hypophysiotropic GnRH1 neurons (40), and the mdGnRH application induced transient Ca^{2+} rise in the pituitary cells (Fig. 2-1 C). The peak amplitude (Δratio of F340/F380) of Ca^{2+} response showed dose dependent changes (1 nM: 0.0080±0.0029, 10 nM: 0.0065±0.0025, 30 nM: 0.0935±0.0057, 100 nM: 0.1471±0.0049, 300 nM: 0.1614±0.0114, 1000 nM: 0.2266±0.0110; n= 55 cells [from 3 fish], 94 [3], 101 [3], 377 [16], 78 [3], 99 [3], respectively; Fig. 2-1 D, E).

Generation of lhb:IP and fshb:IP transgenic medaka

In medaka, GnRH1 neurons in the ventral preoptic area (vPOA) directly project to the pituitary (39). I performed double immunohistochemistry (IHC) for LH or FSH and GnRH (EGFP-immunoreactive in *gnrh1:EGFP* transgenic medaka) and found that GnRH1 fibers project to both LH and FSH cell layers in the pituitary (Fig. 2-2 D, E). To examine the GnRH effect on each gonadotrope (LH cell or FSH cell) separately, I generated transgenic medaka lines that specifically express IP, a genetically encoded calcium indicator, in either LH or FSH cells. I generated transgenic lines using plasmid-based DNA constructs that contain 5' flanking region of *lhb* gene (2.3kb) or *fshb* gene (2.2kb) immediately upstream of IP sequence (Fig. 2-2A). I injected *lhb*:IP construct to 380 fertilized eggs and *fshb*:IP construct to 330 fertilized eggs. I crossed the F0 generation fish and succeeded in obtaining one homozygous transgenic line for each construct. I examined the specificity of IP expression in the pituitary using double labeling of *lhb* or *fshb* mRNA by ISH and IP by EGFP IHC. I found that both of these transgenic lines showed specific expression of inverse-pericam in LH or FSH cells (Fig. 2-2B, C). Therefore, I performed further

experiments using these transgenic lines.

Different Ca^{2+} responses are induced by mdGnRH in LH and FSH cell

I performed cell-type specific Ca^{2+} imaging of individual LH and FSH cells respectively, using these transgenic lines as the whole brain-pituitary preparations. In the LH cells, mdGnRH application induced a rapid and transient Ca^{2+} rise ($\Delta F/F_0$ in vehicle: 0.0107±0.0008, mdGnRH: 0.0258±0.0013; $P < 0.001$; n=118 [4]; Fig. 2-3A, C). On the other hand, the FSH cells showed a slow and long lasting Ca^{2+} responses in response to mdGnRH, in comparison with those in LH cells ($\Delta F/F_0$ in vehicle: 0.0164±0.0017, mdGnRH: 0.0474±0.0025; $P < 0.001$; n=139 [5]; Fig. 2-3, B and D). The half rise time for GnRH responses was compared between LH and FSH cells. The FSH cells showed a significantly longer rise time compared with LH cells (half rise time in LH cells: 20.0±3.36 sec, FSH cells: 49.2±3.16 sec; $P < 0.001$; n=7 averaged traces for each; Fig. 2-3E). In some preparations, I could observe spontaneous Ca^{2+} responses in LH and FSH cells (Fig. 2-4A, D). Among them, the LH cells tended to show simultaneous Ca^{2+} rise more frequently compared with the FSH cells (Fig. 2-4B, C). Their simultaneous events occurred within 30 to 60 second periods. The FSH cells, on the other hand, tended to show less simultaneous events compared with that of LH cells (Fig. 2-4E, F). Interestingly, the FSH cells also showed short-interval spontaneous Ca^{2+} rises in individual cells (Fig. 2-4D), whereas there was no such pattern in the LH cells. In either LH or FSH cells, I did not observe characteristic GnRH-induced Ca^{2+} oscillations, which have been reported for the rat gonadotropes (65). I examined the effects of analog M, a GnRH receptor antagonist (70), on the spontaneous Ca^{2+} fluctuations in my preparation, but they were not completely diminished in either LH or FSH cells, even under high

analog M concentrations, in which neither LH nor FSH cells responded to exogenous application of mdGnRH peptide (data not shown).

GnRH receptor-mediated Ca^{2+} rise is mainly derived from the intracellular store

To examine the source of Ca^{2+} rise, I then performed experiments using various pharmacological agents. I first confirmed that three repetitive applications of GnRH did not significantly change the Ca^{2+} response amplitude in the identical preparation in both LH and FSH cells ($\Delta F/F_0$ in LH cells: 1st GnRH: 0.0286±0.0012, 2nd GnRH: 0.0285±0.0012 (P = 0.9979), 3rd GnRH 0.0281±0.0011 (P = 0.9424), n=105 [3], Fig. 2-5A; FSH cells: 1st GnRH: 0.0491±0.0029, 2nd GnRH: 0.0465±0.0031 (P = 0.7836), 3rd GnRH 0.0468±0.0035 (P = 0.8305), n=120 [4], Fig. 2-5E). Then, I compared the amplitude of GnRH responses in the presence of various receptor antagonists. First, I examined the effect of analog M to confirm that the GnRH-induced Ca^{2+} rise in LH and FSH cells is a GnRH receptor-mediated response. The mdGnRH responses in the presence of 5 μM analog M were severely diminished in both LH and FSH cells ($\Delta F/F_0$ in LH cells: 1st GnRH: 0.0270±0.0011, 2nd GnRH+analog M: 0.0075±0.0006 (P < 0.001), 3rd GnRH 0.0226±0.0006 (P < 0.001), n=135 [4], Fig. 2-5B; FSH cells: 1st GnRH:0.0308±0.0023, 2nd GnRH+analog M: 0.0112±0.0009 (P < 0.001), 3rd GnRH 0.0218±0.0017 (P < 0.001), n=96 [3], Fig. 2-5F), indicating that the responses are mediated by GnRH receptors. To determine whether GnRH-induced Ca^{2+} rise derived from the extracellular Ca^{2+} influx or Ca^{2+} release from the intracellular store, I next examined the GnRH effect in the presence of Cd^{2+}, a broad-spectrum voltage gated Ca^{2+} channel blocker. 100 μM $CdCl_2$ did not change the amplitude of mdGnRH response ($\Delta F/F_0$ in LH cells: 1st GnRH: 0.0208±0.0009, 2nd GnRH+$CdCl_2$: 0.0236±0.0010 (P = 0.0753), 3rd GnRH

0.0233±0.00010 (P = 0.1248), n=85 [3], Fig. 2-5C; FSH cells: 1st GnRH: 0.0593±0.0038, 2nd GnRH+$CdCl_2$: 0.0560±0.0031 (P = 0.7147), 3rd GnRH 0.0497±0.0032 (P = 0.0827), n=125 [3], Fig. 2-5G). As GnRH induces the release of Ca^{2+} from an inositol 1,4,5-triphosphate (IP_3)-sensitive store in the rat gonadotrope (66), I used 2-APB, an IP_3 receptor antagonist. 100 μM 2APB significantly decreased the amplitude of GnRH-induced Ca^{2+} rise in both LH and FSH cells ($\Delta F/F_0$ in LH cells: 1st GnRH: 0.0135±0.0007, 2nd GnRH+analog M: 0.0084±0.0005 (P < 0.001), 3rd GnRH 0.0134±0.0005 (P = 0.9819), n=78 [3], Fig. 2-5D; FSH cells: 1st GnRH: 0.0667±0.0043, 2nd GnRH+2APB: 0.0459±0.0034 (P < 0.001), 3rd GnRH 0.0582±0.0035 (P = 0.1997), n=109 [3], Fig. 2-5H).

Ca^{2+} rise in LH cells in response to the electrical axonal stimulation of GnRH1 neurons can be visualized

In the previous experiments, I stimulated gonadotropes using exogenous applications of GnRH peptide. By taking advantage of the whole brain-pituitary preparation, I next examined Ca^{2+} responses of LH cells by the electrical axonal stimulation of GnRH1 neurons. In medaka, vPOA GnRH1 neurons directly project to the pituitary by forming thick axon bundles (Fig. 2-6A and B). I used the *gnrh1:EGFP* x *lhb:IP* double transgenic medaka to visualize the GnRH1 axon bundles under the fluorescence microscopy. I recorded Ca^{2+} fluctuations from the LH cells while electrically stimulating unilateral GnRH1 fiber bundle with a mono-polar electrode placed on it (Fig. 2-6B). The electrical stimulation (500-μs pulses at +250 μA every 20ms for 20 trains) induced a Ca^{2+} rise in LH cells (Fig. 2-6C), the time course of which was similar to that induced by exogenous mdGnRH application (Fig. 2-3A). The averaged value of peak amplitude ($\Delta F/F_0$) was 0.0118±0.0007, and the average time to peak after stimulation was 52.3±2.27

seconds (n= 224 cells in 18 trial from 10 fish). Prior analog M treatment (5 μM) severely diminished the electrical stimulation-induced Ca^{2+} rise in LH cells (Fig. 2-6 C,D; $\Delta F/F_0$ in LH cells: 1st Stim.: 0.0071±0.0005, 2nd Stim.+analog M: 0.0023±0.0004 ($P < 0.001$), 3rd Stim. 0.0546±0.0005 ($P < 0.05$), n=33 [3], Fig. 2-6C, D). As the sensitivity to the GnRH peptide is different among individuals, I only analyzed data from the stimulation experiment with a complete set of three stimulations.

Discussion

GnRH-induced Ca^{2+} rise in LH and FSH cells can be visualized using the whole brain-pituitary preparation

GnRH was first found as a hypothalamic peptide that stimulates LH release. Just as the name indicates, GnRH has also been shown to stimulate FSH release in addition to LH release (72, 73). However, the mechanisms and properties of FSH release are not well understood in contrast to the great deal of knowledge in LH release. One of the reasons may be that LH and FSH are co-released from a single gonadotrope in mammals. To take advantage of the teleost pituitaries where LH and FSH cells are completely separate, I generated transgenic medaka lines that express a genetically encoded calcium indicator, IP, specifically in the FSH or the LH cells. Until now Ca^{2+} responses in LH cells (not the mammalian gonadotropes which co-express LH and FSH in the same cells) have been studied mainly in goldfish using Fura-2 or Indo-1 (31, 74-76), but there has been no report on the FSH cells. This is probably because of the difficulty of identifying FSH cells from the goldfish dispersed cell culture, because they distinguished the LH cells from the other pituitary cells only by their morphological features (77). The newly generated

transgenic medaka lines in the present Chapter allow us to identify LH and FSH cells by their fluorescence and to record cell type-specific Ca^{2+} responses separately using the whole brain-pituitary preparations in which the neural circuit and the pituitary cell network are kept intact.

GnRH-induced LH release and Ca^{2+} rise in gonadotropes have been well known from the studies in '90s using pituitary cell culture (63-66). GnRH-induced Ca^{2+} rise in the gonadotrope is accompanied by an increase in membrane capacitance, which indicates the occurrence of exocytosis (63-66). This suggests that GnRH-induced Ca^{2+} rise can be an index of the timing of hormone exocytosis from the gonadotropes. LH cells begin to respond to mdGnRH from around 30 nM in my Fura2 experiments (Fig. 2-1D, E). This concentration is rather higher than the other studies in the literature (around 0.01 nM in rat (slice) (78), 1 nM in goldfish and medaka (culture) (76, 79), 0.1 nM in catfish (culture) (80)). The difference seems to arise from the difference in the preparations. As the cells are not directly exposed to the solution in my whole brain-pituitary preparations, they need higher concentration than the other studies. However, I succeeded in detecting small but sufficient Ca^{2+} rise in LH cells by the electrical stimulation of GnRH1 neurons, which is expected to induce small amount of intrinsic GnRH release locally in the pituitary. Therefore, the effective concentration of 30 nM in the present experiment should be considered as a physiological concentration, and the present experiments are considered to represent what occurs *in vivo*. Moreover, the time course and the wave forms of Ca^{2+} response were similar to those induced in goldfish and African catfish LH cells in dispersed pituitary cell culture (74-76, 80). Note that examination of Fura2 based measurements in *lhb*:IP medaka failed to detect responses to GnRH in IP negative cells at least adjacent cells of IP positive cells. These results are consistent with the

fact that no report has shown the surface cells in adenohypophysis but LH cells express GnRH receptors.

In medaka, mdGnRH induced rapid, transient and non-oscillatory Ca^{2+} rise in LH cells. Previous studies in mice, rats and goldfish showed that GnRH induces Ca^{2+} responses in gonadotropes, which are broadly divided into two categories: oscillatory and non-oscillatory responses (64, 65, 76, 78). Unlike these studies, I only observed non-oscillatory Ca^{2+} rise in medaka LH cells, which has also been reported in catfish (80). The GnRH response curve obtained in medaka LH cells in the present study appears to be similar to the non-oscillatory response curve in mice (78).

I demonstrated for the first time that FSH cells also show GnRH receptor-mediated Ca^{2+} rise. In contrast to the LH cells, the GnRH-induced Ca^{2+} rise in FSH cells are slow and long-lasting. The responses in both LH and FSH cells are mediated by GnRH receptors, but their response curves were different from each other. There are some possible explanations. One is that both LH and FSH cells express GnRH receptors, but the difference in signaling cascade downstream of GnRH receptor activation may cause the difference in Ca^{2+} signaling. From the results of tilapia pituitary cell culture, it was suggested that *lhb* and *gpa* or *fshb* transcription were regulated by different signaling cascades downstream of GnRH receptor activation. *lhb* and *gpa* transcription were regulated by GnRH receptor-mediated signals coupled to both PKC-PKA and MAPK pathways, but FSH transcription was mainly regulated by PKA-CREB-CRE pathway (13, 81). However, this applies to the transcription but not the hormone release, and different signaling cascades may be recruited and cause the difference in GnRH-induced Ca^{2+} rise in LH or FSH cells. One of the other possibilities for the difference between LH

and FSH cells is presence/absence or the subtype expression of the regulators of G protein signaling (RGS) protein coupled to GnRH receptors. The RGS proteins interact with active Gα subunits and accelerate their intrinsic GTPase activity of Gα subunits leading to their deactivation and termination of downstream signals. The RGS proteins modify the amplitude and the time course of G protein signaling, including Ca^{2+} signaling, differently according to their subtypes (82). For example, RGS8 modulates both activation and deactivation of $G\alpha_{q/11}$-coupled receptors specifically and in a splicing variant-type dependent manner (83). At least, two family members, RGS3 and RGS10, are implicated in the regulation of GnRH receptor coupling (84). Therefore, LH and FSH cells may have the same signaling cascades that activate IP_3-induced Ca^{2+} release, but the time course of G $G\alpha_{q/11}$ subunit activation may be different because of the difference in the subtype of RGS proteins expressed in the LH and FSH cells. Medaka has three kinds of GnRH receptors, all of which are expressed in the pituitary and coupled with $G\alpha_{q/11}$ signaling pathway (58). However, their distribution in the pituitary and the existence of signaling cascades other than $G\alpha_{q/11}$ are still unknown. Therefore, LH and FSH cells may express different subtype of GnRH receptors, which may cause the difference in Ca^{2+} responses. Further studies should reveal differential regulation of LH and FSH cells.

The present results showed that the main source of GnRH-induced Ca^{2+} rise in both LH and FSH cells is the IP_3-sensitive intracellular Ca^{2+} store (see Fig. 2-5). Although the specificity of 2APB has not been reported to be high enough as a blocker of intracellular Ca^{2+} release, the combined results of my experiments using $CdCl_2$ to block the voltage-dependent influx should argue against the importance of Ca^{2+} influx. The GnRH signaling in gonadotropes has been well-studied in rat (65,

66). These studies showed that GnRH-induced Ca^{2+} rise did not depend on the extracellular Ca^{2+} but the IP_3-sensitive Ca^{2+} stores. Both the Ca^{2+} rise and the hormone release (increase in membrane capacitance) occur in Ca^{2+}-free solution (65). In teleosts, however, there are many contradictory results even in the same species. GnRH-induced gonadotropin release were attenuated by the use of Ca^{2+}-deficient medium or voltage gated Ca^{2+} channel inhibitors (tilapia (85); snakehead (86); goldfish (87)). Concerning the GnRH-induced Ca^{2+} rise in goldfish gonadotropes, extracellular Ca^{2+} was important for GnRH-induced Ca^{2+} rise (31), but in another study the authors showed that extracellular Ca^{2+} deprivation did not affect GnRH-induced Ca^{2+} rise (76). Johnson *et al.* (76), showed different results of the effect of extracellular Ca^{2+} on the GnRH-induced Ca^{2+} rise; treatment of Ca^{2+}-deficient medium or voltage-gated Ca^{2+} channel blockers for a long time may have depleted the intracellular Ca^{2+} store and changed the balance of Ca^{2+} homeostasis. They concluded that GnRH induced Ca^{2+} rise derived from the intracellular store but not from the extracellular Ca^{2+} influx in goldfish LH cells. In this respect, my results are in agreement with this goldfish study and the mammalian studies, and suggest the existence of similar signaling cascades in medaka LH cells. Recently, Strandabø *et al.* (79) reported on the LH cell-specific Ca^{2+} responses to GnRH2 peptide in a dissociated pituitary culture, using Fura-2 imaging with *lhb:EGFP* transgenic medaka. They observed both monophasic and biphasic Ca^{2+} changes evoked by GnRH2 and suggested that the intracellular Ca^{2+} mainly contributes to the first peak, and the extracellular Ca^{2+} contributes to the secondary peak. This apparent discrepancy between the results of Strandabø *et al.* (79) and my present study might be because of the difference in the molecular species of GnRH peptide used for the experiments, preparations, or properties of the

Ca^{2+} indicators. GnRH1 (present result) and GnRH2 (79), may induce different responses, because it has been reported that the signaling cascades to induce Ca^{2+} rise in goldfish dispersed LH cells are different between responses to GnRH2 and those to GnRH3 (reviewed in (74)). I performed GnRH2 peptide application experiments with LH and FSH transgenic fish, but I did not find significant difference in the shape of Ca^{2+} responses between GnRH1 (mdGnRH) and GnRH2 (cGnRH-II) peptides (data not shown). Although I did not perform statistical analysis, the Ca^{2+} responses to GnRH2 peptide tended to be stronger than to GnRH1 peptide. Okubo *et al.* demonstrated that GnRH2 peptide activates all three GnRH receptors more strongly than GnRH1 peptide, and my results are consistent with theirs (58, 59). Furthermore, Strandabø *et al.* used dissociated pituitary cells cultured for 2-7 days after dissociation and were loaded with Fura2-AM. The long-term cell culture may have changed the characteristics of the cells from those of *in vivo* pituitary cells. Other possibilities may include differences in binding and dissociation properties of each calcium indicator, Fura2 and inverse-pericam.

Detection of neural input-induced Ca^{2+} rise in LH cells

In the present study, I observed Ca^{2+} rise in LH cells induced by electrical stimulation of the unilateral GnRH1 axon bundle projecting to the pituitary. The shape and the time course of the response induced by the stimulation were similar to those by exogenous GnRH application, and the Ca^{2+} rise was diminished by GnRH receptor antagonist. These results indicate that electrical stimulation effectively evoked GnRH1 release from the axon terminals of the GnRH1 neurons in the pituitary and that the present preparation is sensitive enough to detect intrinsic GnRH-induced Ca^{2+} rises in the LH cells. It may be noted that the amplitude of the

Ca^{2+} responses induced by electrical stimulation was smaller than that by mdGnRH application (compare with Fig. 2-3C and Fig. 2-6D). There are several possibilities for this difference in the response amplitude. First, it is possible that stronger stimulation was needed to release substantial amount of GnRH peptide from the terminals of GnRH1 neurons. To avoid direct electrical stimulation of LH cells, however, I unfortunately could not use stimulation stronger than +250 μA. Second, I used unilateral electrical stimulation to the GnRH fiber bundle, which may have stimulated only some of the GnRH fibers to result in much weaker Ca^{2+} responses compared with the bath application of GnRH solution. In any case, I here demonstrated for the first time that GnRH neurons actually release GnRH peptides in the pituitary to stimulate the gonadotropes. Furthermore, these results indicate that my transgenic models can be used to analyze not only the direct exogenous input to gonadotropes but also the inputs that are mediated by neural activity in the brain. Next, it should be interesting to reveal the relationship between the electrical activity pattern of GnRH1 neurons and LH release.

I also observed spontaneous Ca^{2+} fluctuations in both LH and FSH cells (Fig. 2-4). LH cells in some preparations showed synchronized small Ca^{2+} fluctuations, which may indicate synchronized neural input to the LH cells or electrical synchronization among the LH cells. The FSH cells showed sufficiently large spontaneous responses compared to the responses stimulated by mdGnRH. Spontaneous Ca^{2+} fluctuation tended to be reduced under analog M treatment but did not completely diminished in both LH and FSH cells (data not shown). This suggests that LH and FSH cells receive inputs from unidentified neurons in addition to GnRH neurons. There are some examples that also suggest the importance of cellular integrations in the pituitary. For example, gonadotropes and

somatotropes are reported to regulate gonadotropin and GH release and transcription each other via autocrine/paracrine release of gonadotropin and GH in grass carp (88). This means that dissociation of pituitary cells may have changed their environment, leading to a change in their gene expression patterns or their activities. Therefore, it is important to keep the networks in the pituitary almost intact for precise analysis. In this respect, my transgenic model should be a powerful tool to study the neural and humoral regulatory mechanisms of LH and FSH release in detail by taking advantage of the whole brain-pituitary *in vitro* preparation.

In summary, I generated transgenic medaka lines that express Ca^{2+} indicators specifically in LH or FSH cells and succeeded for the first time in recording different patterns of Ca^{2+} rises triggered by GnRH in LH and FSH cells separately. This is a remarkable experimental system which allows us to maintain the axonal projections of the GnRH neurons to the pituitary intact by taking advantage of the features of a small teleost brain and pituitary. This model system allows us to analyze the multi-synaptic neuronal circuitry regulating the pituitary functions. Particularly, I should be able to analyze the regulatory mechanisms of FSH release, which has been less intensively studied to date. It should be an exciting in the future to study the neuroendocrine mechanisms of HPG axis regulation, which may include novel regulators of gonadotropin secretion, especially FSH.

Figure legends

Figure 2-1

Ca^{2+} imaging from the whole brain-pituitary preparation using Fura2.

(A) A schematic illustration of medaka pituitary. Left, the whole pituitary seen from the ventral side. The area of gonadotropes is shown in purple. Right, frontal section of the pituitary. The LH and FSH cell layers are shown in pink and blue, respectively. The dotted white square indicates the recording area in Fura2 imaging. (B) Schematic illustration of the experimental setup for Ca^{2+} imaging. (C) Representative Ca^{2+} response to 100 nM mdGnRH from unidentified pituitary cells. Each trace from 15 cells is shown in thin gray lines, and averaged trace from 15 cells is shown in a thick black line. (D) Representative dose responses from an identical preparation. (E) Dose response relationship between mdGnRH peptide concentration and the maximum amplitudes of the Ca^{2+} rise. R, rostral; C, caudal; D, dorsal; V, ventral

Figure 2-2

Generation of transgenic medaka lines.

(A) The gene constructs for the transgenic medaka expressing inverse-pericam (IP) under the control of *lhb* or *fshb* promoters. (B, C) LHβ and FSHβ cell-specific expressions of IP in *lhb:IP* and *fshb:IP* transgenic medaka, respectively. The left pictures show the ventral view of the pituitary of *lhb:IP* and *fshb:IP* transgenic medaka. The white dashed lines indicate the boundaries of the pituitaries. (Scale bar: 50 μm) The right pictures show the frontal sections of the pituitary. Magenta, *lhb/fshb* mRNA ISH; green, EGFP IHC for IP labeling. (Scale bar: 25 μm) (D)

Double IHC for LHβ (magenta) and EGFP (green) in the pituitary of *gnrh1:EGFP* transgenic medaka. The white dashed lines indicate the boundaries of the pituitaries. (Scale bar: 20 μm) (E) Double IHC for FSHβ (magenta) and EGFP (green) in the pituitary of *gnrh1:EGFP* transgenic medaka. (Scale bar: 20 μm) R, rostral; C, caudal

Figure 2-3

LH cells and FSH cells show different Ca^{2+} responses to mdGnRH.

(A,B) Representative traces of Ca^{2+} responses to mdGnRH in *lhb:IP* or *fshb:IP* transgenic medaka. The right graphs show traces from 10 cells (thin gray lines) and averaged trace (thick black line). The left pictures show the analyzed cells (the red circles indicate ROI) corresponding to the right graphs. (Scale bar: 50 μm) Moving average was applied to the traces for every three points. (C, D) The peak amplitudes of responses to vehicle and 50 nM mdGnRH applications in LH cells (C) and FSH cells (D). (E) Time to 50% rise in response to 50 nM mdGnRH application in LH and FSH cells. The LH cells showed significantly quicker Ca^{2+} rise than the FSH cells. ***, $P < 0.001$. R, rostral; C, caudal

Figure 2-4

Spontaneous Ca^{2+} fluctuations in LH and FSH cells.

(A-C) Representative data for spontaneous Ca^{2+} fluctuations in 23 LH cells, indicating simultaneous oscillation of spontaneous Ca^{2+} fluctuations among them. (A) Representative spontaneous traces from the same recording. The detected Ca^{2+} peaks were marked by asterisks. (B) Raster plot of the timing of Ca^{2+} peaks. The shadowed areas correspond to the area including 5 seconds before and after the

peak time detected in (C). (C) Percentage of cells showing Ca^{2+} rise events simultaneously (gray: raw trace, black: 3-point moving averaged trace). Simultaneous Ca^{2+} peaks detected by the analysis are marked by asterisks. (D-F) Representative data for spontaneous Ca^{2+} fluctuations in 35 FSH cells similar to those in (A-C). Asterisks indicate the peaks detected by analysis.

Figure 2-5

GnRH receptor mediated-Ca^{2+} rise is derived from IP_3-sensitive Ca^{2+} store and not from extracellular Ca^{2+} influx in both LH cells and FSH cells.

(A, E) The peak amplitude in repetitive three 50 nM mdGnRH applications in LH cells (A) and FSH cells (E). (B, F) The peak amplitude in 50 nM mdGnRH during 5μM analog M application in LH cells (B) and FSH cells (F). (C, G) The peak amplitude in 100 nM mdGnRH during 100μM $CdCl_2$ application in LH cells (C) and FSH cells (G). (D, H) The peak amplitude in 100 nM mdGnRH during 100 μM 2APB application in LH cells (D) and FSH cells (H). ***, $P < 0.001$.

Figure 2-6

Release of intrinsic GnRH by stimulating GnRH neuron axons induces Ca^{2+} rise in LH cells.

(A) Morphological evidence that vPOA GnRH1 neurons directly project to the LH cells in the pituitary. (a) Schematic illustration of medaka whole brain from the ventral side. The blue square in (a) is magnified in (b). (b) Enlarged view of the POA and pituitary of *gnrh1*:EGFP transgenic medaka, indicating that GnRH1 fibers (white arrowheads) directly project to the pituitary LH cell area (green fibers in the pituitary). (c) Magnified view of the pituitary in (b). For the axonal stimulation of

GnRH1 neurons, I placed a stimulation electrode on the bundle of *gnrh1:EGFP* axons at the yellow arrowhead. (B) Schematic illustration of the experimental setup for the electrical stimulation and Ca^{2+} imaging. I placed the electrode (black triangle) right on the entry of the GnRH1 fiber bundle into the pituitary. The pink area in the pituitary indicates the LH cell area. I recorded Ca^{2+} response from PPD (gray dashed square on the right figure). (C) Representative example of Ca^{2+} responses after electrical axonal stimulation of GnRH1 neurons. The arrows indicate the timing of electrical stimulation. Each graph shows traces from 12 cells (thin gray line) and an averaged trace (thick black line). The moving average was applied to the traces for every three points. (D) The peak amplitude in three times of repetitive GnRH1 fiber stimulations in the LH cells. Five μM analog M was used as an antagonist for GnRH receptor. ***, $P < 0.001$ and *, $P < 0.05$.

Figure 2-1

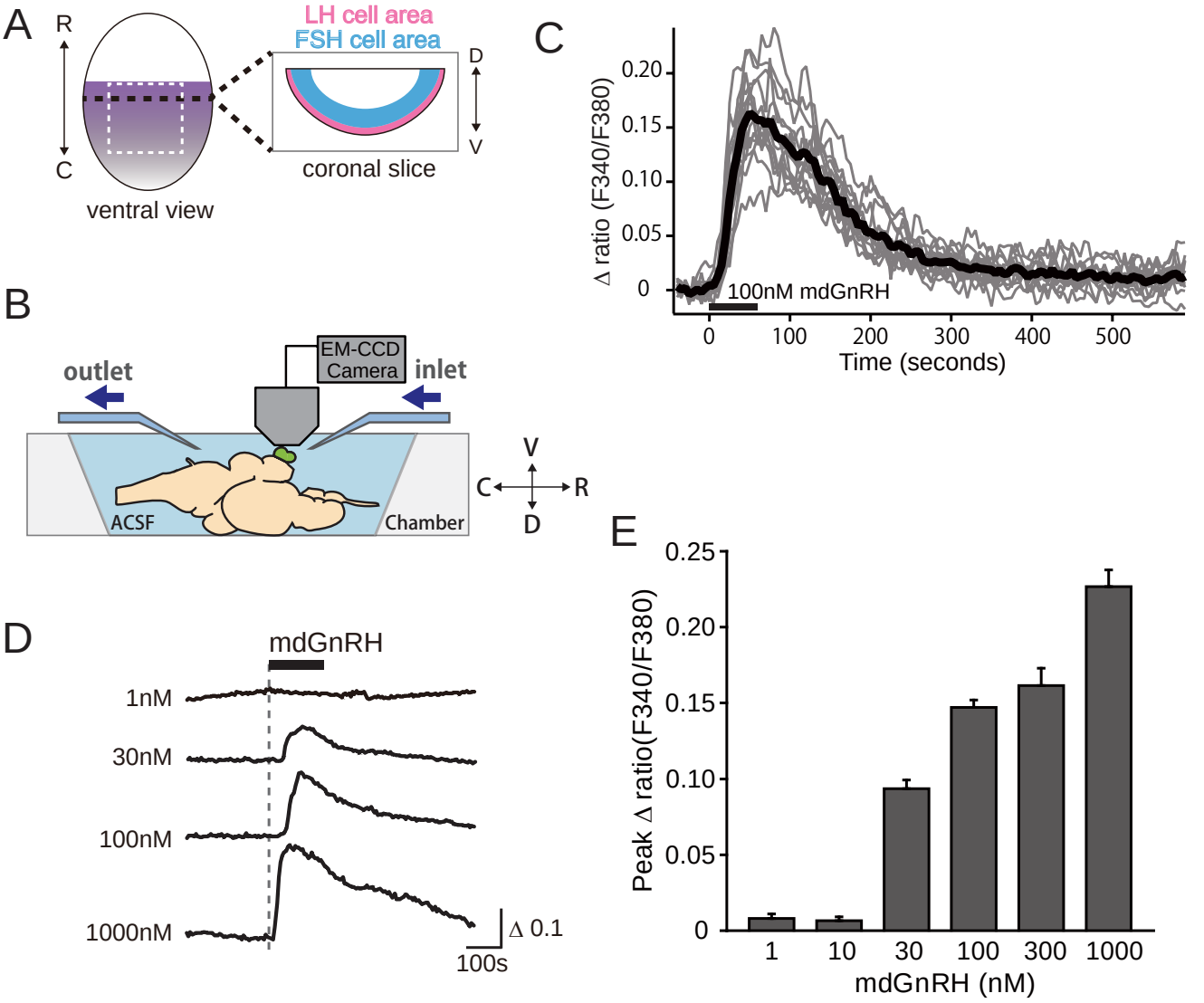
A
R
C
ventral view
LH cell area
FSH cell area
D
V
coronal slice
B
outlet
EM-CCD Camera
inlet
ACSF
Chamber
V
C
R
D
C
Δ ratio (F340/F380)
0.20
0.15
0.10
0.05
0
100nM mdGnRH
0
100
200
300
400
500
Time (seconds)
D
mdGnRH
1nM
30nM
100nM
1000nM
Δ 0.1
100s
E
Peak Δ ratio(F340/F380)
0.25
0.20
0.15
0.10
0.05
0
1
10
30
100
300
1000
mdGnRH (nM)

Figure 2-2

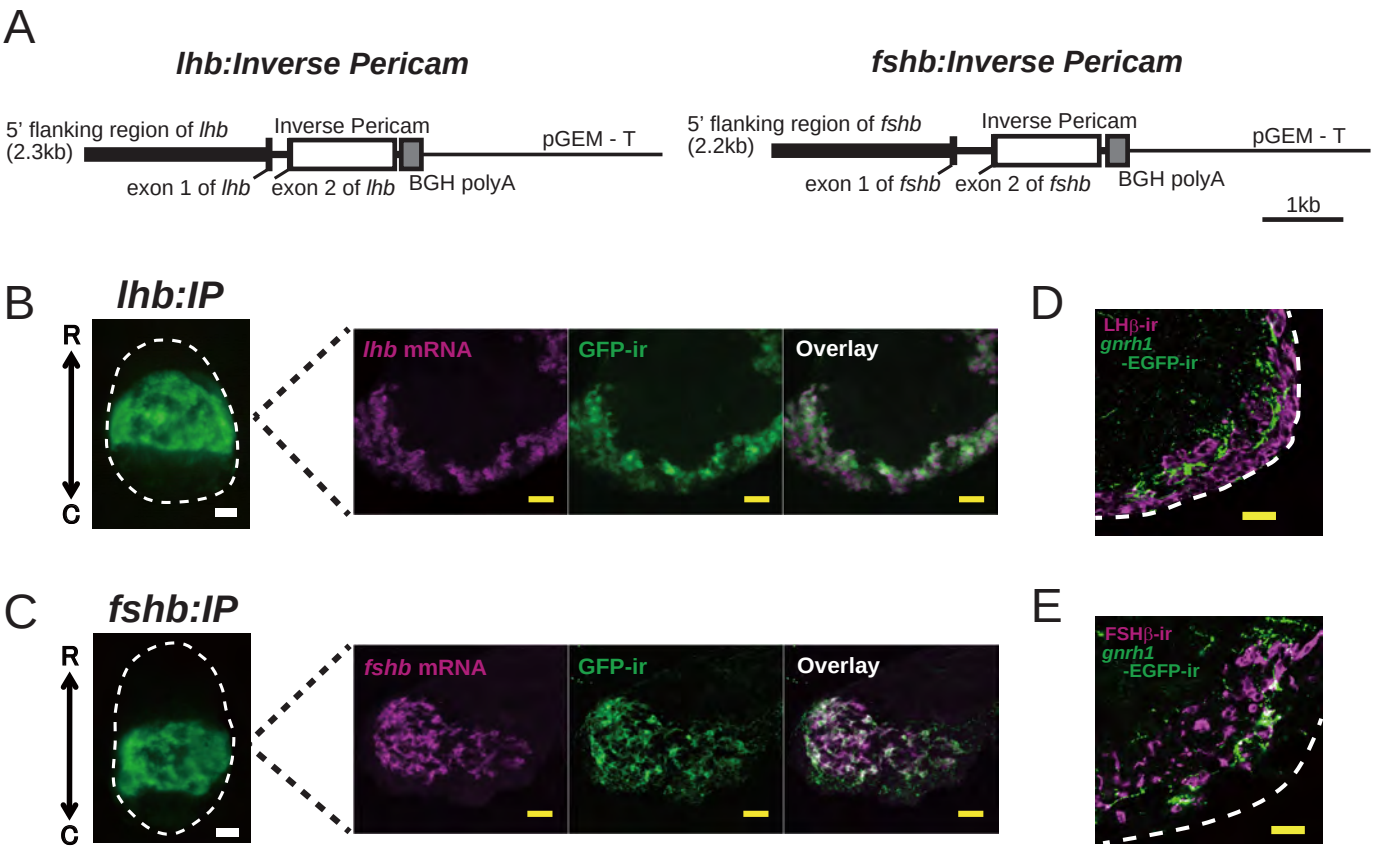
A
lhb:Inverse Pericam
5' flanking region of lhb
(2.3kb)
Inverse Pericam
pGEM - T
exon 1 of lhb
exon 2 of lhb
BGH polyA
fshb:Inverse Pericam
5' flanking region of fshb
(2.2kb)
Inverse Pericam
pGEM - T
exon 1 of fshb
exon 2 of fshb
BGH polyA
1kb
B
lhb:IP
R
C
lhb mRNA
GFP-ir
Overlay
C
fshb:IP
R
C
fshb mRNA
GFP-ir
Overlay
D
LHβ-ir
gnrh1
-EGFP-ir
E
FSHβ-ir
gnrh1
-EGFP-ir

Figure 2-3

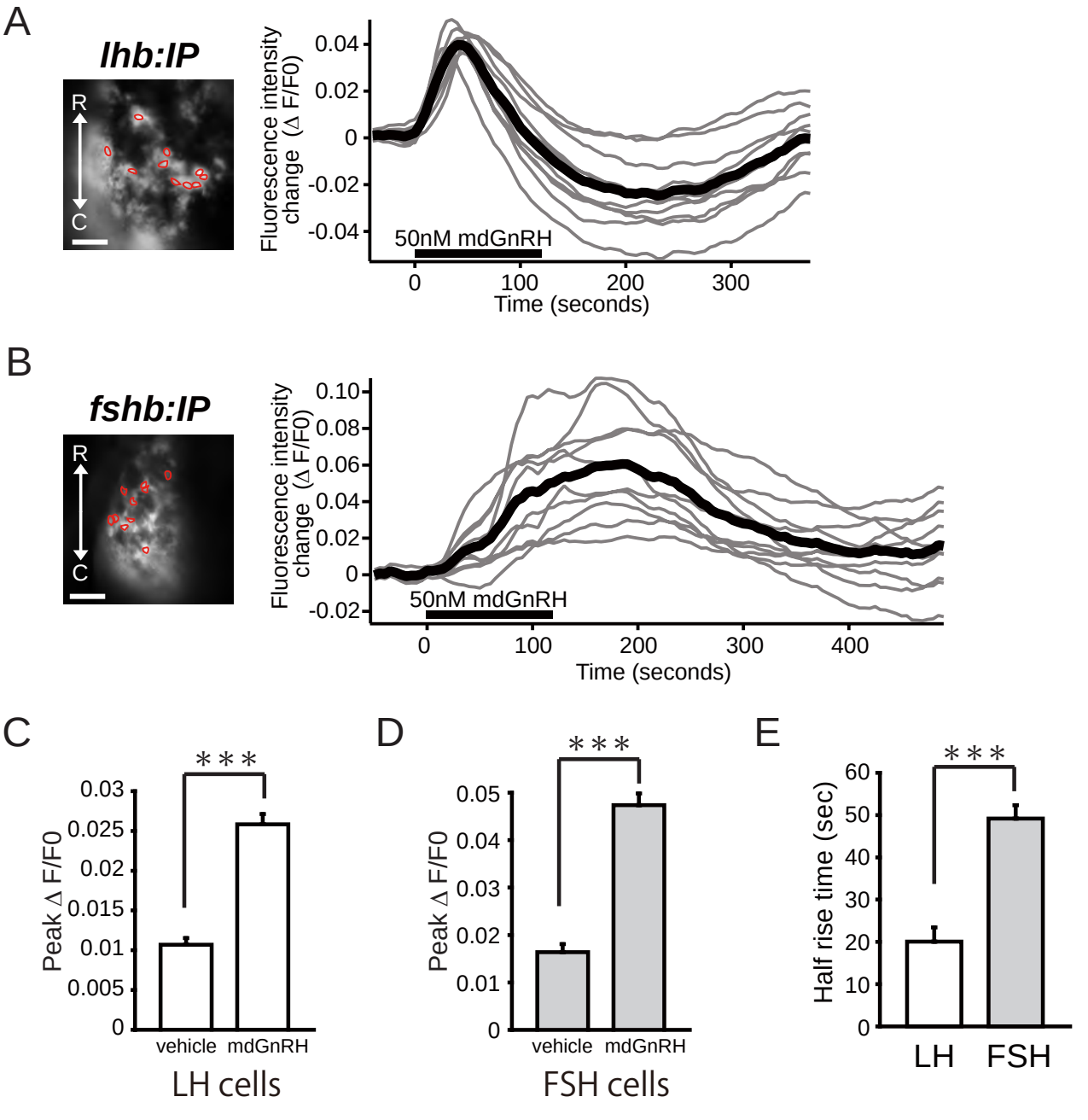
A
lhb:IP
R
C
Fluorescence intensity change (Δ F/F0)
0.04
0.02
0
-0.02
-0.04
50nM mdGnRH
0
100
200
300
Time (seconds)
B
fshb:IP
R
C
Fluorescence intensity change (Δ F/F0)
0.10
0.08
0.06
0.04
0.02
0
-0.02
50nM mdGnRH
0
100
200
300
400
Time (seconds)
C
***
Peak Δ F/F0
0.03
0.025
0.02
0.015
0.01
0.005
0
vehicle
mdGnRH
LH cells
D
***
Peak Δ F/F0
0.05
0.04
0.03
0.02
0.01
0
vehicle
mdGnRH
FSH cells
E
***
Half rise time (sec)
60
50
40
30
20
10
0
LH
FSH

Figure 2-4

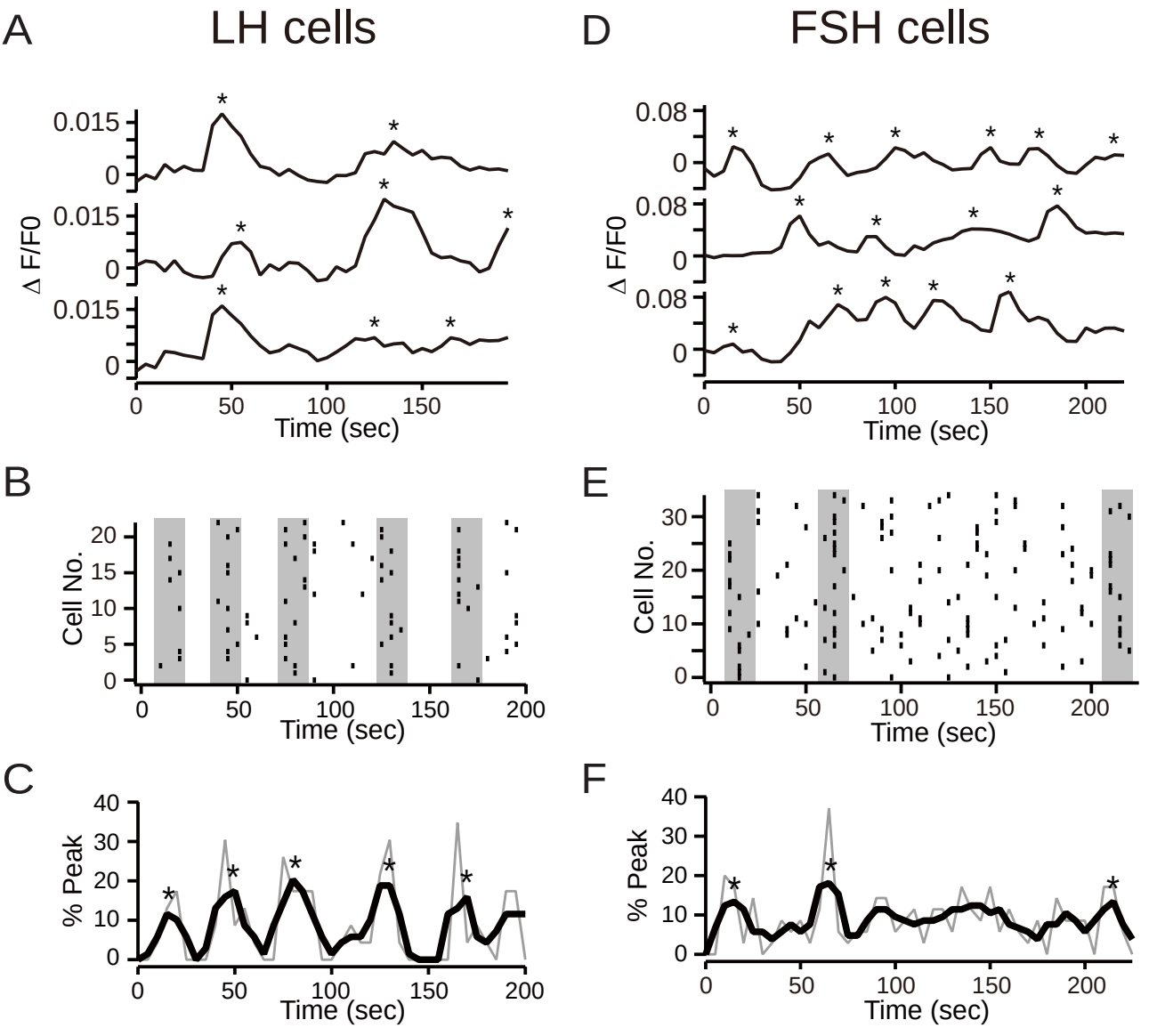

Figure 2-5

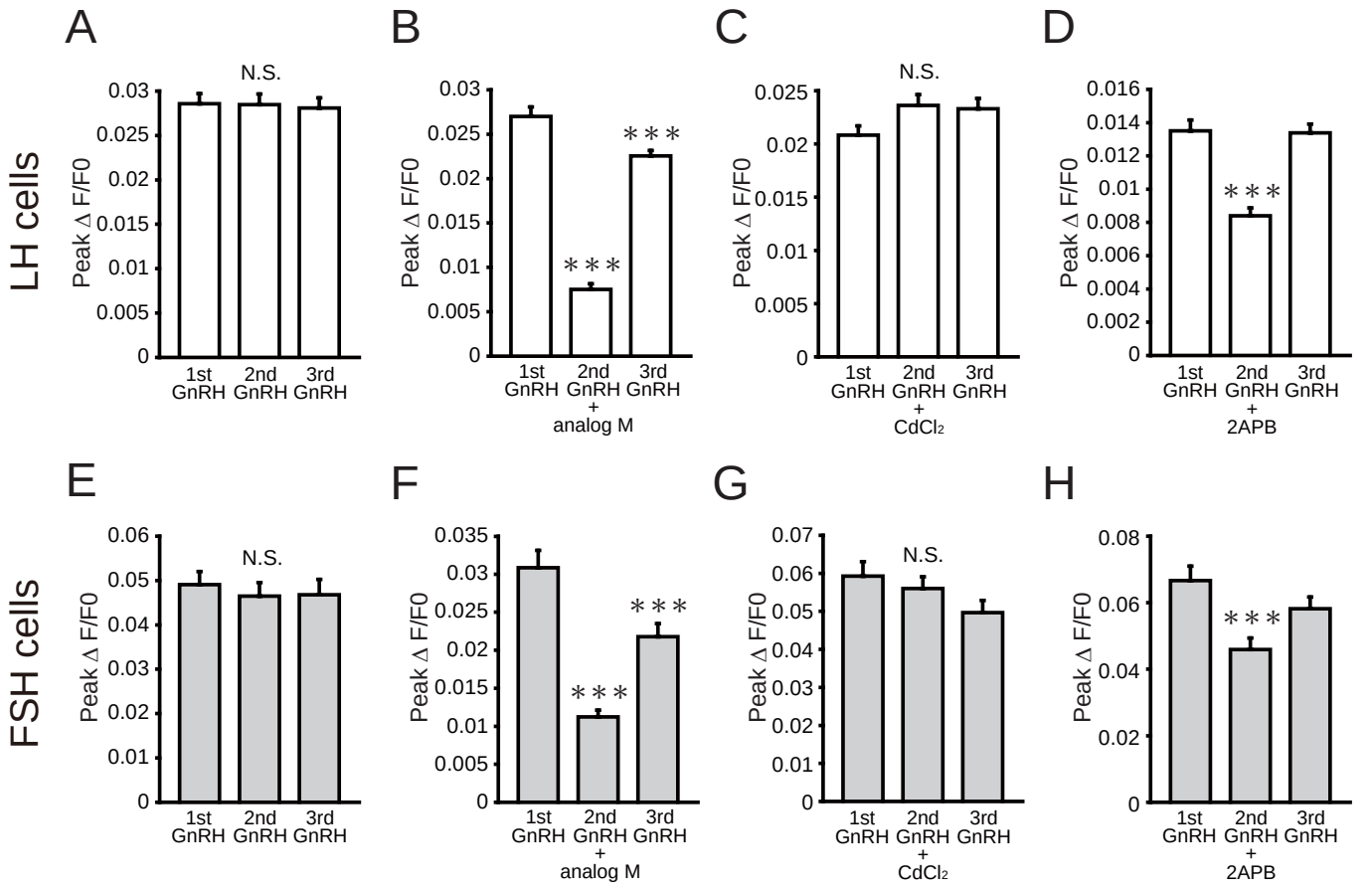
LH cells
FSH cells
A
B
C
D
E
F
G
H
N.S.
***
Peak Δ F/F0
1st GnRH
2nd GnRH
3rd GnRH
2nd GnRH + analog M
2nd GnRH + CdCl2
2nd GnRH + 2APB

Figure 2-6

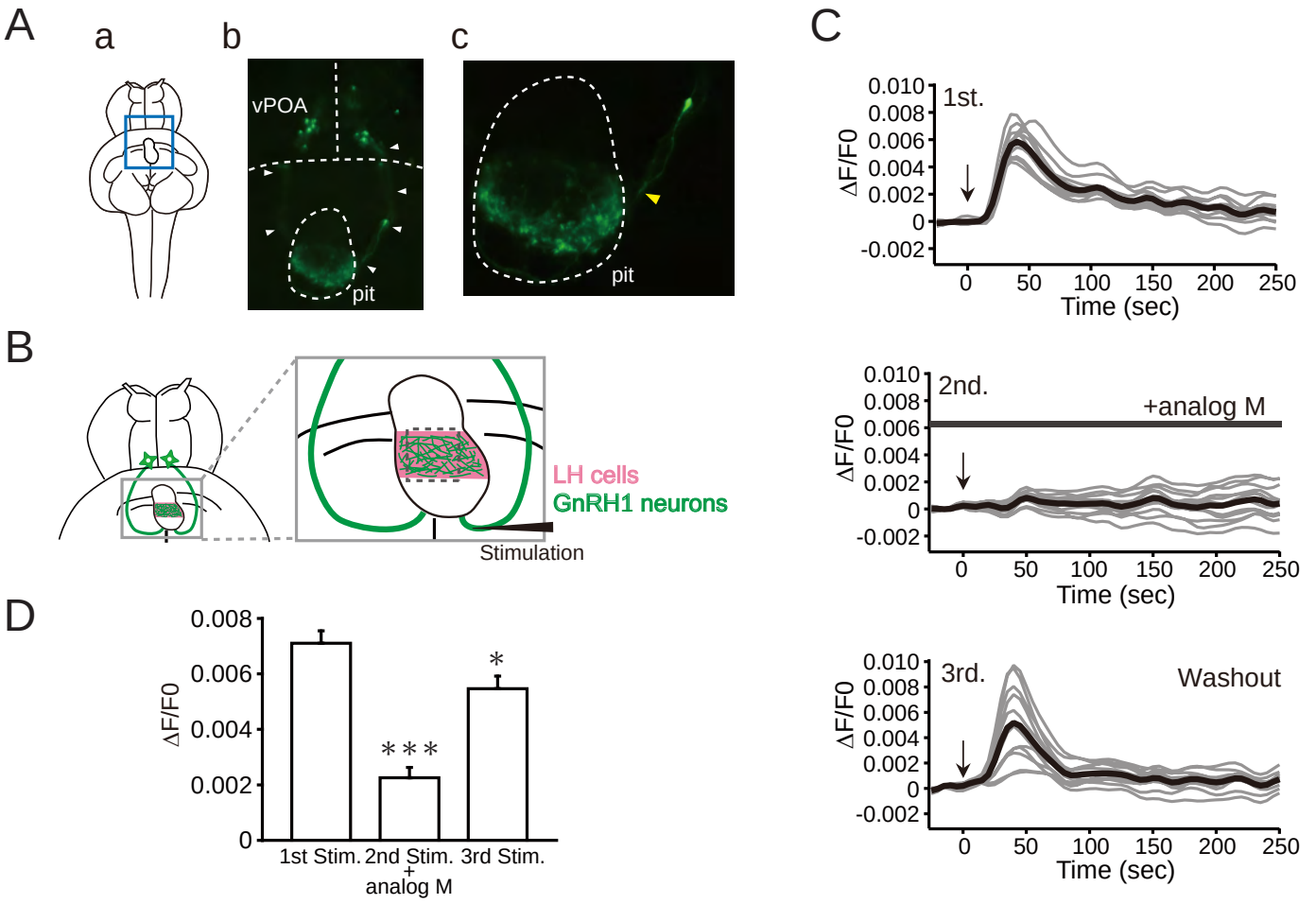
A
a
b
c
vPOA
pit
pit
B
LH cells
GnRH1 neurons
Stimulation
C
1st.
2nd.
+analog M
3rd.
Washout
ΔF/F0
0.010
0.008
0.006
0.004
0.002
0
-0.002
0
50
100
150
200
250
Time (sec)
D
ΔF/F0
0.008
0.006
0.004
0.002
0
* * *
*
1st Stim.
2nd Stim. + analog M
3rd Stim.

Chapter 3

Identification of the Regulator of GnRH1 Neurons in Some Teleosts

Abstract

Hypophysiotropic GnRH neurons are known to constitute the final common pathway for hypothalamic-pituitary-gonadal axis regulation in vertebrates by inducing LH release from the pituitary. During adaptation to environment, GnRH neurons are considered to alter their firing activity in accordance with external environments and endocrine conditions, for example nutritional conditions, state of sexual maturation, and the day length. However, only a few neuronal inputs to GnRH1 neurons have been identified, and the neural mechanisms of such regulation have not been fully understood. To search for the neuroendocrine mechanisms for regulating reproduction according to the environmental and internal states in vertebrates, I analyzed the neural inputs to the GnRH1 neurons.

First, I focused on the neuropeptide kisspeptin, which is known as a potent activator of GnRH1 neuron activity in mammals. Intraperitoneal (i.p.) and intracerebroventricular (i.c.v.) administration of kisspeptin *in vivo* did not induce plasma LH elevation or ovulation in sexually matured female goldfish. Moreover, electrophysiological experiments showed that kisspeptin did not change the firing frequency of GnRH1 neurons in medaka. Next, I focused on a monoamine neurotransmitter dopamine, which has been suggested to have inhibitory effects on the HPG axis. I found close appositions between dopaminergic fibers and GnRH1 cell bodies in the ventral POA (vPOA) and the dopaminergic fibers intertwined with the GnRH fibers in the pituitary. I also demonstrated electrophysiologically that dopamine inhibits neural activity of GnRH1 neurons. In addition, I found that dopamine neurons also show direct projections to LH and FSH cells in the pituitary.

These results suggest that there are common and different components of the

HPG axis regulation between mammals and teleosts; dopamine acts as an inhibitor of HPG axis in both teleosts and mammals, whereas kisspeptin may not be involved in the HPG axis regulation in teleost fish, unlike the previous reports in mammals.

Introduction

The regulators of GnRH1 neuron activities are rather well studied in mammals (reviewed in (49, 51)) but are poorly understood in non-mammalian species. In teleost fish, most of the studies of the HPG axis regulation have been assessed by measuring serum hormone concentrations, and the number of neurobiological studies is quite small. Some candidates have already been suggested as regulators of GnRH1 neuronal activities, especially in the goldfish (89, 90). However, all of these previous results are based on pharmacological studies that measured the amount of GnRH1 peptide released into the serum after injection of drugs to the whole animal, or that released into the culture media or that remaining in the tissue after treating fragments of the pituitary or brain slices with drugs. Although these previous studies may be suggestive for understanding the HPG axis regulation mechanisms in teleost fish, the detailed neuroendocrine regulatory mechanisms, for example, the actual action site of these candidates and the mode of actions on the GnRH1 neuronal activities are still controversial. In this chapter, I focused on two factors, a neuropeptide kisspeptin, which is a candidate for the activator of the HPG axis in mammals, and a monoaminergic neurotransmitter dopamine, which is a candidate of inhibitor of the HPG axis.

First, I examined the effects of kisspeptin. In the last decade, a peptide called kisspeptin, a hypothalamic peptide coded by *Kiss1* gene, has been attracting much attention as a powerful activator of GnRH1 neuron activities in mammals (reviewed in (91)). It has been reported in many mammals, that the kisspeptin receptor, GPR54, is expressed on the GnRH1 neurons, and kisspeptin evokes a conspicuous long-lasting depolarization in >90% of GnRH1 neurons (92), which leads to the

increased release of GnRH and thus strongly stimulates LH release from the pituitary (93-95). It has recently been found that the teleosts possess two paralogous kisspeptin genes, *kiss1* and *kiss2*, and two subtypes of receptors, *gpr54-1* and *gpr54-2* (96, 97). There have also been some studies showing that i.p. administration of kisspeptin increased the release or transcription of gonadotropins or GnRH1 in some fish species (98-101). However, recent studies using specific *in situ* hybridization for *gpr54* in teleosts show that the GnRH1 neurons do not express Gpr54 (102-104), and there has not been any solid evidence for the positive involvement of kisspeptin in the HPG axis regulation in teleosts. Therefore, I examined the possibility of both direct and indirect involvement of kisspeptin on the HPG axis regulation in teleosts. First I examined the *in vivo* effect of kisspeptin on the LH secretion and induction of ovulation. I used the goldfish for these experiments because of the large body of information about reproductive neuroendocrinology and the convenient size for experiments, especially i.p. and i.c.v. administration of drugs. Goldfish is a seasonal breeder, and a method for keeping them sexually mature and that for inducing ovulation followed by radioimmunoassay (RIA) measurement of serum LH concentration have already been established by previous studies (105-108). Next, I examined the effects of kisspeptin on the activity of GnRH1 neurons by using electrophysiological methods in a *gnrh1:EGFP* transgenic medaka.

In Section II, I focused on the roles of dopamine on the HPG axis regulation. The inhibitory effects of dopamine on the HPG axis have been implicated from previous studies, especially in sheep (Reviewed in (109)). A14/A15 dopaminergic neurons in the hypothalamus has been identified, which are considered to be involved in the control of seasonal breeding cycle and of LH pulse frequency in sheep (110-112), and

these neurons are now estimated to regulate the HPG axis via kisspeptin neurons (113). Most of these studies in sheep have been performed pharmacologically *in vivo,* and a detailed study at the cellular level has not yet been done to date. Recently, direct inhibitory effect of dopamine was shown by an electrophysiological study in mice (114). In teleosts, the importance of dopaminergic inhibition in the HPG axis regulation is also known. For example, injections of GnRH analog can induce ovulation only when dopaminergic inhibition was removed by dopamine antagonist in goldfish and eel (106, 115). The other studies in the goldfish suggested that dopamine or dopamine agonist treatment inhibits GnRH and LH release, and dopamine may act on both GnRH1 neurons and gonadotropes in the pituitary. However, action sites and mechanisms of dopaminergic inhibition remain unclear, because these previous studies used whole animal or brain/pituitary slices, and analysis at the cellular level has not yet been performed. In the present thesis, I examined involvement of dopamine in the HPG axis regulation by immunohistochemistry and electrophysiology, focusing on GnRH1 neurons and the pituitary.

Materials and Methods

Section I: Analysis of the effect of kisspeptin on the HPG axis regulation

Animals

For the *in vivo* kisspeptin administration experiments, I used sexually matured female goldfish (*Carassius auratus*). Adult goldfish were purchased from a local dealer in Tokyo at the end of autumn and were kept in a large tank under a 14-hour light and 10-hour dark photoperiod (light on at 8:00 and light off at 22:00) at water

temperature of 12°C at least two weeks before use in the experiments. The goldfish were fed trout pellets once or twice a day. For the electrophysiological experiments, I used *gnrh1:EGFP* (7) transgenic medaka. All the medaka were maintained in pairs under a 14-hour light and 10-hour dark photoperiod (light on at 8:00 and light off at 22:00) at water temperature of 27°C. We used sexually matured female and male medaka that spawned for at least three consecutive days. The medaka were fed two to three times a day with live brine shrimp and flake food. All animals were maintained and used in accordance with the Guidelines of the University of Tokyo for the Use and Care of Experimental Animals.

In vivo administration of drugs

LHRH-A (synthetic Luteinizing Hormone-Releasing Hormone analog; [des-Gly^{10}, D-Ala^{6}]-LH-RH ethylamide acetate salt hydrate) was dissolved in a fish saline (0.7% NaCl solution; plasma Na^+ and Cl^- ion concentration in carp (*Cyprinus carpio*) (116) and goldfish (control condition in (117)) is around 120 mM) and was injected i.p. (0.1μg/g body weight (BW)). Pimozide (PIM) was suspended in a vehicle of 0.7% NaCl with 0.1% sodium metabisulfite and was injected i.p. at 10μg/g BW. The control groups were given an equivalent volume of saline and/or the PIM vehicle. The decapeptide of medaka Kiss1 (Kiss1-10: YNLNSFGLRY-NH_2, believed to be the core peptide sequence for its physiological function) and the dodecapeptide of medaka Kiss2 (Kiss2-12: SKFNYNPFGLRF-NH_2) were synthesized (Sigma-Aldrich Japan, Tokyo, Japan; Bonac Corporation, Kurume, Japan, respectively). Synthetic Kiss1-10 and FTM145 (4-fluorobenzoyl-Phe-Gly-ψ[(*E*)-CH=CH]-Leu-Arg-Trp-NH_2; GPR54 agonist (118-121) gift from Dr. Shinya Oishi, Kyoto University) was dissolved in saline and injected i.p. (0.1 μg or 1 μg/g BW) or i.c.v. (0.1nmol).

Synthetic Kiss2-12 was first dissolved in DMSO and was diluted with saline (0.02% DMSO in final concentration) and was injected i.p. (0.1 μg /g BW) or i.c.v. (0.1 nmol). In the experiments, the animals were divided into three groups; 1) those receiving i.p. administration on a short time scale, 2) those receiving i.p. administration on a long time scale, and 3) those receiving i.c.v. administration. The ovulation was confirmed by the release of a stream of ripe translucent oocytes from the ovipore following application of a slight pressure to the abdomen (105). In Group 1 (i.p. administration of a long time scale), PIM was injected 12 hours prior to the co-injection of peptide and PIM (0hr) according to the previous study in goldfish using LHRH-A (106), and the blood was sampled just before the first injection of PIM (-12hr), 24 hours and 48 hours after peptide injection (Fig. 3-2A). In Group 2 (i.p. administration of a short time scale), PIM was injected three hours prior to the co-injection of peptide and PIM according to the previous study in goldfish using kisspeptin (100), and the blood was sampled just before the injection of peptide and PIM (0hr), two hours and six hours after that (Fig. 3-3A). In Group 3 (i.c.v. administration), PIM was injected i,p, 12 hours prior to the i.c.v. injection of peptide (0hr), and the blood was sampled just before the first injection of PIM (-12hr), just before the injection of peptide (0hr), 0.5 hour and 3 hours after peptide injection. In all experiments, ovulation was checked until three days after the peptide injection (Fig. 3-4A).

Blood sampling and radioimmunoassay (RIA)

The blood samples were taken from the caudal vasculature with a heparinized syringe and needle according to the above-mentioned schedules. The blood samples were centrifuged at 3,000 g, and the plasma was stored at -20°C until the assay. The

plasma LH concentrations were determined by a double antibody radioimmunoassay (RIA) using a silver carp GtH RIA (107), which measures glycoprotein GtH. The present RIA system has been validated for the goldfish by obtaining parallelism for serial dilutions of plasma samples collected from ovulated females (108).

Luciferase Assays

The luciferase assay experiments were performed as described previously (103). The cDNA fragments containing full-length open reading frames of *gpr54-1* and *gpr54-2* were subcloned into the expression vector pcDNA3.1 (Invitrogen). COS-7 cells were grown on 24-well plate at 37°C in Dulbecco's modified Eagle's medium (DMEM), supplemented with 10% fetal bovine serum. The plasmid DNAs (100 ng/well) were transfected into monolayer culture cells with either pSRE-Luc or pCRE-Luc (100 ng/well; Clontech, Palo Alto, CA), and pRL-CMV containing the Renilla luciferase reporter gene (2.5 ng/well; Promega, Madison, WI), using Lipofectamine LTX (Invitrogen). The cells were maintained in a serum-free medium for 24 hours. After that, they were incubated with various concentrations (from 0 to 10^{-6} M) of medaka Kiss1, Kiss2, or FTM145 for six hours and then harvested and analyzed. Luciferase activity in the cell extract was measured using Dual-Glo Luciferase Assay System (Promega) with Lumat LB9507 (EB & G Berthold, Bad Wildbad, Germany). The transfection experiments were performed in more than triplicate and were repeated at least three times.

Electrophysiology

For the electrophysiological analysis, I used a *gnrh1:EGFP* transgenic medaka line

(7). The fish were anesthetized by immersion in tricaine methanesulfonate (dissolved 0.02% in tap water) and then decapitated. Targeted single-unit extracellular loose-patch recordings were performed using *in vitro* whole-brain preparations as previously described (7).

Data analysis

All values are shown as mean ± SEM. For the analysis of plasma LH levels, Dunnet's multiple comparison tests were performed for the average concentration level for each time period (significance levels were < 0.05). For electrophysiological experiments, the number of action currents for one minute was counted. The number of action currents from two minutes to one minute before Kiss1-10 application were counted as "Before", from one minute to two minutes after the start of Kiss1-10 application as "During", and from five minutes to six minutes after the start of washout as "Washout". The relative firing rate were calculated by dividing each number of action currents by that of "Before". Steel's multiple comparison tests were performed for the comparison of relative firing rate (significance levels were < 0.05).

Section II: Analysis of the effect of dopamine on the HPG axis regulation

Animals

For the electrophysiological and morphological experiments, I used male and female wild type drR medaka (*Oryzias latipes*) and transgenic medaka (*gnrh1:EGFP* (7), *lhb:inverse-pericam (IP)*, and *fshb:IP* (39)). All the medaka were maintained in pairs under a 14-hour light and 10-hour dark photoperiod (lights on at 8:00 and lights off at 22:00) at water temperature of 27°C. We used sexually mature female

and male medaka that spawned for at least three consecutive days. The medaka were fed two to three times a day with live brine shrimp and flake food. All the animals were maintained and used in accordance with the guidelines of the University of Tokyo for the Use and Care of Experimental Animals.

Electrophysiology

For the electrophysiological analysis, I used a *gnrh1:EGFP* transgenic medaka line (7). Fish were anesthetized by immersion in tricaine methanesulfonate (dissolved 0.02% in tap water) and then decapitated. Targeted single-unit extracellular loose-patch recordings were performed in *in vitro* whole-brain preparations as previously described (7). Dopamine Hydrochloride was purchased from Funakoshi (Tokyo, Japan) and was dissolved into water.

Data analysis

All the values are shown as mean ± SEM. For electrophysiological experiments, the number of action currents for one minute was counted. The number of action currents from two minutes to one minute before DA application were counted as "Before", from 0.5 minutes to 1.5 minutes after the start of DA applicationas "During", and from two minutes to three minutes after the start of washoutas "Washout". Relative firing rate were calculated by dividing each number of action currents by that of "Before". Steel's multiple comparison tests were performed for the comparison of relative firing rate (significance levels were < 0.05).

Histology

The brain and pituitary was fixed by 4% paraformaldehyde in PBS. The fixed

tissues were frontally cryo-sectioned at 30 μm using a cryostat (CM 3050S, Leica microsystems, Wetzlar, Germany) and was mounted onto MAS-GP typeA coated glass slides (Matusnami, Osaka, Japan) as described before (30). For double labeling immunohistochemistry (IHC) for GnRH1 neurons and tyrosine hydroxylase (TH) -immunoreactive (ir) neurons, I used *gnrh1:EGFP* transgenic medaka. The somata and fibers of GnRH1 neurons were visualized by anti-EGFP antiserum (68) (diluted 1:1000 with PBST) and AlexaFluor488 conjugated anti-rabbit IgG (diluted 1:800 with PBST; Invitrogen, Carlsbad, CA). TH-ir neurons were visualized by anti-TH antibody (Millipore, diluted 1:750 with PBST) and AlexaFluor555 conjugated anti-mouse IgG (diluted 1:800 with PBST; Invitrogen). For double labeling immunohistochemistry (IHC) for LH or FSH cells and TH-ir fibers, I used *lhb:IP* or *fshb:IP* transgenic medaka. The LH or FSH cells were visualized immunohitochemically by anti-EGFP antiserum (68) (diluted 1:1000 with PBST) and AlexaFluor488 conjugated anti-rabbit IgG (diluted 1:800 with PBST; Invitrogen). TH-ir fibers were visualized in the same way as described above. The sections were coverslipped with CC/Mount (Diagnostic BioSystems, Pleasanton, CA). The fluorescence was observed under a confocal laser-scanning microscope LSM-710 (Carl Zeiss, Oberkochen, Germany) at 1-μm optical section.

Results

Section I: Analysis of the effects of kisspeptin on the HPG axis regulation

FTM145 activates two subtypes of teleost Gpr54, Gpr54-1 and Gpr54-2

In *in vivo* experiment, I used not only teleost kisspeptins but also FTM145, a GPR54 agonist which is chemically modified to be resistant to matrix

metalloproteinase (MMP) hydrolysis and has a longer half-life period, because kisspeptin itself is known to be easily cleaved by MMP within an hour in serum (118), and a single injection of kisspeptin may not be enough to induce ovulation *in vivo*. Because FTM145 was originally synthesized as an agonist for mammalian GPR54, I first confirmed the activity of FTM145 against the teleost Gpr54. Teleosts have two subtypes of Gpr54, Gpr54-1 and Gpr54-2 (96, 97). Since the both medaka Gpr54s have already been cloned, and luciferase assay with intrinsic kisspeptins, Kiss1-10 and Kiss2-12, have already been reported (103), I performed a luciferase reporter assay for the two types of Gpr54 receptors in medaka, Gpr54-1 and Gpr54-2, and compared the effect of FTM145 with those of intrinsic medaka kisspeptin peptides. The luciferase assay showed that FTM145 significantly activate both Gpr54-1 and Gpr54-2 (Fig. 3-1B). FTM145 activated both SRE- and CRE-driven luciferase reporter gene like Kiss1-10 and Kiss2-12 (Fig. 3-1, (B) and (D) were modified from (103)). These results indicate that FTM145 can activate not only mammalian Gpr54 but also two types of teleost Gpr54.

Intraperitoneal administration of kisspeptins on a long time scale

In order to verify the ovulation-inducing potency of kisspeptin, I performed an *in vivo* experiment using the same protocol as reported by Chang *et al.* (106), in which they showed that i.p. injection of PIM+LHRHA to matured goldfish induced serum LH increase and ovulation. I performed an i.p. injection of FTM145 in the same manner as LHRHA injection. I injected PIM (10 μg/gBW) i.p. twice, 12 hours before and at the same time with the peptide injection, to disinhibit the dopaminergic inhibition and collected the blood three times, according to a previous literature (106). The experimental procedure is shown in Fig. 3-2A. Only the PIM+LHRHA

injection increased the plasma LH level 24 hours and 48 hours after the peptide injections, but the FTM145 injection did not increase it (PIM+saline -12 hr: 18.73±1.71, 24 hr: 21.24±6.98 (N.S.), 48 hr: 19.54±6.01 (N.S.) (n =3); PIM+FTM145 (0.1 μg/gBW) -12 hr: 16.99±5.05, 24 hr: 12.08±4.43 (N.S.), 48 hr: 12.93±1.52 (N.S.) (n =4); PIM+FTM145 (1 μg/gBW) -12 hr: 20.11±5.13, 24 hr: 19.72±3.25 (N.S.), 48 hr: 15.10±2.82 (N.S.) (n =4); PIM+LHRHA (0.1 μg/gBW) -12 hr: 12.68±2.36, 24 hr: 121.62±9.77 (**, P = 0.0049), 48 hr: 83.38±25.33 (*, P = 0.036) (n =3)). The ovulation was checked until 60 hours after the peptide injections, and only the PIM+LHRHA injected fish (3/3) ovulated.

Intraperitoneal administration of kisspeptins on a short time scale

If the kisspeptins stimulate the HPG axis in the upstream of the GnRH neurons, instead of directly stimulating the GnRH neurons, the induction of plasma LH increase by kisspeptin may be delayed from that by stimulation with LHRHA. However, Li *et al.* (100) reported that i.p. injection of kisspeptin induced a significant increase in serum LH level in goldfish on a shorter time scale than LHRHA injection in Chang *et al.* (106). As they did not mention induction of ovulation, I performed an *in vivo* experiment using the same protocol as reported by Li *et al.* (100) and verified the ovulation-inducing potency of kisspeptins. I injected PIM (10 μg/gBW) i.p. twice, three hours before and at the same time with the peptide injection and collected the blood three times, according to the previous literature (100). The experimental procedure is shown in Fig. 3-3A. I used medaka kisspeptins, Kiss1-10 and Kiss2-12, because the amino acid sequence for those kisspeptins were almost the same for medaka and goldfish (100) (Fig. 3-1A). I also injected FTM145 in two concentrations, 0.1 μg/gBW and 1 μg/gBW (ten times higher

than the other peptides). As the induction of serum LH elevation and ovulation by LHRHA have already been reported (106), I used LHRHA as a positive control. LHRHA is a potent GnRH analog, and LHRHA injection is expected to cause direct stimulation of pituitary by GnRH.

In none of the experimental groups, saline only, PIM+saline, PIM+Kiss1-10 (0.1 μg/gBW), PIM+Kiss2-12 (0.1 μg/gBW), PIM+FTM145 (0.1 μg/gBW and 1 μg/gBW), and LHRHA (0.1 μg/gBW) the peptide injections increased the plasma LH levels either 2 hours or 6 hours afterwards. Only 2 hours after PIM+FTM145 (1 μg/gBW), the injection significantly decreased the plasma LH concentration (saline only 0 hr: 10.91±1.78, 2 hr: 8.96±0.43 (N.S.), 6 hr: 8.34±0.79 (N.S.) (n =3); PIM+saline 0 hr: 11.80±2.85, 2 hr: 11.34±1.94 (N.S.), 6 hr: 9.88±3.62 (N.S.) (n =3); PIM+FTM145 (0.1μg/gBW) 0 hr: 10.45±4.44, 2 hr: 13.59±1.91 (N.S.), 6 hr: 12.21±3.85 (N.S.) (n =3); PIM+FTM145 (1 μg/gBW) 0 hr: 15.92±4.28, 2 hr: 3.35±1.79 (*, P = 0.035), 6 hr: 10.11±1.63 (N.S.) (n =3); PIM+Kiss1-10 (0.1 μg/gBW) 0 hr: 8.58±1.14, 2 hr: 7.58 ±1.08 (N.S.), 6 hr: 10.34±3.22 (N.S.) (n =3); PIM+Kiss2-12 (0.1 μg/gBW) 0 hr: 11.32 ±1.13, 2 hr: 8.87±0.77 (N.S.), 6 hr: 9.79±0.38 (N.S.) (n =3); PIM+LHRHA (0.1 μg/gBW) 0 hr: 21.04±2.21, 2 hr: 22.04±5.05 (N.S.), 6 hr: 32.49±7.08 (N.S.) (n =3). The ovulation was checked until 60 hours after the peptide injections, but only PIM+LHRHA injected fish (3/3) ovulated, which suggests that the peptide injection itself is working as expected.

Intraventricular administration of kisspeptins

Considering that it may still be possible that i.p.-injected peptide did not reach the brain, I performed i.c.v injection of peptides. First, I injected PIM i.p., and 12 hours after that, I injected peptides into the third ventricle of the brain. I collected

the blood according to the time schedule, to see whether i.c.v. injection of kisspeptin elevates the serum LH level, as reported in rats (94). The experimental procedure is shown in Fig. 3-4A. Neither FTM145 nor Kiss2-12 increased the plasma LH level at any time point (PIM+saline -12 hr: 6.73±1.18, 0 hr: 10.40±2.16 (N.S.), 0.5 hr, 9.38 ±2.39 (N.S.), 3 hr, 12.03±2.46 (N.S.) (n =4); PIM+DMSO (0.02%) -12 hr: 8.40±1.89, 0 hr: 9.23±2.03 (N.S.), 0.5 hr, 8.27±0.72 (N.S.), 3 hr, 14.88±2.60 (N.S.) (n =4); PIM+FTM145 (0.1 nmol) -12 hr: 8.51±0.67, 0 hr: 10.24±1.45 (N.S.), 0.5 hr, 12.60± 4.11 (N.S.), 3 hr, 14.54±4.97 (N.S.) (n =4); PIM+Kiss2-12 (0.1 nmol) -12 hr: 13.19± 2.88, 0 hr: 12.45±0.85 (N.S.), 0.5 hr, 19.54±6.88 (N.S.), 3 hr, 16.04±2.84 (N.S.) (n =4)). Similarly, no fish ovulated after i.c.v. injection of FTM145 or Kiss2-12 peptides.

Effects of kisspeptins on GnRH1 neuronal activities

Next, I examined possible effects of kisspeptins on the neuronal activity of GnRH1 neurons. For this experiment, I used transgenic medaka to identify GnRH1 neurons. Since the absence of Gpr54 on the GnRH1 neurons has already been reported in medaka (17), I examined the possibility of indirect effect of kisspeptin on the GnRH1 neurons using whole brain preparations, in which neural circuits are kept almost intact.

I recorded neural activity of GnRH1 neurons by using loose-cell patch clamp and compared the firing frequency before and after the application of medaka Kiss1-10. Representative traces are shown in Fig. 3-5A. The application of 1 μM Kiss1-10 did not change the firing frequency of GnRH1 neurons (During 0.81±0.18; Washout 1.08±0.28 (N.S.), Fig. 3-5B).

Section II: Analysis of the effects of dopamine on the HPG axis regulation

Dopaminergic projections in the vicinity of GnRH1 cell bodies in vPOA and fibers in the pituitary

To elucidate the dopaminergic regulation of the HPG axis, I first examined the presence of the dopaminergic projection to vPOA GnRH1 neurons. I performed double labeling immunohistochemistry using a *gnrh1:EGFP* transgenic medaka, by combining immunohistochemistry for dopaminergic neurons using the anti-tyrosine hydroxylase (TH) antibody and that for GnRH1 neurons using the anti-EGFP antibody. TH is the enzyme responsible for catalyzing the conversion of the amino acid L-tyrosine to L-DOPA (precursor of DA) and has been used as a maker for the DA neurons. Many TH-ir fibers were found in the vicinity of GnRH1 cell bodies in vPOA (Fig. 3-6A). The vPOA GnRH1 neurons directly project to the pituitary (7) and some GnRH1 fibers intertwined with TH-ir fibers in the pituitary (Fig. 3-6B).

Dopamine inhibits firing activity of GnRH1 neurons

Next, I examined the effects of dopamine on the neural activity of GnRH1 neurons. I performed loose-cell patch clamp recordings from vPOA GnRH1 neurons of *gnrh1:EGFP* transgenic medaka. Dopamine application significantly inhibited the neural activity of GnRH1 neurons. Representative trances are shown in Fig. 3-7A. Relative firing rates compared to the initial firing rate under each concentration of dopamine are as follows: 100 μM DA During: 0.15±0.13, Washout: 0.62±0.34 (n=6); 50 μM DA During: 0.17±0.14 (**, P=0.0041), Washout: 0.52±0.29 (**, P=0.0041) (n=6); 10 μM DA During: 0.10±0.15 (**, P=0.0010), Washout: 0.63±0.31 (*, P=0.010) (n=5); 1 μM DA During: 0.31±0.27 (*, P=0.0010), Washout: 1.03±0.31 (N.S.) (n=5); 100 nM DA During: 0.78±0.27 (N.S.), Washout: 0.78±0.27 (N.S.) (n=5) (Fig. 3-7B). Dopamine also inhibited the GnRH1 neural activity in a dose

dependent manner (Fig. 3-7C).

Dopamine neuron innervates both LH and FSH cells

DA is known to inhibit basal and GnRH-induced LH release in goldfish both *in vivo* and *in vitro* (122-124). Since I found direct innervation of TH-ir fibers to the pituitary in medaka, I examined whether TH-ir axons project to the gonadotropes. I performed a double labeling immunohistochemistry using *lhb:IP* or *fshb:IP* transgenic medaka and labeled dopaminergic neurons with the anti-TH antibody and LH or FSH cells with the anti-EGFP antibody (labeling IP). TH-ir fibers were found to invade both the LH (Fig. 3-8A) and the FSH cell layers (Fig. 3-8B).

Discussion

In Chapter3, I searched for the regulators of GnRH1 neurons. In teleosts, some candidates have already been suggested as regulators of GnRH1 neuronal activities from pharmacological studies, For example, dopamine is known to inhibit the release of GnRH from brain slices including POA and the anterior hypothalamus (60, 125), and noradrenaline and serotonin stimulate the release of GnRH (126). Intraperitoneal injection of RFRP, a kind of RF-amide peptides, first found in birds as an inhibitor of gonadotropin release (GnIH) (reviewed in (127)), reduced the expression level of GnRH in the hypothalamus (128). NPY, which is suggested to be involved in the regulation of feeding in fish and mammals (129, 130), stimulates the release of GnRH from the GnRH terminals in the pituitary or in the brain slices containing POA (131). Out of these candidates, I focused on kisspeptin and dopamine.

The effects of kisspeptin on the HPG axis regulation

In order to examine the involvement of kisspeptin in the HPG axis regulation, I performed *in vivo* administration of kisspeptin and electrophysiological study of GnRH1 neurons. In the former experiment, I used goldfish because of their convenience for *in vivo* experiments. I performed both i.p. and i.c.v. injection of kisspeptin and its durable agonist FTM145, because the previous protocol in which GnRH successfully induced ovulation. Although, both subcutaneous administration (93) and i.c.v. administration (94, 95) of kisspeptin are reported to induce significant elevation of serum LH and ovulation in rodents, kisspeptin and FTM145 did not induce plasma LH elevation in goldfish. Because I succeeded in inducing ovulation with LHRH-A in goldfish in both long and short time scale experiments, goldfish that I used for *in vivo* experiments were sufficiently mature to ovulate. The reason I could not detect plasma LH elevation on a short time scale may be that the timing of blood sampling was too early to detect the LH surge in those fish. From these results, it is strongly suggested that kisspeptin do not have as strong effects on LH release in goldfish as reported in mammals. In addition, kisspeptin did not change the firing frequency of medaka GnRH1 neurons in an electrophysiological study. In some earlier reports on kisspeptin effects, teleost kisspeptin was expected as one of the potent activators of GnRH1 neurons just like they are in mammals. However, the absence of Gpr54 on GnRH1 neurons have recently been reported in cichlid, medaka and sea bass (102-104), and the differences in kisspeptin system between mammals and teleosts are beginning to be recognized.

Although my experiments are designed to detect both direct and indirect activations of the HPG axis via GnRH1 neurons, none of the results showed any

activation of HPG axis by kisspeptin. The pervious study (100) showed that i.p. injection of only 0.01 μg/gBW of kisspeptin without pimozide increased serum LH only two hours after peptide injection. Chang *et al.* (106) showed that co-injection of pimozide with LHRHA increase the amount and accelerate the serum LH elevation and LHRHA injection solely is not enough for induction of ovulation (106, 124). The serum LH elevation shown in Li *et al.* (100) may not be the LH elevation via activation of GnRH1 neurons in the brain, because LHRHA+PIM injected fish did not show serum LH elevation six hours after LHRHA injection in my study (Fig. 3-2B) and LH elevation only two hours after kisspeptin injection is too fast to activate LH secretion via GnRH1 neuron stimulation. However, kisspeptin did not induce an elevation of intracellular Ca^{2+} in LH cells using Ca imaging with *lh:IP* transgenic medaka (Kondo *et al.*, unpublished, Master thesis) and the possibility of direct stimulation of pituitary by kisspeptin is low.

Taken together with the previous studies, the present results strongly suggest that, in goldfish and medaka, kisspeptin may not modulate GnRH1 neurons, at least in the same manner as in mammals, and kisspeptin may have some functions other than the HPG axis regulation. For example, it has been recently reported that vasotocin and isotocin (orthologs of mammalian vasopressin and oxytocin, respectively) neurons in nucleus preopticus pars magnocellularis express *gpr54-2* by dual *in situ* hybridization in medaka (103). Because isotocin and vasotocin neurons are suggested to be involved in the regulation of social behaviors including sex behaviors and aggressive behaviors, kisspeptin may regulate these functions in teleosts (132).

The effects of dopamine on the HPG axis regulation

The inhibitory effect of dopamine on reproduction has been previously suggested, but the mechanisms of inhibition have not been clarified in either mammals or teleosts. As one of the candidate regulators of GnRH1 neurons, I examined the functions of dopamine in the HPG axis regulation.

I demonstrated the dopaminergic projections to the somata of vPOA GnRH1 neurons and the close interactions between the GnRH1 fibers and the dopaminergic fibers in the pituitary. From these anatomical observations, it is strongly suggested that dopamine acts on GnRH1 neurons at both the cell bodies and the axon terminals. As expected, the dopamine application to GnRH1 neurons inhibited the firing activity of GnRH1 neurons. I also found direct axonal projections of dopaminergic neurons to both LH and FSH cells. These results suggest that dopamine neurons inhibit the HPG axis at two levels; at the level of the GnRH1 neuron cell bodies and the gonadotropes (Fig. 3-9).

The physiological actions of dopamine are mediated by five distinct but closely related G protein-coupled receptors, D1, D2, D3, D4 and D5, which are divided into two major groups: the D1 (D1 and D5 subtypes) and D2 (D2, D3 and D4 subtypes) classes of dopamine receptors (133). The D1 class receptors are known as "stimulatory" receptors coupled with G_s signaling pathway, and the D2 class receptors as "inhibitory" receptors coupled with G_i signaling pathway (133). In my study, I found dopaminergic input to both GnRH1 neurons and gonadotropes in medaka, but the identity of dopamine receptor subtypes mediating the effects remained to be studied. There are some implications from previous studies as to the subtypes of dopamine receptors involved in the HPG axis regulation. In sheep, D2 receptor mediated dopamine signal inhibits serum LH elevation (110, 112). However, Liu and Herbison (114) showed that both D1 and D2 receptors are involved in the

inhibition of neural activity of GnRH1 neurons by electrophysiological experiments in mice. In addition, it has been suggested that D1 agonists inhibit GnRH release from the hypothalamic brain slices, and D2 agonists inhibit LH release from the pituitary in goldfish (60, 125). These two results in the mice and goldfish appear to contradict with each other, because D1 and D2 receptors should have opposite effects on the HPG axis regulations. More detailed investigations at the cellular level are necessary to understand the dopaminergic inhibition mechanisms of the HPG axis.

To summarize, the present study provides the first insights into the regulator of teleost GnRH1 neurons by using anatomical and physiological analyses at the single neuron level. Dopamine was suggested to inhibit the HPG axis at both GnRH1 neuron and gonadotrope levels, similar to mammals. However, kisspeptin, one of the strongest activator of GnRH1 neurons in mammals, did not show any involvement in the HPG axis regulation in medaka nor in goldfish. At present, medaka is the only teleost fish in which one can analyze the neural activity of GnRH1 neurons efficiently by using GFP transgenic animals. Thus, the present medaka model will be a promising tool to discover the direct regulator of GnRH1 neurons and to reveal the difference and similarity of the HPG axis regulations between mammals and non-mammalian vertebrates such as teleosts.

Figure legends

Figure 3-1

Luciferase assays for the activation of two types of receptors, Gpr54-1 and Gpr54-2, by GPR54 agonist, FTM145.

(A) Comparison of amino acid sequences of predicted mature kisspeptin in medaka and goldfish and FTM145. (B~E) Medaka Gpr54-1 (B, C) or Gpr54-2 (D, E) cDNA was transfected to COS-7 cells with SRE-luc or CRE-luc vector. Various concentrations of FTM145 (B, D) and Kiss1-10, and Kiss2-12 (C, E) were applied to the culture medium, and the luciferase activity was measured. The results are indicated as mean±SEM, each of which was conducted in more than triplicates. The data are expressed as the ratio of changes in luciferase activity over the control renilla luciferase activity. (C) and (E) were modified from (103).

Figure 3-2

Plasma LH levels and % ovulated fish after intraperitoneal (i.p.) administration of kisspeptins on a long time scale in goldfish.

(A) Experimental procedure for i.p. administration on a long time scale. (B) Plasma LH levels (ng/mL) at -12 hours, 24 hours and 48 hours from peptide administrations and % ovulated fish 60 hours after peptide administrations.

Figure 3-3

Plasma LH levels and % ovulated fish after intraperitoneal (i.p.) administration of kisspeptins on a short time scale in goldfish.

(A) Experimental procedure for i.p. administration on a short time scale. (B) Plasma

LH levels (ng/mL) at 0 hour, 2 hours and 6 hours from peptides administration and % ovulated fish 60 hours after peptide administrations.

Figure 3-4

Plasma LH levels and % ovulated fish after intracerebroventricular (i.c.v.) administration of kisspeptins in goldfish.

(A) Experimental procedure for i.c.v. administration. (B) Plasma LH levels (ng/mL) at -12 hours, 0 hour, 0.5 hours and 3 hours from peptide administrations and % ovulated fish 60 hours after peptide administrations.

Figure 3-5

Effects of kisspeptin on medaka GnRH1 neuronal activities.

(A) Representative traces before, during, and after (washout) administration of Kiss1-10, recorded by loose-cell patch clamp. (B) Relative firing rate before, during, and after administration of Kiss1-10.

Figure 3-6

Dopaminergic projections to the GnRH1 cell bodies and fibers in the pituitary.

TH-ir fibers are shown in magenta, and GnRH1 neurons are in green. TH-ir fibers project in the vicinity of GnRH1 neurons in vPOA (A) and some GnRH1 fibers intertwine with TH-ir fibers in the pituitary (B).

Figure 3-7

Dopamine inhibits firing activity of vPOA GnRH1 neurons.

(A) Representative traces of the inhibitory effects of dopamine on the GnRH1 neural

activities. (B) The firing rate changes during and after application of dopamine in each concentration. (C) Dose dependency of dopamine on the inhibition rate of GnRH1 neural activities.

Figure 3-8

The axons of the dopamine neurons invade both the LH and FSH cell layers, suggesting that both LH cells (A, green) and FSH cells (B, green) are innervated by TH-ir fibers (magenta) in the pituitary.

Figure 3-9

Schematic diagram illustrating a working hypothesis on the dual pathways for dopaminergic inhibition in the HPG axis regulation.

Figure 3-1

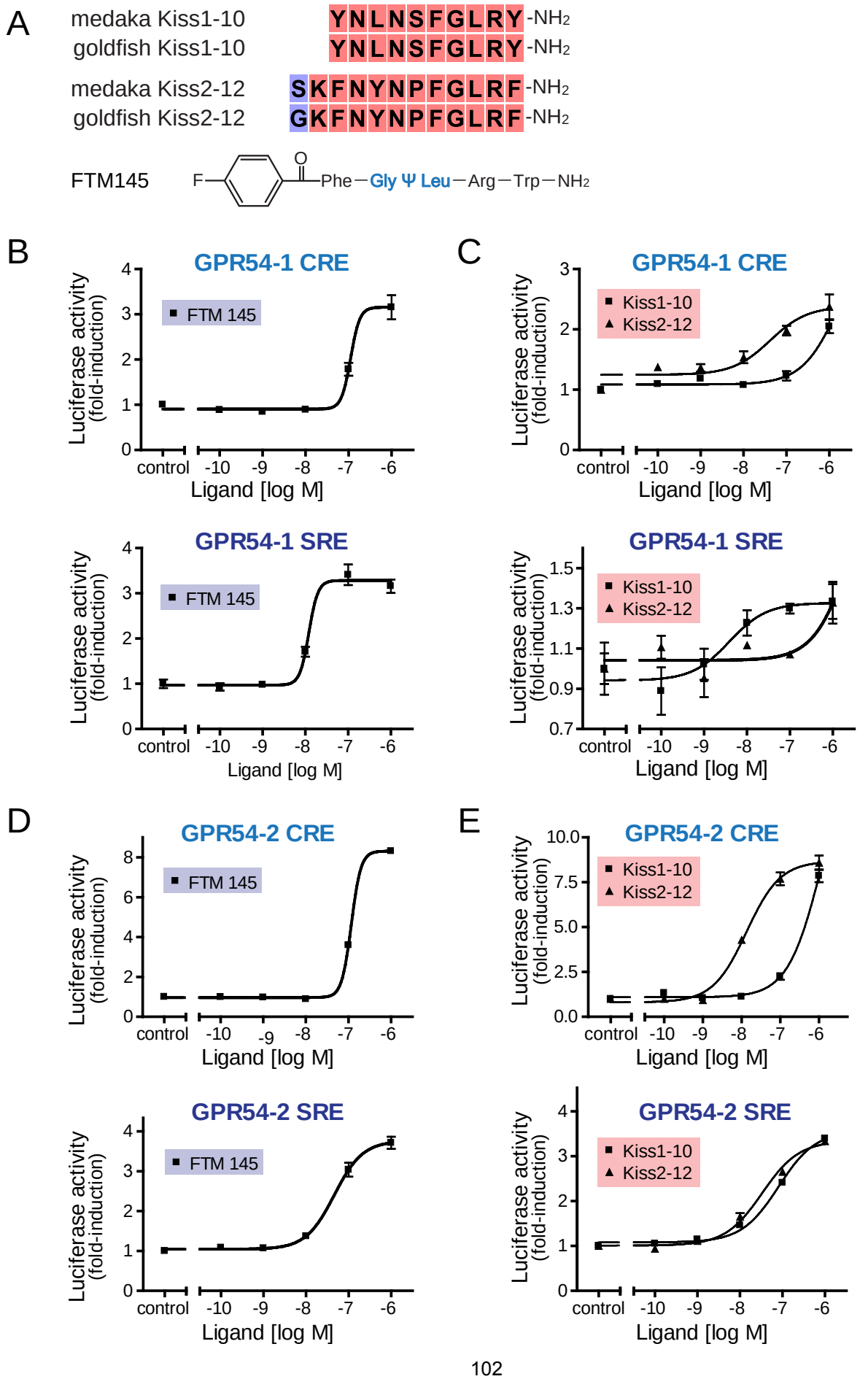
A
medaka Kiss1-10 YNLNSFGLRY-NH2
goldfish Kiss1-10 YNLNSFGLRY-NH2
medaka Kiss2-12 SKFNYNPFGLRF-NH2
goldfish Kiss2-12 GKFNYNPFGLRF-NH2
FTM145 F Phe Gly Ψ Leu Arg Trp NH2
B
GPR54-1 CRE
FTM 145
Luciferase activity (fold-induction)
Ligand [log M]
C
GPR54-1 CRE
Kiss1-10
Kiss2-12
GPR54-1 SRE
GPR54-1 SRE
D
GPR54-2 CRE
GPR54-2 CRE
E
GPR54-2 SRE
GPR54-2 SRE
control -10 -9 -8 -7 -6

Figure 3-2

A

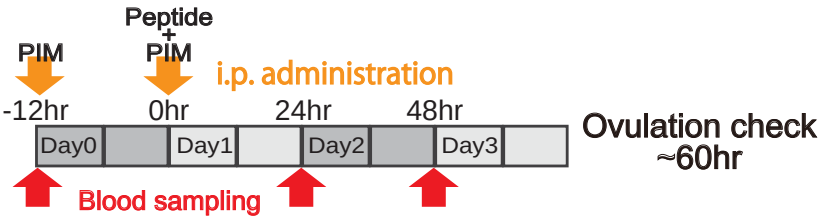
Peptide
+
PIM
PIM
i.p. administration
-12hr
0hr
24hr
48hr
Day0
Day1
Day2
Day3
Ovulation check
~60hr
Blood sampling

B

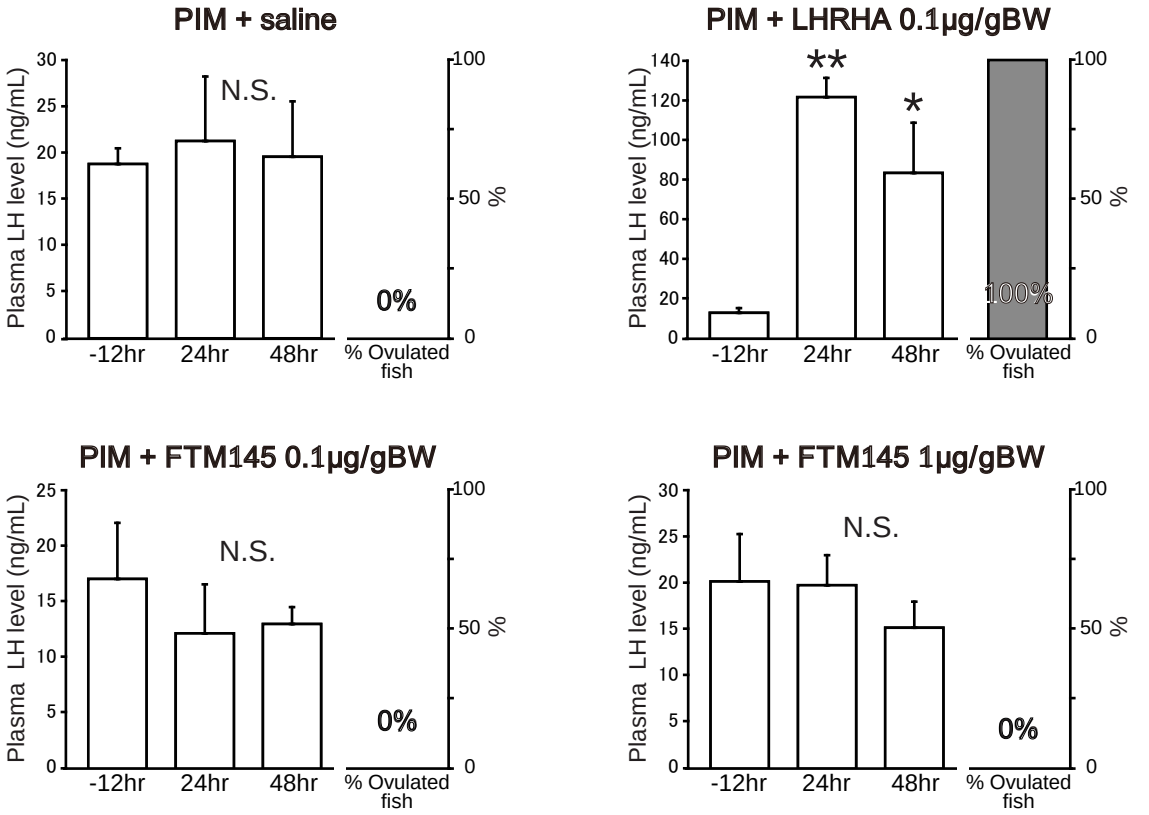
PIM + saline
Plasma LH level (ng/mL)
N.S.
0%
-12hr
24hr
48hr
% Ovulated fish
%
PIM + LHRHA 0.1µg/gBW
**
*
100%
PIM + FTM145 0.1µg/gBW
N.S.
0%
PIM + FTM145 1µg/gBW
N.S.
0%

Figure 3-3

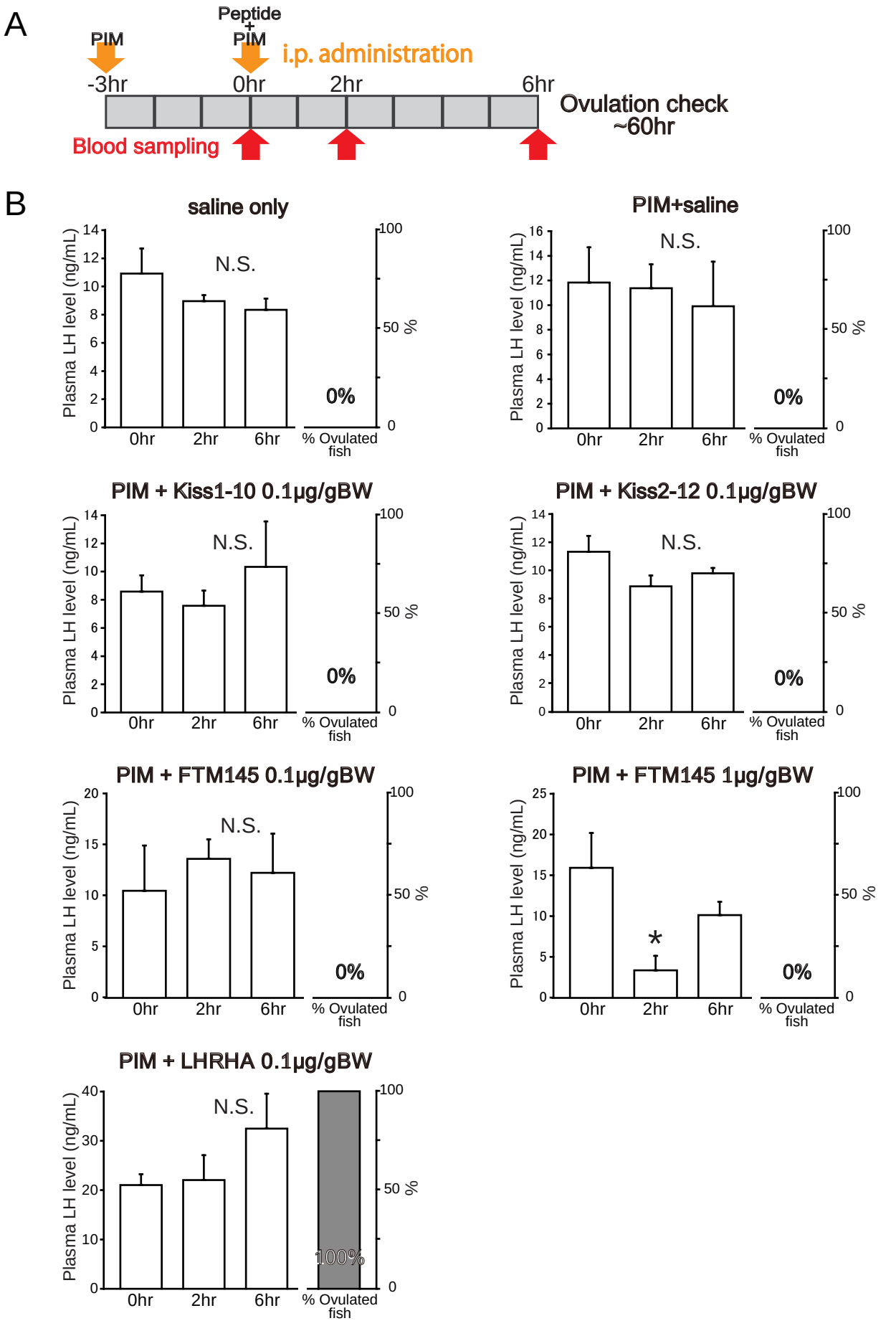
A
PIM
Peptide
+
PIM
i.p. administration
-3hr
0hr
2hr
6hr
Ovulation check
~60hr
Blood sampling
B
saline only
PIM+saline
PIM + Kiss1-10 0.1μg/gBW
PIM + Kiss2-12 0.1μg/gBW
PIM + FTM145 0.1μg/gBW
PIM + FTM145 1μg/gBW
PIM + LHRHA 0.1μg/gBW
Plasma LH level (ng/mL)
N.S.
*
0%
100%
50 %
% Ovulated fish
0hr
2hr
6hr

Figure 3-4

A

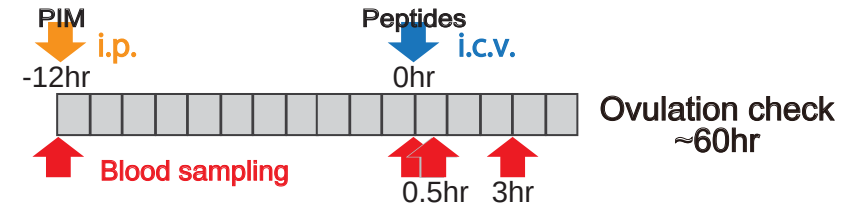
PIM
i.p.
-12hr
Peptides
i.c.v.
0hr
Ovulation check
~60hr
Blood sampling
0.5hr
3hr

B

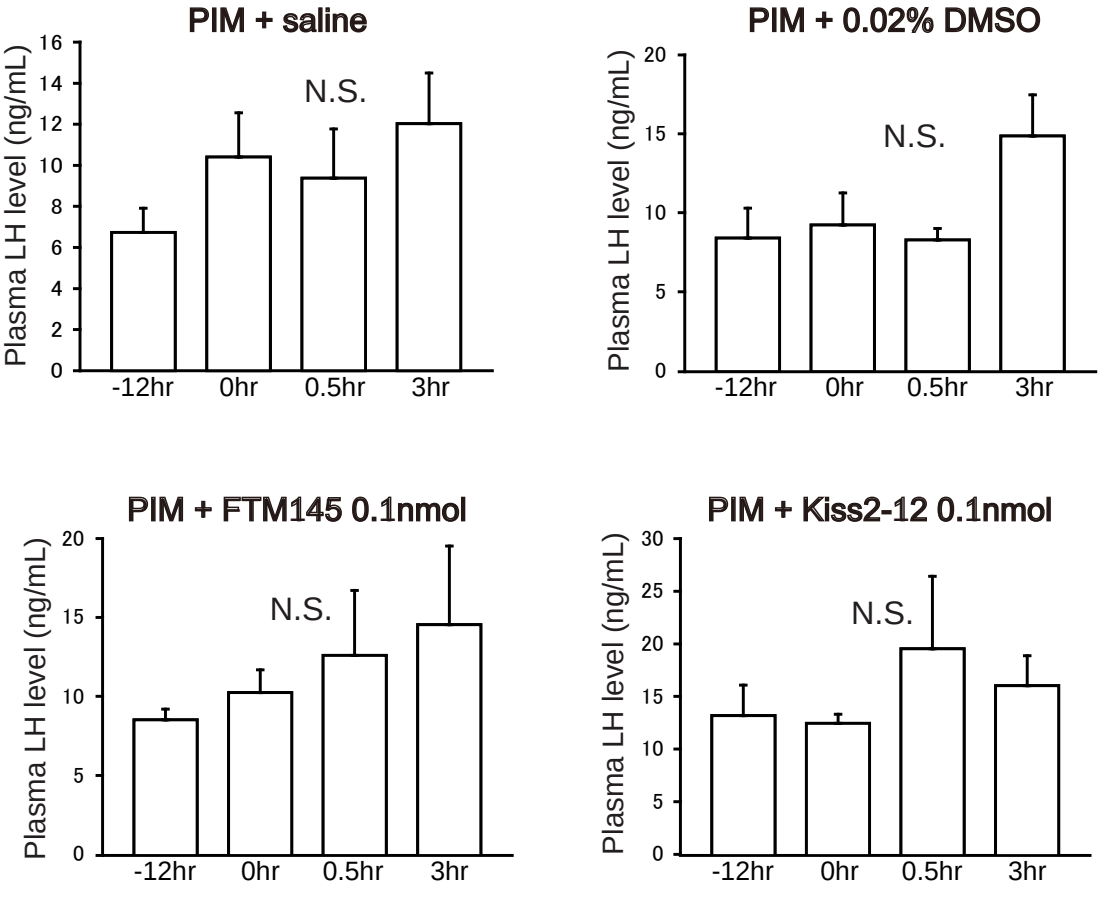
PIM + saline
Plasma LH level (ng/mL)
N.S.
-12hr
0hr
0.5hr
3hr
PIM + 0.02% DMSO
Plasma LH level (ng/mL)
N.S.
-12hr
0hr
0.5hr
3hr
PIM + FTM145 0.1nmol
Plasma LH level (ng/mL)
N.S.
-12hr
0hr
0.5hr
3hr
PIM + Kiss2-12 0.1nmol
Plasma LH level (ng/mL)
N.S.
-12hr
0hr
0.5hr
3hr

Figure 3-5

A

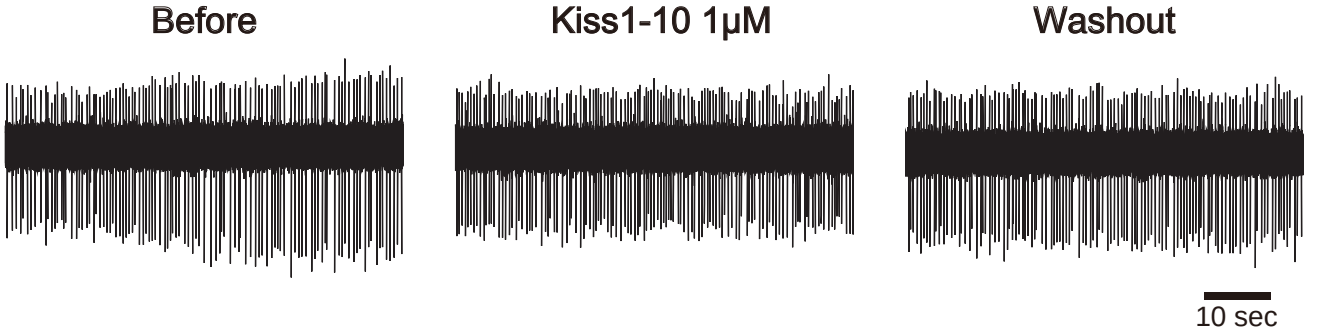
Before
Kiss1-10 1μM
Washout
10 sec

B

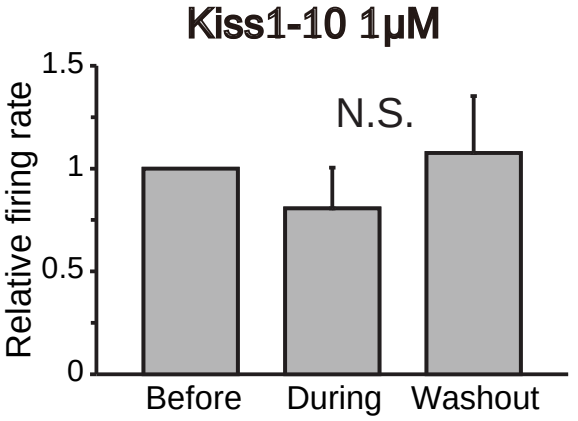
Kiss1-10 1μM
Relative firing rate
1.5
1
0.5
0
N.S.
Before
During
Washout

Figure 3-6

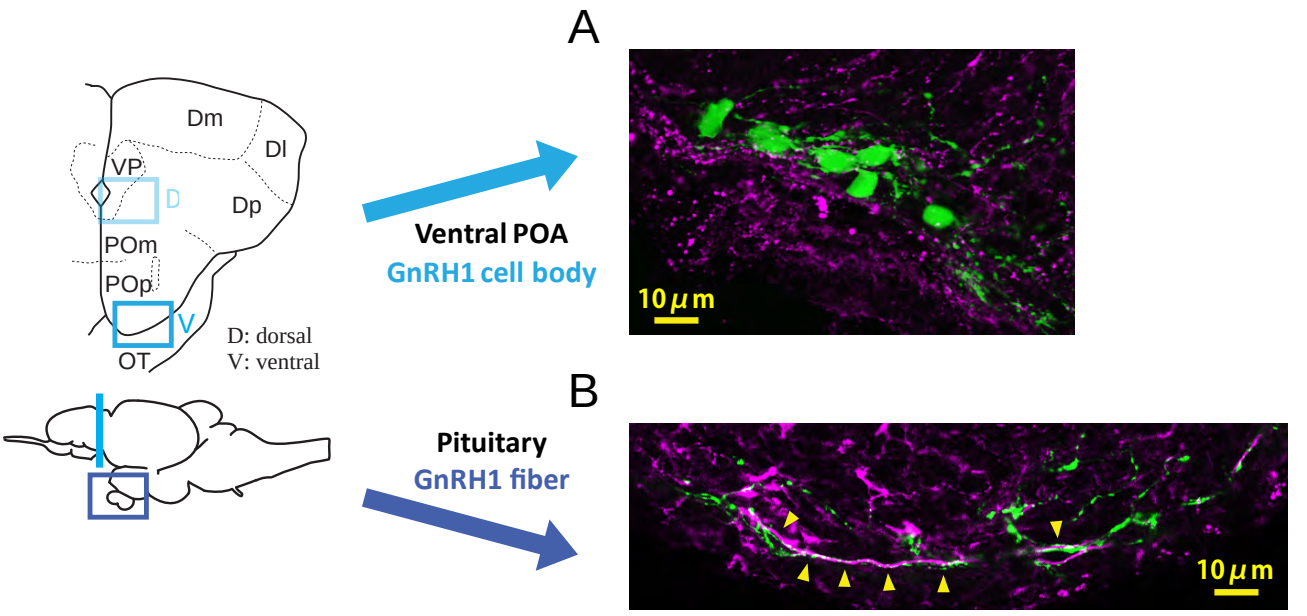
A
Dm
Dl
VP
D
Dp
POm
POp
V
OT
D: dorsal
V: ventral
Ventral POA
GnRH1 cell body
10 μm
B
Pituitary
GnRH1 fiber
10 μm

Figure 3-7

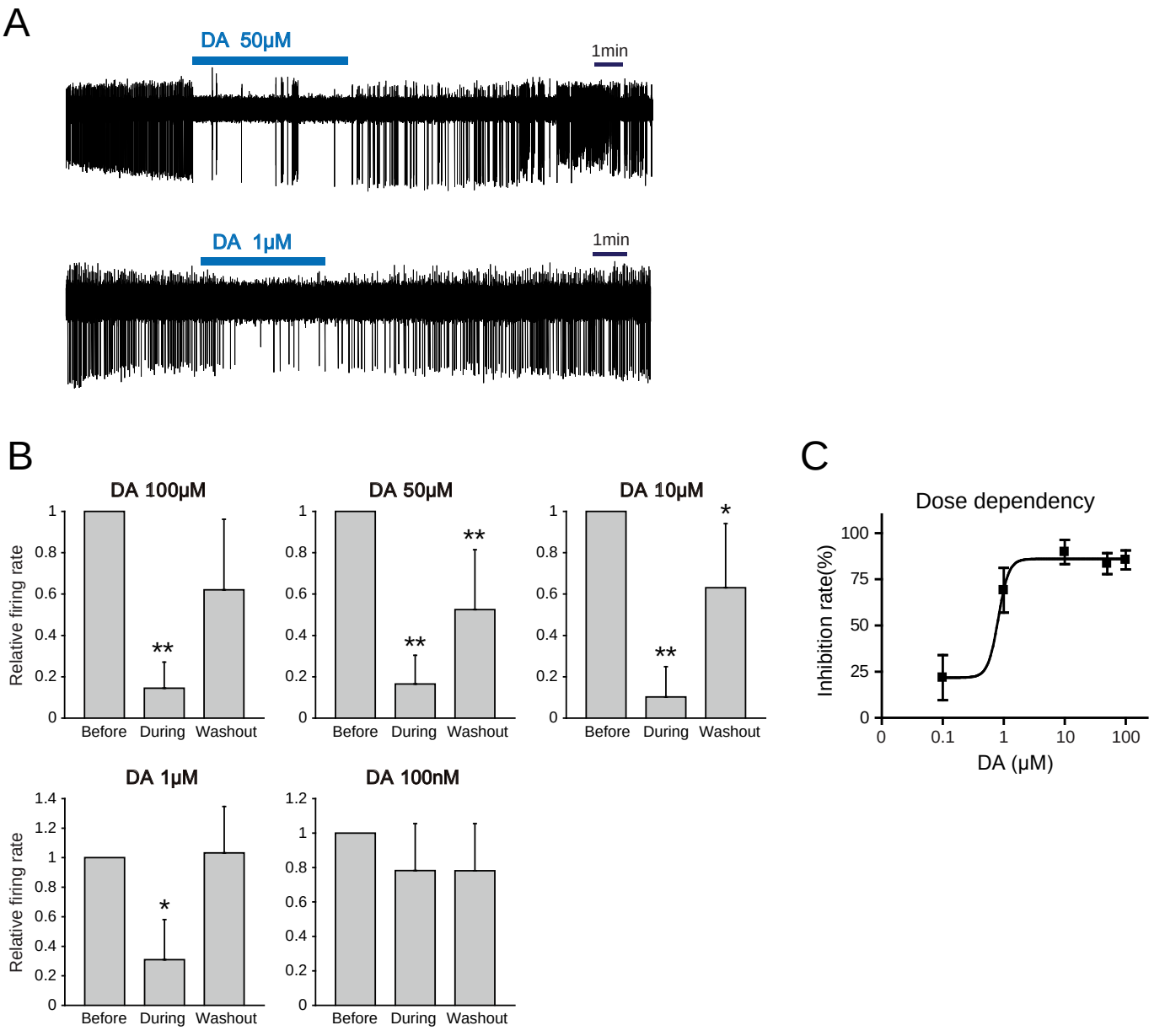
A
DA 50μM
1min
DA 1μM
1min
B
DA 100μM
DA 50μM
DA 10μM
DA 1μM
DA 100nM
Relative firing rate
Before
During
Washout
C
Dose dependency
Inhibition rate(%)
DA (μM)

Figure 3-8

A

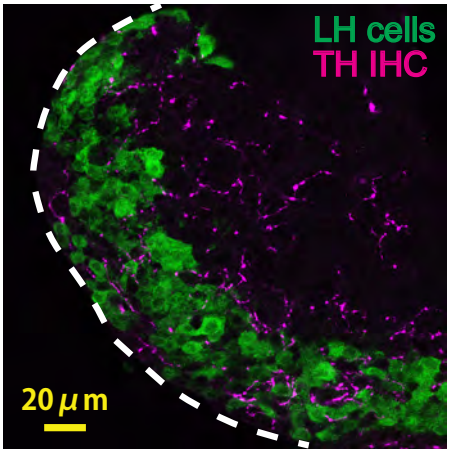

B

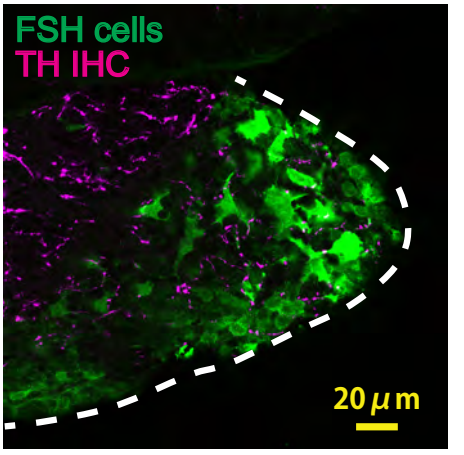

Figure 3-9

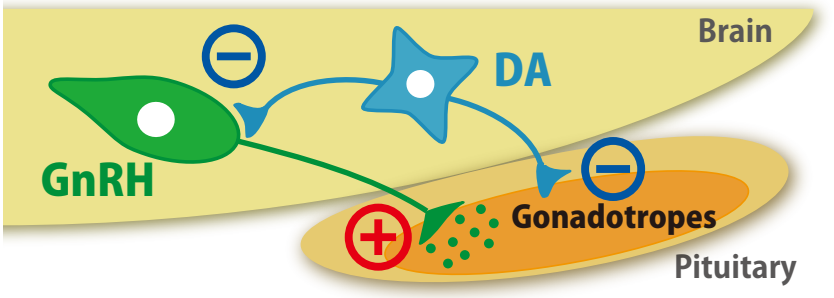

General Discussion

The present thesis aimed at analyzing the basic principles of the HPG axis regulation mechanisms in vertebrates by using teleost fishes, medaka and goldfish, as models, with special reference to the hypophysiotropic GnRH1 neurons.

In Chapter 1, I showed the time-of-day changes in the GnRH1 neuronal activities and the gonadotropin mRNA expressions in the pituitary to establish the bases for studying the HPG axis regulation mechanisms in medaka. I recorded the neuronal activity of pituitary-projecting vPOA GnRH1 neurons and found time-of-day dependent changes in neuronal activities; the overall firing activity in the afternoon was higher than in the morning, and they peaked before the estimated LH surge timing. This increase of neuronal activity may initiate the LH surge and subsequently trigger ovulation. This is the first report in vertebrates showing the time-of-day dependent changes in the electrical activity of GnRH1 neurons in the neural circuit-intact brain without manipulations of the sex steroid milieu by taking advantage of the characteristics of a daily ovulating small teleost, medaka.

Concerning the dynamic changes in the spontaneous activity of GnRH1 neurons, there have been some reports on the occurrence of time-of-day dependent changes in GnRH1 neuronal activity using an ovariectomized and estradiol-treated (OVX+E) mice model (48). In the intact mice, serum 17β-estradiol (E2) concentration fluctuates along the estrous cycle and shows LH surge and ovulation every four or five days, whereas the OVX+E mice whose E2 level is kept at high concentration are supposed to mimic the proestrous phase of estrous cycle and show LH surge-like serum LH rise in every afternoon (48). In females, the ovarian steroid hormones exert both negative and positive feedback to modulate GnRH1 neuron functions and pituitary responsiveness to GnRH peptide. At proestrous phase, estradiol feedback switches from negative to positive action, causing the GnRH surge (15, 17, 18). In

such daily surge model experiments, the neuronal activities were measured only during artificially mimicked proestrous-like phase, and there have been no report concerning other phases of the estrous cycle. However, the spontaneous firing rate of GnRH1 neurons was low in the morning (AM) and high in the afternoon (PM) in the OVX+E mice, and no such difference was apparent in the OVX mice. In addition, the neuronal activity of the GnRH1 neurons in the OVX+E mice is lower than that of the OVX mice in AM and higher in PM, suggesting the existence of estrogen positive and negative feedback on GnRH1 neuronal activities; E2 facilitates the GnRH neuronal activity in AM and suppresses that in PM (48). By using a quantitative expression analysis in the OVX and sex steroid-treated medaka, the sex steroids have been shown to have a positive feedback effect on LH concerning mRNA expression in the medaka pituitary (30), which is completely opposite to the mammalian gonadotropin response to sex steroids (reviewed in (134)), and negative feedback regulation on LH have not been demonstrated in teleosts. In my experiments, the firing frequency of GnRH1 neurons tended to be the lowest prior to the estimated time of LH surge in medaka (around 16:00 to 17:00) and the highest after that (Fig. 1-2 E and F, group d and e, not statically significant). In medaka, plasma E2 concentration fluctuates in a day and is lowest at the latter of the lighting period (comparable to around 16:00 in my experiments) (135). This result may imply the existence of both negative and positive feedback mechanisms by sex steroid on GnRH1 neuronal activities also in medaka.

The time-of-day dependent changes in GnRH1 neuronal activities in both our study and the previous studies using mice suggest that some kinds of circadian neural mechanisms may be important for the regulation of GnRH neuronal activities. There are reports in rodents suggesting that signals arising from the

suprachiasmatic nucleus (SCN), which is known as the candidate master biological clock in mammalian brain, affect the hypothalamic neuronal functions such as the regulation of timing of LH surge (reviewed in (53)). However, in teleosts, the notion of master circadian clock has not yet been established. Therefore, we still do not know what the actual trigger of time-of-day changes in the activity of GnRH1 neurons in our teleost model is. Because most teleosts have rather transparent body compared with mammals, and non-mammalian vertebrates express various opsin-like photoreceptors widely outside the retina (136), certain information from light maybe transmitted to the GnRH1 neurons. Thus, the sex steroid concentration and the information from light may act as triggers in teleosts. Because the trigger of LH surge is important for the maintenance of estrous cycle, the comparison among animals of differences in the trigger of LH surge should be an interesting future topic for the elucidation of the common mechanisms of the HPG axis regulation in vertebrates.

In Chapter 1, I discussed the activities of single GnRH1 neurons. On the other hand, it has been suggested from various studies in mammals that coordination of activity of multiple GnRH neurons probably underlies two different modes of rhythmic GnRH release, GnRH pulses and surges. For example, single unit activity extracted from hypothalamic multiunit electrical recordings during LH release (MUA volleys) has indicated changes in activity of multiple neurons (137). In addition, total GnRH peptide content in GnRH neurons have been estimated to be approximately 1.0 pg/cell (138), and 30% of which likely comprises the releasable pool of GnRH peptides. The levels of GnRH in the hypophyseal portal vessels during a pulse (139, 140) (several hundred pg/ml) suggest that multiple GnRH neurons are probably involved in the release of LH. However, the mechanisms for synchronous

firing in the hypothalamic GnRH neurons are unknown, and there are quite a small number of studies that shows the coordinated activity of hypophysiotropic GnRH1 neurons (141). One of the reasons which make difficult to elucidate the coordinated activities of GnRH1 neurons is a sparse distribution of GnRH1 neurons in the brain (4). The other one may be a technical problem in that mammalian brain researchers inevitably use brain slices for physiological experiments, in which neural circuits are disrupted during slicing. In fact, some reports suggest that the GnRH1 neuronal activities and the mode and/or frequency of synaptic inputs to the GnRH1 neurons vary depending on the cutting direction of the brain slices and their thickness (50, 142). There are some implications about the interactions among individual GnRH1 neurons. From the electron microscopic studies of mice GnRH1 neurons, dendro-dendritic interactions between GnRH1 neurons are reported (143). The dendrites of the great majority of GnRH neurons (86%) form multiple close appositions with dendrites of other GnRH neurons, and puncta and zonula adherens were found connecting adjacent dendritic elements of GnRH neurons. Also, individual afferent axon terminals were found to synapse with multiple GnRH neuron dendrites in bundles. Of course, coordinated activities of hypophysiotropic GnRH1 neurons have not yet been identified in teleosts. In medaka, vPOA GnRH1 neurons directly project to the pituitary by forming distinctive thick fiber bundles (39). In those axon bundles, GnRH1 fibers are closely apposed to each other, and some kind of electrical interactions, such as electrical field effects, may be working among the axons of GnRH1 neurons in the bundles. Our whole brain preparation should prove to be a potent tool to study such synchronization mechanisms of GnRH1 neuron activities.

Next, in Chapter 2, I analyzed the effects of GnRH on the release of LH and FSH

separately. Despite the different secretory profiles of LH and FSH, many previous studies focused on LH release by GnRH, and the mechanisms of differential regulation of the release of two types of gonadotropins by GnRH are still unknown. Therefore, I generated transgenic medaka lines that express fluorescent Ca^{2+} indicator proteins in either LH or FSH cells to analyze intracellular Ca^{2+} dynamics separately. I performed a cell-type specific Ca^{2+} imaging of LH and FSH cells and demonstrated that LH and FSH cells show different modes of Ca^{2+} rise induced by GnRH. Since the Ca^{2+} rise can be considered as the indicator of exocytotic release of hormones from the gonadotropes, these results indicate that the differential LH and FSH release patterns are induced by GnRH. Because of the technical limitations, I have not yet been able to measure the released hormones themselves and cannot determine the actual hormone release patterns. However, the Ca^{2+} rise generally is a good indicator to know the timing of exocytosis. The previous electron microscopic study in rat gonadotropes showed that LH and FSH tend to be packaged into different kind of vesicle in identical cell, LH in small secretory granules and FSH in large secretory granules (144). In mammals, gonadotropes may control the different secretory pattern of each gonadotropin via different regulation of each kind of secretory vesicle. I also observed spontaneous Ca^{2+} fluctuations in both LH and FSH cells and found that the pattern of spontaneous Ca^{2+} fluctuation was different between LH and FSH cells. Spontaneous Ca^{2+} fluctuations tended to be reduced under GnRH antagonist treatment but did not completely diminish in both LH and FSH cells. This suggests that LH and FSH cells receive additional inputs from unidentified non-GnRH neurons, and such inputs may be different between LH and FSH cells. In this respect, the study of gonadotropes using teleosts, in which LH and FSH cells are separated as different cell groups, should go a long way towards the

understanding of the neuroendocrine regulation mechanisms of each cell group, and we may be able to find out a novel regulatory mechanism for gonadotropin secretion by using the novel experimental model as shown here in Chapter 2.

In Chapter 3, I searched for neural inputs to the GnRH1 neurons to study the control mechanisms of GnRH1 neurons, focusing on two molecules, kisspeptin and dopamine (DA). In mammals, the kisspeptin signaling is now considered to be essential for the HPG axis regulation; kisspeptin strongly activates GnRH1 neuronal activities and induces serum LH elevation and ovulation. However, unlike in mammals, neither *in vivo* i.p. nor i.c.v. administration of kisspeptin induced plasma LH elevation and ovulation in sexually mature goldfish. In addition, kisspeptin did not change the firing frequency of GnRH1 neurons in medaka. In contrast, DA, which has been suggested to have inhibitory effects on the HPG axis in some mammals telosts, significantly inhibited the GnRH1 neuronal activities in medaka. I also found close appositions between DA neurons and GnRH1 neurons in both vPOA and the pituitary. In addition, LH and FSH cells were innervated by dopaminergic fibers.

In spite of many reports on the mammalian kisspeptin actions as a potent activator of GnRH1 neuronal activity, I could never find any positive effects of kisspeptin on the activation of the HPG axis in medaka or goldfish. Combined with the recent reports that demonstrated the absence of Gpr54 (kisspeptin receptor) on GnRH1 neurons in some teleosts (102-104), it is strongly suggested that, in teleosts, kisspeptin may not modulate GnRH1 neurons in the same manner as that of mammals; it may not even regulate the HPG axis in non-mammalian species in general. Recently, the involvement of kisspeptin systems in various physiological functions other than reproduction have been shown in teleosts. For example, in

medaka, a subpopulation of vasotocin and isotocin neurons express *gpr54-2* mRNA, and these neurons are suggested to be related to the regulation of social behaviors (103). In the European sea bass, *gpr54-2* mRNA is expressed in somatostatin neurons and NPY neurons, which are suggested to be related to the control of GH secretion and feeding, respectively (104). Interestingly, mammals and most of the non-mammalian vertebrates possess kisspeptin systems, and only avian species seem to have lost kisspeptin systems; both the genes for kisspeptin and its receptor GPR54 are lacking in birds (96). In spite of the absence of kisspeptin system, the avian species retain a normal ability of reproduction. This fact implies a possibility that kisspeptin system originally had some physiological functions other than the HPG axis regulation and have evolved and specialized as a regulator of HPG axis regulation in mammals. In this hypothesis, non-mammalian vertebrates including teleosts may have some kind of regulatory mechanisms to regulate GnRH1 neurons other than kisspeptin neurons, and those mechanisms may be truly essential for the HPG axis regulation. Until now, *Kiss1* or *Gpr54* gene knockout animals have been reported only in mammals, human (hereditary disorder) and rodents. Therefore, gene knockout studies in non-mammalian vertebrates, which have become available as TALEN or CRISPR/Cas9 technology, may provide novel insights into the understanding of the candidate original function(s) of the kisspeptin systems in the near future.

By contrast, the inhibitory effect of DA on the HPG axis studied in Chapter 3 seems to be common between mammals and teleosts. There are several reports that measured serum LH and GnRH concentrations after treating animals with DA agonist and antagonist in both mammals and teleosts (60, 110-112, 125). However, the direct inhibitory effect of DA on the GnRH1 neurons were shown for the first

time by electrophysiological study in mice, quite recently (114) and needs further detailed analysis in future. In Chapter 3, I demonstrated that DA inhibits the activities of GnRH1 neurons for the first time in teleosts, and this inhibitory effect appears to be similar to that shown in mice (114). In fact, the inhibitory effect of DA on the GnRH1 neuronal activities was significant but transient. Although such transient inhibitions on GnRH1 neuronal activities themselves may not have a potent influence on the total GnRH release at the pituitary, DA treatment significantly inhibited GnRH release from the hypothalamic brain explants (60, 125). Dopaminergic inhibition may have additional effects other than mere inhibition of GnRH1 neuronal activities, e.g., inhibition of transcription of GnRH or modulation of the control neural circuit for GnRH1 neurons. I also showed a possible direct inhibition on LH and FSH cells. The direct dopaminergic inhibitory effects on LH release or synthesis have been suggested in both mammals (145-147) and teleosts (61, 115, 148, 149). Overall, the dopaminergic inhibitions on both GnRH1 neurons and LH cells (gonadotropes in mammal) are possibly common to many vertebrates. As the number of studies on the dopamine effects on FSH cells is rather small, elucidation of the differential regulation of DA on gonadotropes should be interesting.

In summary, the present thesis revealed several novel aspects of the HPG axis regulation mechanisms in teleost fishes with special focus on the hypophysiotropic GnRH1 neurons and the pituitary, by taking advantage of medaka as a model system for the study of such mechanisms in vertebrates. The HPG axis regulation mechanisms in vertebrates have been studied for a long time; more than 40 years have passed after the discovery of GnRH, and considerable amount of knowledge on the individual components of the HPG axis regulation has been accumulated until

now. However, we are still far from the comprehensive understanding of the entire neural circuitry for the HPG axis regulation mechanisms, because the cellular level analysis of the neural circuitry for the HPG axis regulation under nearly intact physiological conditions has been fairly difficult. I believe that my medaka model will go a long way towards the elucidation of the long-standing problems in the neuroendocrine study of reproduction and provide profound insights into the truly essential common regulatory mechanisms of vertebrate reproduction through the comparison of studies in various mammalian as well as non-mammalian vertebrate species.

Acknowledgements

I heartily express my great gratitude to Professor Yoshitaka Oka, Laboratory of Biological Signaling, Department of Biological Sciences, Graduate School of Science, The University of Tokyo, for his constant guidance, encouragement, and valuable discussion during the course of my study. I am also indebted to Drs. Min Kyun Park, Yasuhisa Akazome, Shinji Kanda (Graduate school of Science), Hideki Abe (Graduate School of Bioagricultural Sciences, Nagoya University), Kataaki Okubo (Graduate School of Agricultural and Life Sciences, The University of Tokyo) for their instruction, discussion, and encouragement. I am deeply grateful to Drs. Kei-ichiro Maeda, Hiroko Tsukamura, Yasuhisa Uenoyama, Naoyuki Yamamoto (Graduate School of Bioagricultural Sciences, Nagoya University) and for their helpful advice and discussion, and Drs. Toyoji Kaneko (Graduate School of Agricultural and Life Sciences, The University of Tokyo) and Makito Kobayashi (International Christian University) for providing experimental space and material. I also greatly thank Mr. Masato Aikawa, Ms. Akiko Takahashi, Chika Kondo and all the member of the Laboratory of Biological Signaling for their helpful support. I sincerely wish to thank Ms. Miho Kyokuwa and Hisako Kohno for their excellent animal care.

I am sincerely grateful to Prof. Kazuo Emoto, Associate Prof. Susumu Hyodo (Atmosphere and Ocean Research Institute, The University of Tokyo), Kataaki Okubo and Min Kyun Park for critical reading of the present thesis and valuable discussion.

Finally, I would like to express my deep gratitude to my parents, Yutaka and Mari Karigo and my sister, Satomi Naoi, for their constant financial support and encouragement.

References

1. **Amoss M, Burgus R, Blackwell R, Vale W, Fellows R, Guillemin R** 1971 Purification, amino acid composition and N-terminus of the hypothalamic luteinizing hormone releasing factor (LRF) of ovine origin. Biochem Biophys Res Commun 44:205-210
2. **Matsuo H, Baba Y, Nair RM, Arimura A, Schally AV** 1971 Structure of the porcine LH- and FSH-releasing hormone. I. The proposed amino acid sequence. Biochem Biophys Res Commun 43:1334-1339
3. **Schally AV, Arimura A, Kastin AJ, Matsuo H, Baba Y, Redding TW, Nair RM, Debeljuk L, White WF** 1971 Gonadotropin-releasing hormone: one polypeptide regulates secretion of luteinizing and follicle-stimulating hormones. Science 173:1036-1038
4. **Herbison AE** 2006 Physiology of the Gonadotropin-Releasing Hormone Neuronal Network. In: Neill JD ed. The Physiology of Reproduction. Third ed. St. Louis, MO: Elsevier; p1415-1482
5. **Bushnik TL, Fernald RD** 1995 The population of GnRH-containing neurons showing socially mediated size changes project to the pituitary in a teleost, *Haplochromis burtoni*. Brain Behav Evol 46:371-377
6. **Yamamoto N, Oka Y, Yoshimoto M, Sawai N, Albert JS, Ito H** 1998 Gonadotropin-releasing hormone neurons in the gourami midbrain: a double labeling study by immunocytochemistry and tracer injection. Neurosci Lett 240:50-52
7. **Karigo T, Kanda S, Takahashi A, Abe H, Okubo K, Oka Y** 2012 Time-of-day-dependent changes in GnRH1 neuronal activities and gonadotropin mRNA expression in a daily spawning fish, medaka. Endocrinology 153:3394-3404
8. **Spergel DJ, Kruth U, Hanley DF, Sprengel R, Seeburg PH** 1999 GABA- and glutamate-activated channels in green fluorescent protein-tagged gonadotropin-releasing hormone neurons in transgenic mice. J Neurosci 19:2037-2050
9. **Suter KJ, Song WJ, Sampson TL, Wuarin JP, Saunders JT, Dudek FE, Moenter SM** 2000 Genetic targeting of green fluorescent protein to gonadotropin-releasing hormone neurons: characterization of whole-cell electrophysiological properties and morphology. Endocrinology 141:412-419
10. **Suter KJ, Wuarin JP, Smith BN, Dudek FE, Moenter SM** 2000 Whole-cell

recordings from preoptic/hypothalamic slices reveal burst firing in gonadotropin-releasing hormone neurons identified with green fluorescent protein in transgenic mice. Endocrinology 141:3731-3736

11. **Kato M, Ui-Tei K, Watanabe M, Sakuma Y** 2003 Characterization of voltage-gated calcium currents in gonadotropin-releasing hormone neurons tagged with green fluorescent protein in rats. Endocrinology 144:5118-5125
12. **Greenwood AK, Fernald RD** 2004 Social regulation of the electrical properties of gonadotropin-releasing hormone neurons in a cichlid fish (*Astatotilapia burtoni*). Biol Reprod 71:909-918
13. **Yaron Z, Gur G, Melamed P, Rosenfeld H, Elizur A, Levavi-Sivan B** 2003 Regulation of fish gonadotropins. Int Rev Cytol 225:131-185
14. **Gorbman A** 1995 Olfactory origins and evolution of the brain-pituitary endocrine system: facts and speculation. Gen Comp Endocrinol 97:171-178
15. **Sarkar DK, Chiappa SA, Fink G, Sherwood NM** 1976 Gonadotropin-releasing hormone surge in pro-oestrous rats. Nature 264:461-463
16. **Clarke IJ, Thomas GB, Yao B, Cummins JT** 1987 GnRH secretion throughout the ovine estrous cycle. Neuroendocrinology 46:82-88
17. **Moenter SM, Caraty A, Locatelli A, Karsch FJ** 1991 Pattern of gonadotropin-releasing hormone (GnRH) secretion leading up to ovulation in the ewe: existence of a preovulatory GnRH surge. Endocrinology 129:1175-1182
18. **Pau KY, Berria M, Hess DL, Spies HG** 1993 Preovulatory gonadotropin-releasing hormone surge in ovarian-intact rhesus macaques. Endocrinology 133:1650-1656
19. **Stacey NE, MacKenzie DS, Marchant TA, Kyle AL, Peter RE** 1984 Endocrine changes during natural spawning in the white sucker, *Catostomus commersoni*. I. Gonadotropin, growth hormone, and thyroid hormones. Gen Comp Endocrinol 56:333-348
20. **Shimizu A, Aida K, Hanyu I** 1985 Endocrine profiles during the short reproductive cycle of an autumn-spawning bitterling, *Acheilognathus rhombea*. Gen Comp Endocrinol 60:361-371
21. **Kobayashi M, Aida K, Hanyu I** 1988 Hormone changes during the ovulatory cycle in goldfish. Gen Comp Endocrinol 69:301-307
22. **Blaustein JD, Tetel MJ, Ricciardi KH, Delville Y, Turcotte JC** 1994 Hypothalamic ovarian steroid hormone-sensitive neurons involved in female sexual behavior. Psychoneuroendocrinology 19:505-516
23. **McEwen BS, Jones KJ, Pfaff DW** 1987 Hormonal control of sexual behavior

in the female rat: molecular, cellular and neurochemical studies. Biol Reprod 36:37-45

24. **Mong JA, Pfaff DW** 2003 Hormonal and genetic influences underlying arousal as it drives sex and aggression in animal and human brains. Neurobiol Aging 24 Suppl 1:S83-88; discussion S91-82

25. **Kerdelhue B, Brown S, Lenoir V, Queenan JT, Jr., Jones GS, Scholler R, Jones HW, Jr.** 2002 Timing of initiation of the preovulatory luteinizing hormone surge and its relationship with the circadian cortisol rhythm in the human. Neuroendocrinology 75:158-163

26. **Bronson FH, Vom Saal FS** 1979 Control of the preovulatory release of luteinizing hormone by steroids in the mouse. Endocrinology 104:1247-1255

27. **Okubo K, Sakai F, Lau EL, Yoshizaki G, Takeuchi Y, Naruse K, Aida K, Nagahama Y** 2006 Forebrain gonadotropin-releasing hormone neuronal development: insights from transgenic medaka and the relevance to X-linked Kallmann syndrome. Endocrinology 147:1076-1084

28. **Kanda S, Akazome Y, Matsunaga T, Yamamoto N, Yamada S, Tsukamura H, Maeda K, Oka Y** 2008 Identification of KiSS-1 product kisspeptin and steroid-sensitive sexually dimorphic kisspeptin neurons in medaka (*Oryzias latipes*). Endocrinology 149:2467-2476

29. **Yamamoto N, Parhar IS, Sawai N, Oka Y, Ito H** 1998 Preoptic gonadotropin-releasing hormone (GnRH) neurons innervate the pituitary in teleosts. Neurosci Res 31:31-38

30. **Kanda S, Okubo K, Oka Y** 2011 Differential regulation of the luteinizing hormone genes in teleosts and tetrapods due to their distinct genomic environments--insights into gonadotropin beta subunit evolution. Gen Comp Endocrinol 173:253-258

31. **Mollard P, Kah O** 1996 Spontaneous and gonadotropin-releasing hormone-stimulated cytosolic calcium rises in individual goldfish gonadotrophs. Cell Calcium 20:415-424

32. **Liu TC, Jackson GL** 1990 17-beta-estradiol potentiates luteinizing hormone glycosylation and release induced by veratridine, diacylglycerol, and phospholipase C in rat anterior pituitary cells. Neuroendocrinology 51:642-648

33. **Klausen C, Chang JP, Habibi HR** 2001 The effect of gonadotropin-releasing hormone on growth hormone and gonadotropin subunit gene expression in the pituitary of goldfish, *Carassius auratus*. Comp Biochem Physiol B Biochem Mol Biol 129:511-516

34. **Kandel-Kfir M, Gur G, Melamed P, Zilberstein Y, Cohen Y, Zmora N,**

Kobayashi M, Elizur A, Yaron Z 2002 Gonadotropin response to GnRH during sexual ontogeny in the common carp, *Cyprinus carpio*. Comp Biochem Physiol B Biochem Mol Biol 132:17-26

35. **Mateos J, Mananos E, Carrillo M, Zanuy S** 2002 Regulation of follicle-stimulating hormone (FSH) and luteinizing hormone (LH) gene expression by gonadotropin-releasing hormone (GnRH) and sexual steroids in the Mediterranean Sea bass. Comp Biochem Physiol B Biochem Mol Biol 132:75-86
36. **Mitani Y, Kanda S, Akazome Y, Zempo B, Oka Y** 2010 Hypothalamic Kiss1 but not Kiss2 neurons are involved in estrogen feedback in medaka (*Oryzias latipes*). Endocrinology 151:1751-1759
37. **Iwamatsu T** 1978 Studies on oocyte maturation of the medaka, *Oryzias latipes*. V. On the structure of steroids that induce maturation *in vitro*. J Exp Zool 204:401-408
38. **Dalkin AC, Burger LL, Aylor KW, Haisenleder DJ, Workman LJ, Cho S, Marshall JC** 2001 Regulation of gonadotropin subunit gene transcription by gonadotropin-releasing hormone: measurement of primary transcript ribonucleic acids by quantitative reverse transcription-polymerase chain reaction assays. Endocrinology 142:139-146
39. **Karigo T, Aikawa M, Kondo C, Abe H, Kanda S, Oka Y** 2014 Whole brain-pituitary *in vitro* preparation of the transgenic medaka (*Oryzias latipes*) as a tool for analyzing the differential regulatory mechanisms of LH and FSH release. Endocrinology 155:536-547
40. **Okubo K, Nagahama Y** 2008 Structural and functional evolution of gonadotropin-releasing hormone in vertebrates. Acta physiologica (Oxford, England) 193:3-15
41. **Wayne NL, Kuwahara K, Aida K, Nagahama Y, Okubo K** 2005 Whole-cell electrophysiology of gonadotropin-releasing hormone neurons that express green fluorescent protein in the terminal nerve of transgenic medaka (*Oryzias latipes*). Biol Reprod 73:1228-1234
42. **Kanda S, Nishikawa K, Karigo T, Okubo K, Isomae S, Abe H, Kobayashi D, Oka Y** 2010 Regular pacemaker activity characterizes gonadotropin-releasing hormone 2 neurons recorded from green fluorescent protein-transgenic medaka. Endocrinology 151:695-701
43. **Oka Y, Matsushima T** 1993 Gonadotropin-releasing hormone (GnRH)-immunoreactive terminal nerve cells have intrinsic rhythmicity and project widely in the brain. J Neurosci 13:2161-2176
44. **Oka Y** 2010 Electrophysiological characteristics of gonadotrophin-releasing

hormone 1-3 neurones: insights from a study of fish brains. J Neuroendocrinol 22:659-663

45. **Nunemaker CS, DeFazio RA, Moenter SM** 2002 Estradiol-sensitive afferents modulate long-term episodic firing patterns of GnRH neurons. Endocrinology 143:2284-2292

46. **Abe H, Terasawa E** 2005 Firing pattern and rapid modulation of activity by estrogen in primate luteinizing hormone releasing hormone-1 neurons. Endocrinology 146:4312-4320

47. **Williams CL, Thalabard JC, O'Byrne KT, Grosser PM, Nishihara M, Hotchkiss J, Knobil E** 1990 Duration of phasic electrical activity of the hypothalamic gonadotropin-releasing hormone pulse generator and dynamics of luteinizing hormone pulses in the rhesus monkey. Proc Natl Acad Sci U S A 87:8580-8582

48. **Christian CA, Mobley JL, Moenter SM** 2005 Diurnal and estradiol-dependent changes in gonadotropin-releasing hormone neuron firing activity. Proc Natl Acad Sci U S A 102:15682-15687

49. **Christian CA, Moenter SM** 2010 The neurobiology of preovulatory and estradiol-induced gonadotropin-releasing hormone surges. Endocr Rev 31:544-577

50. **Christian CA, Moenter SM** 2007 Estradiol induces diurnal shifts in GABA transmission to gonadotropin-releasing hormone neurons to provide a neural signal for ovulation. J Neurosci 27:1913-1921

51. **Moenter SM** 2010 Identified GnRH neuron electrophysiology: a decade of study. Brain Res 1364:10-24

52. **Sun J, Chu Z, Moenter SM** 2010 Diurnal *in vivo* and rapid *in vitro* effects of estradiol on voltage-gated calcium channels in gonadotropin-releasing hormone neurons. J Neurosci 30:3912-3923

53. **Chappell PE, Goodall CP, Tonsfeldt KJ, White RS, Bredeweg E, Latham KL** 2009 Modulation of gonadotrophin-releasing hormone secretion by an endogenous circadian clock. J Neuroendocrinol 21:339-345

54. **Van der Beek EM, Horvath TL, Wiegant VM, Van den Hurk R, Buijs RM** 1997 Evidence for a direct neuronal pathway from the suprachiasmatic nucleus to the gonadotropin-releasing hormone system: combined tracing and light and electron microscopic immunocytochemical studies. J Comp Neurol 384:569-579

55. **de la Iglesia HO, Meyer J, Schwartz WJ** 2003 Lateralization of circadian pacemaker output: Activation of left- and right-sided luteinizing hormone-releasing hormone neurons involves a neural rather than a

humoral pathway. J Neurosci 23:7412-7414

56. **Hickok JR, Tischkau SA** 2010 *In vivo* circadian rhythms in gonadotropin-releasing hormone neurons. Neuroendocrinology 91:110-120

57. **Pawson AJ, Faccenda E, Maudsley S, Lu ZL, Naor Z, Millar RP** 2008 Mammalian type I gonadotropin-releasing hormone receptors undergo slow, constitutive, agonist-independent internalization. Endocrinology 149:1415-1422

58. **Okubo K, Ishii S, Ishida J, Mitani H, Naruse K, Kondo M, Shima A, Tanaka M, Asakawa S, Shimizu N, Aida K** 2003 A novel third gonadotropin-releasing hormone receptor in the medaka *Oryzias latipes*: evolutionary and functional implications. Gene 314:121-131

59. **Okubo K, Nagata S, Ko R, Kataoka H, Yoshiura Y, Mitani H, Kondo M, Naruse K, Shima A, Aida K** 2001 Identification and characterization of two distinct GnRH receptor subtypes in a teleost, the medaka *Oryzias latipes*. Endocrinology 142:4729-4739

60. **Yu KL, Peter RE** 1992 Adrenergic and dopaminergic regulation of gonadotropin-releasing hormone release from goldfish preoptic-anterior hypothalamus and pituitary *in vitro*. Gen Comp Endocrinol 85:138-146

61. **Van Goor F, Goldberg JI, Chang JP** 1998 Dopamine-D2 actions on voltage-dependent calcium current and gonadotropin-II secretion in cultured goldfish gonadotrophs. J Neuroendocrinol 10:175-186

62. **Childs GV** 2006 Gonadotropes and Lactotropes. In: Neill JD ed. The Physiology of Reproduction. Third ed. St. Louis, MO: Elsevier; p1492-1539

63. **Kwiecien R, Hammond C** 1998 Differential management of Ca^{2+} oscillations by anterior pituitary cells: a comparative overview. Neuroendocrinology 68:135-151

64. **Thomas P, Waring DW** 1997 Modulation of stimulus-secretion coupling in single rat gonadotrophs. J Physiol 504 (Pt 3):705-719

65. **Tse A, Tse FW, Almers W, Hille B** 1993 Rhythmic exocytosis stimulated by GnRH-induced calcium oscillations in rat gonadotropes. Science 260:82-84

66. **Tse FW, Tse A, Hille B, Horstmann H, Almers W** 1997 Local Ca^{2+} release from internal stores controls exocytosis in pituitary gonadotrophs. Neuron 18:121-132

67. **Nagai T, Sawano A, Park ES, Miyawaki A** 2001 Circularly permuted green fluorescent proteins engineered to sense Ca^{2+}. Proc Natl Acad Sci U S A 98:3197-3202

68. **Tamamaki N, Nakamura K, Furuta T, Asamoto K, Kaneko T** 2000 Neurons in Golgi-stain-like images revealed by GFP-adenovirus infection *in vivo*.

Neurosci Res 38:231-236

69. **Ogiwara K, Fujimori C, Rajapakse S, Takahashi T** 2013 Characterization of luteinizing hormone and luteinizing hormone receptor and their indispensable role in the ovulatory process of the medaka. PLoS ONE 8:e54482

70. **Murthy CK, Nahorniak CS, Rivier JE, Peter RE** 1993 *In vitro* characterization of gonadotropin-releasing hormone antagonists in goldfish, *Carassius auratus*. Endocrinology 133:1633-1644

71. **Urano A** 1971 Monamine oxidase in the hypothalamo-hypophysial region of the teleosts, *Anguilla japonica* and *Oryzias latipes*. Z Zellforsch Mikrosk Anat 114:83-94

72. **Ando H, Swanson P, Kitani T, Koide N, Okada H, Ueda H, Urano A** 2004 Synergistic effects of salmon gonadotropin-releasing hormone and estradiol-17β on gonadotropin subunit gene expression and release in masu salmon pituitary cells *in vitro*. Gen Comp Endocrinol 137:109-121

73. **Dickey JT, Swanson P** 2000 Effects of salmon gonadotropin-releasing hormone on follicle stimulating hormone secretion and subunit gene expression in coho salmon (*Oncorhynchus kisutch*). Gen Comp Endocrinol 118:436-449

74. **Chang JP, Johnson JD, Sawisky GR, Grey CL, Mitchell G, Booth M, Volk MM, Parks SK, Thompson E, Goss GG, Klausen C, Habibi HR** 2009 Signal transduction in multifactorial neuroendocrine control of gonadotropin secretion and synthesis in teleosts-studies on the goldfish model. Gen Comp Endocrinol 161:42-52

75. **Johnson JD, Klausen C, Habibi H, Chang JP** 2003 A gonadotropin-releasing hormone insensitive, thapsigargin-sensitive Ca^{2+} store reduces basal gonadotropin exocytosis and gene expression: comparison with agonist-sensitive Ca^{2+} stores. J Neuroendocrinol 15:204-214

76. **Johnson JD, VanGoor F, Jobin RM, Wong CJ, Goldberg JI, Chang JP** 2000 Agonist-specific Ca^{2+} signaling systems, composed of multiple intracellular Ca^{2+} stores, regulate gonadotropin secretion. Mol Cell Endocrinol 170:15-29

77. **Van Goor F, Goldberg JI, Wong AO, Jobin RM, Chang JP** 1994 Morphological identification of live gonadotropin, growth-hormone, and prolactin cells in goldfish (*Carassius auratus*) pituitary-cell cultures. Cell Tissue Res 276: 253-261

78. **Sanchez-Cardenas C, Hernandez-Cruz A** 2010 GnRH-Induced $[Ca^{2+}]_i$-signalling patterns in mouse gonadotrophs recorded from acute pituitary slices *in vitro*. Neuroendocrinology 91:239-255

79. **Strandabo RA, Hodne K, Ager-Wick E, Sand O, Weltzien FA, Haug TM** 2013 Signal transduction involved in GnRH2-stimulation of identified LH-producing gonadotropes from lhb-GFP transgenic medaka (*Oryzias latipes*). Mol Cell Endocrinol 372:128-139
80. **Bosma PT, Kolk SM, Rebers FE, Lescroart O, Roelants I, Willems PH, Schulz RW** 1997 Gonadotrophs but not somatotrophs carry gonadotrophin-releasing hormone receptors: receptor localisation, intracellular calcium, and gonadotrophin and GH release. J Endocrinol 152:437-446
81. **Gur G, Bonfil D, Safarian H, Naor Z, Yaron Z** 2002 GnRH signaling pathways regulate differentially the tilapia gonadotropin subunit genes. Mol Cell Endocrinol 189:125-134
82. **Hollinger S, Hepler JR** 2002 Cellular regulation of RGS proteins: modulators and integrators of G protein signaling. Pharmacol Rev 54:527-559
83. **Saitoh O, Murata Y, Odagiri M, Itoh M, Itoh H, Misaka T, Kubo Y** 2002 Alternative splicing of RGS8 gene determines inhibitory function of receptor type-specific Gq signaling. Proc Natl Acad Sci U S A 99:10138-10143
84. **Millar RP, Lu ZL, Pawson AJ, Flanagan CA, Morgan K, Maudsley SR** 2004 Gonadotropin-releasing hormone receptors. Endocr Rev 25:235-275
85. **Levavi-Sivan B, Yaron Z** 1993 Intracellular mediation of GnRH action on GTH release in tilapia. Fish Physiol Biochem 11:51-59
86. **Mukhopadhyay B, Biswas R, Bhattacharya S** 1995 Gonadotropin releasing hormone stimulation of cyclic 3',5'-AMP in the pituitary cell of a teleost (*Channa punctatus, Bloch*) requires extracellular calcium: its relationship to gonadotropin release. Gen Comp Endocrinol 97:353-365
87. **Jobin RM, Neumann CM, Chang JP** 1996 Roles of calcium and calmodulin in the mediation of acute and sustained GnRH-stimulated gonadotropin secretion from dispersed goldfish pituitary cells. Gen Comp Endocrinol 101:91-106
88. **Zhou H, Wang X, Ko WK, Wong AO** 2004 Evidence for a novel intrapituitary autocrine/paracrine feedback loop regulating growth hormone synthesis and secretion in grass carp pituitary cells by functional interactions between gonadotrophs and somatotrophs. Endocrinology 145:5548-5559
89. **Trudeau VL** 1997 Neuroendocrine regulation of gonadotrophin II release and gonadal growth in the goldfish, *Carassius auratus*. Rev Reprod 2:55-68
90. **Zohar Y, Munoz-Cueto JA, Elizur A, Kah O** 2010 Neuroendocrinology of reproduction in teleost fish. Gen Comp Endocrinol 165:438-455
91. **Oakley AE, Clifton DK, Steiner RA** 2009 Kisspeptin signaling in the brain.

Endocr Rev 30:713-743

92. **Han SK, Gottsch ML, Lee KJ, Popa SM, Smith JT, Jakawich SK, Clifton DK, Steiner RA, Herbison AE** 2005 Activation of gonadotropin-releasing hormone neurons by kisspeptin as a neuroendocrine switch for the onset of puberty. J Neurosci 25:11349-11356
93. **Matsui H, Takatsu Y, Kumano S, Matsumoto H, Ohtaki T** 2004 Peripheral administration of metastin induces marked gonadotropin release and ovulation in the rat. Biochem Biophys Res Commun 320:383-388
94. **Kinoshita M, Tsukamura H, Adachi S, Matsui H, Uenoyama Y, Iwata K, Yamada S, Inoue K, Ohtaki T, Matsumoto H, Maeda K** 2005 Involvement of central metastin in the regulation of preovulatory luteinizing hormone surge and estrous cyclicity in female rats. Endocrinology 146:4431-4436
95. **Gottsch ML, Cunningham MJ, Smith JT, Popa SM, Acohido BV, Crowley WF, Seminara S, Clifton DK, Steiner RA** 2004 A role for kisspeptins in the regulation of gonadotropin secretion in the mouse. Endocrinology 145:4073-4077
96. **Akazome Y, Kanda S, Okubo K, Oka Y** 2010 Functional and evolutionary insights into vertebrate kisspeptin systems from studies of fish brain. J Fish Biol 76:161-182
97. **Kanda S, Oka Y** 2013 Structure, Synthesis, and Phylogeny of Kisspeptin and its Receptor. In: Kauffman AS, Smith JT eds. Kisspeptin Signaling in Reproductive Biology. Advances in Experimental Medicine and Biology: Springer; 9-26
98. **Felip A, Zanuy S, Pineda R, Pinilla L, Carrillo M, Tena-Sempere M, Gomez A** 2009 Evidence for two distinct *KiSS* genes in non-placental vertebrates that encode kisspeptins with different gonadotropin-releasing activities in fish and mammals. Mol Cell Endocrinol 312:61-71
99. **Kitahashi T, Ogawa S, Parhar IS** 2009 Cloning and expression of *kiss2* in the zebrafish and medaka. Endocrinology 150:821-831
100. **Li S, Zhang Y, Liu Y, Huang X, Huang W, Lu D, Zhu P, Shi Y, Cheng CH, Liu X, Lin H** 2009 Structural and functional multiplicity of the kisspeptin/GPR54 system in goldfish (*Carassius auratus*). J Endocrinol 201:407-418
101. **Selvaraj S, Ohga H, Kitano H, Nyuji M, Yamaguchi A, Matsuyama M** 2013 Peripheral administration of Kiss1 pentadecapeptide induces gonadal development in sexually immature adult scombroid fish. Zoolog Sci 30:446-454
102. **Grone BP, Maruska KP, Korzan WJ, Fernald RD** 2010 Social status

regulates kisspeptin receptor mRNA in the brain of *Astatotilapia burtoni*. Gen Comp Endocrinol 169:98-107

103. **Kanda S, Akazome Y, Mitani Y, Okubo K, Oka Y** 2013 Neuroanatomical evidence that kisspeptin directly regulates isotocin and vasotocin neurons. PLoS One 8:e62776

104. **Escobar S, Servili A, Espigares F, Gueguen MM, Brocal I, Felip A, Gomez A, Carrillo M, Zanuy S, Kah O** 2013 Expression of kisspeptins and kiss receptors suggests a large range of functions for kisspeptin systems in the brain of the European sea bass. PLoS ONE 8:e70177

105. **Stacey NE, Cook AF, Peter RE** 1979 Ovulatory surge of gonadotropin in the goldfish, *Carassius auratus*. Gen Comp Endocrinol 37:246-249

106. **Chang JP, Peter RE** 1983 Effects of pimozide and des Gly^{10},[$D\text{-}Ala^{6}$]luteinizing hormone-releasing hormone ethylamide on serum gonadotropin concentrations, germinal vesicle migration, and ovulation in female goldfish, *Carassius auratus*. Gen Comp Endocrinol 52:30-37

107. **Kobayashi M, Aida K, Hanyu I** 1985 Radioimmunoassay for silver carp gonadotropin. Bull Japan Soc Sci Fish 49:1783-1787

108. **Kobayashi M, Aida K, Hanyu I** 1986 Gonadotropin surge during spawning in male goldfish. Gen Comp Endocrinol 62:70-79

109. **Smith JT, Clarke IJ** 2010 Seasonal breeding as a neuroendocrine model for puberty in sheep. Mol Cell Endocrinol 324:102-109

110. **Thiery JC, Gayrard V, Le Corre S, Viguie C, Martin GB, Chemineau P, Malpaux B** 1995 Dopaminergic control of LH secretion by the A15 nucleus in anoestrous ewes. J Reprod Fertil Suppl 49:285-296

111. **Thiery JC, Martin GB, Tillet Y, Caldani M, Quentin M, Jamain C, Ravault JP** 1989 Role of hypothalamic catecholamines in the regulation of luteinizing hormone and prolactin secretion in the ewe during seasonal anestrus. Neuroendocrinology 49:80-87

112. **Havern RL, Whisnant CS, Goodman RL** 1994 Dopaminergic structures in the ovine hypothalamus mediating estradiol negative feedback in anestrous ewes. Endocrinology 134:1905-1914

113. **Goodman RL, Maltby MJ, Millar RP, Hileman SM, Nestor CC, Whited B, Tseng AS, Coolen LM, Lehman MN** 2012 Evidence that dopamine acts via kisspeptin to hold GnRH pulse frequency in check in anestrous ewes. Endocrinology 153:5918-5927

114. **Liu X, Herbison AE** 2013 Dopamine regulation of gonadotropin-releasing hormone neuron excitability in male and female mice. Endocrinology 154:340-350

115. **Vidal B, Pasqualini C, Le Belle N, Holland MC, Sbaihi M, Vernier P, Zohar Y, Dufour S** 2004 Dopamine inhibits luteinizing hormone synthesis and release in the juvenile European eel: a neuroendocrine lock for the onset of puberty. Biol Reprod 71:1491-1500

116. **Evans DH** 1993 Osmotic and ionic regulation. In: Evans DH ed. The Physiology of Fishes. Boca Raton, FL: CRC Press; p315-341

117. **Sinha AK, Liew HJ, Diricx M, Kumar V, Darras VM, Blust R, De Boeck G** 2012 Combined effects of high environmental ammonia, starvation and exercise on hormonal and ion-regulatory response in goldfish (*Carassius auratus L.*). Aquat Toxicol 114-115:153-164

118. **Tomita K, Oishi S, Ohno H, Peiper SC, Fujii N** 2008 Development of novel G-protein-coupled receptor 54 agonists with resistance to degradation by matrix metalloproteinase. J Med Chem 51:7645-7649

119. **Inoue N, Sasagawa K, Ikai K, Sasaki Y, Tomikawa J, Oishi S, Fujii N, Uenoyama Y, Ohmori Y, Yamamoto N, Hondo E, Maeda K, Tsukamura H** 2011 Kisspeptin neurons mediate reflex ovulation in the musk shrew (*Suncus murinus*). Proc Natl Acad Sci U S A 108:17527-17532

120. **Tomita K, Niida A, Oishi S, Ohno H, Cluzeau J, Navenot JM, Wang ZX, Peiper SC, Fujii N** 2006 Structure-activity relationship study on small peptidic GPR54 agonists. Bioorg Med Chem 14:7595-7603

121. **Tomita K, Oishi S, Cluzeau J, Ohno H, Navenot JM, Wang ZX, Peiper SC, Akamatsu M, Fujii N** 2007 SAR and QSAR studies on the N-terminally acylated pentapeptide agonists for GPR54. J Med Chem 50:3222-3228

122. **Chang JP, Peter RE, Crim LW** 1984 Effects of dopamine and apomorphine on gonadotropin release from the transplanted pars distalis in goldfish. Gen Comp Endocrinol 55:347-350

123. **Chang JP, MacKenzie DS, Gould DR, Peter RE** 1984 Effects of dopamine and norepinephrine on *in vitro* spontaneous and gonadotropin-releasing hormone-induced gonadotropin release by dispersed cells or fragments of the goldfish pituitary. Life Sci 35:2027-2033

124. **Chang JP, Peter RE, Nahorniak CS, Sokolowska M** 1984 Effects of catecholaminergic agonists and antagonists on serum gonadotropin concentrations and ovulation in goldfish: evidence for specificity of dopamine inhibition of gonadotropin secretion. Gen Comp Endocrinol 55:351-360

125. **Yu KL, Peter RE** 1990 Dopaminergic regulation of brain gonadotropin-releasing hormone in male goldfish during spawning behavior. Neuroendocrinology 52:276-283

126. **Yu KL, Rosenblum PM, Peter RE** 1991 *In vitro* release of

gonadotropin-releasing hormone from the brain preoptic-anterior hypothalamic region and pituitary of female goldfish. Gen Comp Endocrinol 81:256-267

127. **Tsutsui K, Bentley GE, Ubuka T, Saigoh E, Yin H, Osugi T, Inoue K, Chowdhury VS, Ukena K, Ciccone N, Sharp PJ, Wingfield JC** 2007 The general and comparative biology of gonadotropin-inhibitory hormone (GnIH). Gen Comp Endocrinol 153:365-370
128. **Qi X, Zhou W, Li S, Lu D, Yi S, Xie R, Liu X, Zhang Y, Lin H** 2013 Evidences for the regulation of GnRH and GTH expression by GnIH in the goldfish, *Carassius auratus*. Mol Cell Endocrinol 366:9-20
129. **Mercer RE, Chee MJ, Colmers WF** 2011 The role of NPY in hypothalamic mediated food intake. Front Neuroendocrinol 32:398-415
130. **Matsuda K, Sakashita A, Yokobori E, Azuma M** 2012 Neuroendocrine control of feeding behavior and psychomotor activity by neuropeptideY in fish. Neuropeptides 46:275-283
131. **Peng C, Chang JP, Yu KL, Wong AO, Van Goor F, Peter RE, Rivier JE** 1993 Neuropeptide-Y stimulates growth hormone and gonadotropin-II secretion in the goldfish pituitary: involvement of both presynaptic and pituitary cell actions. Endocrinology 132:1820-1829
132. **Godwin J, Thompson R** 2012 Nonapeptides and social behavior in fishes. Horm Behav 61:230-238
133. **Beaulieu JM, Gainetdinov RR** 2011 The physiology, signaling, and pharmacology of dopamine receptors. Pharmacol Rev 63:182-217
134. **Shupnik MA** 1996 Gonadal hormone feedback on pituitary gonadotropin genes. Trends Endocrinol Metab 7:272-276
135. **Soyano K, Saito T, Nagae M, Yamauchi K** 1993 Effects of thyroid hormone on gonadotropin-induced steroid production in medaka, *Oryzias latipes*, ovarian follicles. Fish Physiol Biochem 11:265-272
136. **Foster RG, Hankins MW** 2002 Non-rod, non-cone photoreception in the vertebrates. Prog Retin Eye Res 21:507-527
137. **Cardenas H, Ordog T, O'Byrne KT, Knobil E** 1993 Single unit components of the hypothalamic multiunit electrical activity associated with the central signal generator that directs the pulsatile secretion of gonadotropic hormones. Proc Natl Acad Sci U S A 90:9630-9634
138. **Maurer JA, Wray S** 1999 Luteinizing hormone-releasing hormone quantified in tissues and slice explant cultures of postnatal rat hypothalami. Endocrinology 140:791-799
139. **Sisk CL, Richardson HN, Chappell PE, Levine JE** 2001 *In vivo*

gonadotropin-releasing hormone secretion in female rats during peripubertal development and on proestrus. Endocrinology 142:2929-2936

140. **Harris GC, Levine JE** 2003 Pubertal acceleration of pulsatile gonadotropin-releasing hormone release in male rats as revealed by microdialysis. Endocrinology 144:163-171
141. **Abe H, Keen KL, Terasawa E** 2008 Rapid action of estrogens on intracellular calcium oscillations in primate luteinizing hormone-releasing hormone-1 neurons. Endocrinology 149:1155-1162
142. **Constantin S, Piet R, Iremonger K, Hwa Yeo S, Clarkson J, Porteous R, Herbison AE** 2012 GnRH neuron firing and response to GABA *in vitro* depend on acute brain slice thickness and orientation. Endocrinology 153:3758-3769
143. **Campbell RE, Gaidamaka G, Han SK, Herbison AE** 2009 Dendro-dendritic bundling and shared synapses between gonadotropin-releasing hormone neurons. Proc Natl Acad Sci U S A 106:10836-10840
144. **Inoue K, Kurosumi K** 1984 Ultrastructural immunocytochemical localization of LH and FSH in the pituitary of the untreated male rat. Cell Tissue Res 235:77-83
145. **Gregory SJ, Townsend J, McNeilly AS, Tortonese DJ** 2004 Effects of prolactin on the luteinizing hormone response to gonadotropin- releasing hormone in primary pituitary cell cultures during the ovine annual reproductive cycle. Biol Reprod 70:1299-1305
146. **Mutiara S, Kanasaki H, Harada T, Miyazaki K** 2006 Dopamine D(2) receptor expression and regulation of gonadotropin alpha-subunit gene in clonal gonadotroph LbetaT2 cells. Mol Cell Endocrinol 259:22-29
147. **Swartz SR, Moberg GP** 1986 Effects of epinephrine, norepinephrine, and dopamine on gonadotropin-releasing hormone-induced secretion of luteinizing hormone *in vitro*. Endocrinology 118:2425-2431
148. **Vacher C, Mananos EL, Breton B, Marmignon MH, Saligaut C** 2000 Modulation of pituitary dopamine D_1 or D_2 receptors and secretion of follicle stimulating hormone and luteinizing hormone during the annual reproductive cycle of female rainbow trout. J Neuroendocrinol 12:1219-1226
149. **Wang X, Zhao T, Wei H, Zhou H** 2011 Regulation of dopamine D2 receptor expression in grass carp pituitary cells: a possible mechanism for dopaminergic modification of luteinizing hormone synthesis. Gen Comp Endocrinol 173:48-55